理學博士學位論文

Dictyostelium discoideum 분화과정에서 glutathione 매개 cAMP 신호 전달체계

Glutathione-mediated cAMP signal pathway during development in *Dictyostelium discoideum*

2017年　2月

서울大學校 大學院

生命科學部

李　香　美

Glutathione-mediated cAMP signal pathway during development in *Dictyostelium discoideum*

by

Hyang-Mi Lee

Advisor:

Professor Sa-Ouk Kang, Ph. D.

A Thesis Submitted in Partial Fulfillment
of the Requirements for
the Degree of Doctor of Philosophy

February, 2017

School of Biological Science

Graduate School

Seoul National University

ABSTRACT

Glutathione (GSH, γ-glutamyl-L-cysteinylglycine) is the most prevalent reducing thiol-containing compound in eukaryotic cells and plays indispensable roles in multicellular development. However, the function of glutathione synthetase (*gshB*/GSS), the final-step enzyme of GSH biosynthesis, on development of *Dictyostelium discoideum* has not been clearly investigated.

Herein, it was found that the overexpression of *gshB* (*gshB*^{oe}) facilitates a significant increase of the intracellular GSH levels during both early and late development, which leads to developmental defects, such as the mound-arrest phenotype and the reduced spore formation. Moreover, in wild-type (KAx3) cells, addition of exogenous GSH led to similar defects to those characteristic of *gshB*^{oe} cells. To investigate the effects of increased intracellular GSH level by *gshB* overexpression on *Dictyostelium* development in more detail, the cAMP-mediated aggregation and cell-type differentiation were examined. First, when cells were allowed to develop at low cell densities, *gshB*^{oe} cells were not able to form aggregates and streams. *gshB*^{oe} cells exhibited multiple pseudopodia, indicating a lack of axial polarity during aggregation. In addition, *gshB*^{oe} cells exhibited abnormal fluctuating pattern in F-actin polymerization in response to cAMP stimulation.

Next, during differentiation, *gshB*^{oe} cells showed remarkable differences in the cell-type proportioning with KAx3 cells. In the mounds of *gshB*^{oe} cells, pre-stalk cells were increased relative to those in KAx3 mounds, whereas pre-spore cells were remarkably decreased, which was consistent with the reduced sporulation of *gshB*^{oe} cells.

Based on these results, the expression pattern of the essential components of the cAMP signaling pathway (*carA*/cAR1/cAMP receptor 1, *gpaB*/Gα2/G protein alpha subunit 2, *gpbA*/Gβ/G protein beta subunit, and *acaA*/ACA/adenylyl cyclase A), which are developmental regulators, was examined in *gshB*^{oe} cells. As the result, the expression level of *carA* and *gpaB* was upregulated, especially after 8 h of development. Similarly, in *gshB*^{oe} cells, the intracellular cAMP concentration were significantly 4.5-fold higher than those of KAx3 cells at 8 h after the onset of development.

To further investigate the effect of *gshB* overexpression on the cAMP signaling pathway, the mutant strains which constitutively expressed *carA* and *gpaA* (*carA*^{oe} and *gpaB*^{oe}, respectively) were generated. During developmental processes, *gpaB*^{oe} cells displayed the defects in multicellular aggregation and F-actin polymerization characteristic of *gshB*^{oe} cells, which may be as a secondary response to abnormally elevated cAMP concentrations, but *carA*^{oe} cells did not. Furthermore, *gpaB*^{oe} cells exhibited phenocopies of *gshB*^{oe} cells in cell-type

proportioning, such as the increased pre-stalk cells and the decreased pre-spore cells. Interestingly, *gpaB* knockdown in *gshB*^{oe} cells (*gpaB*^{as}/*gshB*^{oe}) partially rescued the defects of *gshB*^{oe} cells. *gpaB*^{as}/*gshB*^{oe} cells produced fruiting bodies with small sori and were able to form aggregates and streams at low cell densities. These results suggest that the developmental defects associated with *gshB*^{oe} cells may be caused by increased *gpaB* expression and high intracellular cAMP concentrations.

Additionally, there was the distinction in Gα2-GFP localization between KAx3 and *gshB*^{oe} cells. In KAx3 cells, Gα2-GFP was uniformly expressed prior to cAMP stimulation and rapidly translocated to the plasma membrane after cAMP stimulation. However, in *gshB*^{oe} cells, Gα2-GFP was strongly localized at the plasma membrane both before and after the addition of cAMP, implying that GSH could also regulate Gα2 localization.

Taken together, these findings suggest that GSH regulates developmental stage and cell-type proportioning by upregulating cAMP signaling pathway via modulation of Gα2 expression and localization during the development of *Dictyostelium*. These results will provide insights into the general mechanisms underlying cell development involved in GSH-mediated signaling.

Key words: Glutathione, Glutathione synthetase, cAR1-mediated cAMP signaling, G protein alpha 2, *Dictyostelium discoideum*

CONTENTS

List of Tables

List of Figures

List of Abbreviations

GSH	glutathione (thiol-reduced form)
GSSG	glutathione (disulfide-oxidized form)
GCS	γ-glytamylcysteine synthetase
GSS	glutathione synthetase
NAD(P)H	nicotinamide adenine dinucleotide (phosphate)
ATP	adenosine triphosphate
cAMP	3',5'-cyclic adenosine monophosphate
FAD(H_2)	flavine adenine nucleotide (hydroquinone form)
cAR1	cAMP receptor 1
Gα2	G protein alpha 2 subunit
Gβγ	G protein beta gamma subunits
ACA	adenylyl cyclase A
PDE	phosphodiesterase
EDTA	Ethylenediaminetetraacetic acid
PIP3	phosphatidylinositol (3,4,5)-triphosphate
PTEN	phosphatase and tensin homolog
DIF	differentiation inducing factor
mBBR	monobromobimane
NEM	N-methylmaleimide
TFA	trifluoroacetic acid
TRITC	tetramethylrhodamine
MOPS	4-morpholinepropanesulfonic acid
GFP	green fluorescent protein

I. INTRODUCTION

1. Glutathione

1.1. An overview of glutathione

Glutathione (GSH) is a ubiquitous tripeptide, γ-L-glutamyl-L-cysteinylglycine (Scheme 1A), found in most plants, microorganisms, and all mammalian tissues (Meister and Anderson, 1983). It is the most abundant non-protein thiol, being in the millimolar range in most cells. Eukaryotic cells have three major reservoirs of GSH: Almost 90% of cellular GSH are in the cytosol, 10% in the mitochondria, and a small percentage in the endoplasmic reticulum (Hwang, *et al.*, 1992; Meredith and Reed, 1982).

In cells, glutathione is present in two forms: Thiol-reduced form (GSH) and disulfide-oxidized form (GSSG). Under normal physiological conditions, glutathione is maintained in the reduced formed (GSH) by the action of glutathione reductase and NAD(P)H. Therefore, the intracellular ratio of GSH to GSSG is high in most eukaryotic cells (Akerboom, *et al.*, 1982; Wu, *et al.*, 2004). Because of the cysteine residue, GSH lacks the toxicity, and is suitable as a cellular thiol "redox buffer" to maintain a given thiol/disulfide redox potential. The free sulfhydryl moiety of the cysteine residue confers high redox potential E'_0 = -0.33 V and nucleophilic properties on the tripeptide. And the γ-glutamyl linkage promotes intracellular stability (Sies, 1999).

GSH serves vital functions, including detoxifying electrophiles; maintaining the essential thiol status of proteins; scavenging free radicals; providing a reservoir for cysteine; and modulating cellular events (gene expression, DNA and protein synthesis, cell proliferation and apoptosis, signal transduction, immune response, and protein glutathionylation) (Meister, 1994; Sies, 1999). GSH deficiency contributes to oxidative stress and the pathogenesis of many diseases

(Alzheimer disease, Parkinson's disease, cystic fibrosis, sickle cell anemia, HIV, AIDS, cancer, and diabetes) (Wu, *et al.*, 2004).

1.2. Glutathione biosynthesis

The synthesis of GSH from glutamate, cysteine, and glycine is catalyzed sequentially by two cytosolic enzymes, γ-glutamylcysteine synthetase (GCS) and glutathione synthetase (GSS) (Scheme 1B).

The first enzyme, γ-glutamylcysteine synthetase (GCS) is sometimes called glutamate cysteine ligase (GCL) and rate-limiting enzyme in *de novo* synthesis of GSH (Meister, 1983). It has been demonstrated that GCS expression is regulated by diverse stimuli in a cell specific manner. Especially, nuclear factor $_{K}$B up-regulates GCS expression in response to oxidant stress, inflammatory cytokines, and buthionine sulfoximine-induced GSH depletion (Lu, 2000; Townsend, *et al.*, 2003). GCS activity also seems to be regulated by cellular thiol antioxidant balance and is favored in animal cells because of the high affinity and activity of GSS. However, GSH itself regulates the activity of GCS by a negative feedback mechanism (Meister and Anderson, 1983).

In mammals, GCS is a heterodimer consisting of a catalytically active heavy subunit (73 kDa) and a light regulatory subunit (31 kDa) (Lu, 2000). GCS heavy subunit has all of the catalytic activity, but in vitro experiments with rat kidney GCS, unless complex with GCS light subunit, it has exquisite sensitivity to feedback inhibition by GSH and a high K_m for glutamate. The K_m values of mammalian GCS for glutamate and cysteine are 1.7 and 0.15 mmol/L, respectively, which are similar to the concentrations of glutamate (2-4 mmol/L) and cysteine (0.15-0.25 mmol/L) in rat liver (Griffith, 1999). The cDNA of mammalian and yeast GCS shows the highest degree of similarity (90-95%)

(Griffith and Mulcahy, 1999). Moreover, *Dictyostelium discoideum* GCS shares approximately 48%, 47%, and 43% sequence identities at the amino acid level with the protein of *Drosophila melanogaster*, *Homo sapiens*, and *Schizosaccharomyces pombe*, respectively.

The second enzyme of *de novo* GSH biosynthesis is glutathione synthetase (GSS) (Scheme 1B). This enzyme is a homodimer of 118 kDa, and is responsible for the addition of glycine to γ-glutamylcysteine produced by GCS to form GSH. Only a few findings have been reported on the gene expression encoding GSS. In the yeast *Saccharomyces cerevisiae*, GSS expression is increased by heat-shock stress in a Yap1p-dependent fashion, and consequently the intracellular GSH level is increased (Sugiyama, *et al.*, 2000). In addition, agents that induce both GCS subunits also induce GSS. For example, the treatment of hepatocytes or rats with diethyl maleate, buthionine sulfoximine, *tert*-butylhydroquinone, or thioacetamide, which increases the expression of GCS subunits, then increases the GSS expression, which accordingly increases the GSH synthesis capacity (Huang, *et al.*, 2000). Meanwhile, GSS is not subject to feedback inhibition by GSH.

Much less is known about the role of GSS in regulating intracellular GSH level. Recent studies suggest that GCS and GSS are coordinately regulated and GSS induction can further enhance GSH biosynthesis (Huang, *et al.*, 2000; Yang, *et al.*, 2002). The K_m values of mammalian GSS for ATP and glycine are ~0.04 and 0.9 mmol/L, respectively, which are lower than intracellular concentrations of ATP (2–4 mmol/L) and glycine (1.5–2 mmol/L) in rat liver (Njalsson, *et al.*, 2001). In *S. cerevisiae*, however, GSS was dispensable for growth under both normal and oxidative stress conditions, which is due to an accumulation of γ-glutamylcysteine (Grant, *et al.*, 1997).

A

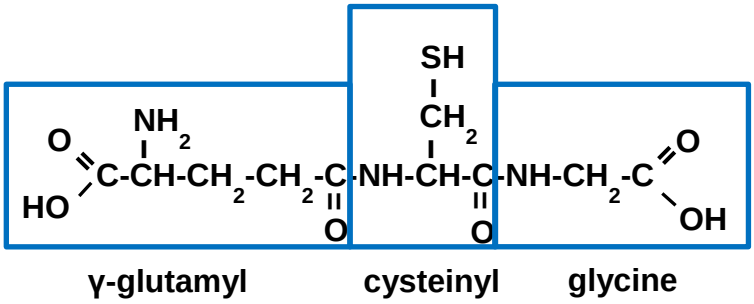

B

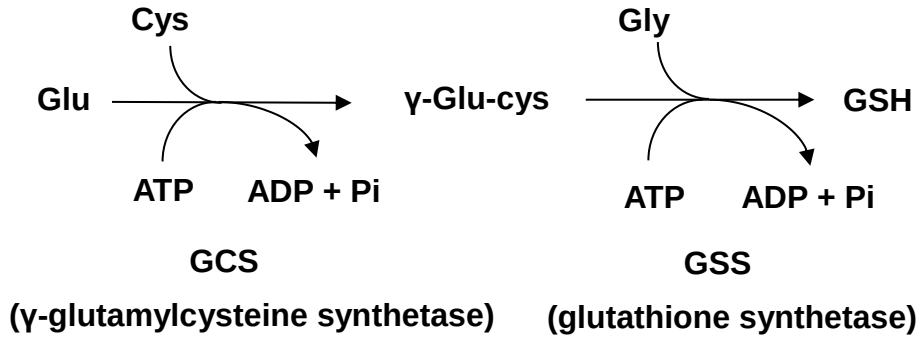

Scheme 1. Chemical structure and enzymatic synthesis of GSH. (A) Chemical structure of GSH. (B) Enzymatic biosynthesis of GSH. GCS; γ-glutamylcysteine synthetase, GSS; glutathione synthetase.

1.3. Glutathione metabolism

Glutamate plays a regulatory role in GSH synthesis. When extracellular glutamate concentrations are high, cysteine uptake is competitively inhibited by glutamate and thereby resulting in reduced GSH synthesis (Tapiero, *et al.*, 2002). Instead, glutamate competes with GSH binding to GCS. When intracellular glutamate concentrations are unusually high, therefore, GSH biosynthesis is enhanced and its concentrations is significantly high (Griffith, 1999). The breakdown of GSH is catalyzed by an enzyme, γ-glutamyl transpeptidase (GGT) that transfers γ-glutamyl moiety of GSH to an acceptor that may be amino acids, peptides, water (forming glutamate), or GSH itself. GGT also leaves the cysteine product to preserve intracellular homeostasis of oxidative stress (Yokoyama, 2007).

Since cysteine is readily oxidized to cystine in oxygenated solutions, the intracellular pool of cysteine is small. Thus, factors (insulins and growth factors) that stimulate cysteine uptake increase intracellular GSH concentrations. In addition, the increased supply of its precursors (cystine, *N*-acetyl cysteine, and L-2-oxothiazolidine-4-carboxylate) enhances GSH synthesis (Townsend, *et al.*, 2003). Because cysteine generated from methionine catabolism via the transsulfuration pathway serves as a substrate for GCS, dietary methionine can replace cysteine to support GSH synthesis *in vivo*.

The evidence indicates that the dietary amino acid balance has an important effect on GSH homeostasis (Lu, 2000). In particular, 5-oxoproline is as a metabolite in the glutathione cycle, and is converted to glutamate by 5-oxoprolinase. Thus, an increase in urinary excretion of 5-oxoproline is a useful indicator of reduced availability of cysteine and/or glycine for GSH synthesis *in vivo*.

Glutathione peroxidase catalyzes the reduction of hydroperoxides by reduced glutathione. GSH is also converted to GSSG by transhydrogenation, which catalyzes via sulfhydryldisulfide interchange, the scission as well as formation of disulfide bonds in many diverse proteins. Reduction of GSSG to GSH is mediated by the widely distributed glutathione reductase (GR) that uses NADPH. Moreover, GSH is converted to GSSG by free radicals.

1.4. The roles of glutathione in cellular functions

Glutathione participates in many cellular reactions. First, GSH is one of the most studied antioxidants that prevent excessive oxidation of sensitive cellular components. GSH also involved in the detoxification of products from ROS-promoted oxidation of lipids and many other products of ROS interaction with cellular components (Ceaser, *et al.*, 2004; Siems, *et al.*, 2010; Zhu, *et al.*, 2009). The thiyl radicals formed from these reactions can also combine with other molecules, which leads to the formation of oxidized glutathione (GSSG). Then, GSSG is reduced to GSH by the NADPH-dependent glutathione reductase (GR). Therefore, the glutathione couple GSH/GSSH is a critically important redox player and together with other redox active couples, such as NAD(P)/NAD(P)H and FAD/$FADH_2$, regulates and maintains cellular redox status. Glutathione deficiency results in oxidative stress, which causes aging and the pathogenesis of many diseases (Townsend, *et al.*, 2003).

Second, GSH is involved in the detoxification of many toxic metabolites produced as side-products of the normal cellular metabolism. For example, methylglyoxal (2-oxopropanal) is one of these, and it can be generated by enzymatically and non-enzymatically (Inagi, *et al.*, 2010; Martins, *et al.*, 2001). Glycolysis appears to be the main source of methylglyoxal, where it is produced

from triose phosphates, particularly due to spontaneously decomposition of glyceraldehyde-3-phosphate (Kalapos, 2008; Murata, *et al.*, 1986). Methylglyoxal toxicity is based on its capacity to interact with any molecule containing free amino groups. Methylglyoxal may be involved in ROS generation. GSH acts as a cofactor in the system of methylglyoxal elimination which consists of two enzymes called glyoxalases. The first enzyme in this reaction glyoxalase I catalyzes the isomerization of hemiacetal adducts, which are formed in a spontaneous reaction between a glutathione and aldehydes such as methylglyoxal:

$$\text{glutathione} + \text{methylglyoxal} \leftrightarrow \text{hemithioacetal adduct} \leftrightarrow \text{(R)-S-lactoylglutathione}$$

The second enzyme, glyoxalase II, catalyzes the hydrolysis of the product of the above reaction:

$$\text{(R)-S-lactoylglutathione} + H_2O \rightarrow \text{D(-)lactic acid} + \text{GSH}$$

This pathway is the main route for methylglyoxal catabolism in yeast and mammals (Cho, *et al.*, 1998; Murata, *et al.*, 1986; Penninckx, *et al.*, 1983).

Third, GSH relates to its impact on signal transduction of gene expression inside cells, which is linked to two well-established redox sensitive transcription factors, nuclear factor κB (NF-κB) and activator protein-1 (Sen, 1998; Sen and Packer, 1996). Extremely high or low levels of oxidized glutathione results in less than optimal activation of these transcription factors. Also, glutathione status has been investigated for its role in tumor necrosis factor-α induced activation of NF-κB. Tumor necrosis factor-α is highly related to muscle wasting conditions

such as cancer cachexia, AIDS, and other muscle inflammatory conditions. Therefore, maintaining optimal cellular levels of glutathione is important for effective cellular function by changing cellular redox homeostasis (Lushchak, 2012; Sies, 1999).

Finally, GSH regulates cell growth, proliferation, and cell death. Vernoux and colleagues discovered a role of intracellular GSH in the G1-S transition in plants during the cloning of GCS (Vernoux, *et al.*, 2000). Additionally, recent evidence suggests that an increased GSH level is associated with an early proliferative response, and is required for the cell to enter the S phase (Chaudhuri, *et al.*, 1997). GSH also modulates cell death at both apoptosis and necrosis by regulating redox state of specific thiol residues of proteins, including NF-κB, stress kinases, and caspases involved in cell death (Galter, *et al.*, 1994).

1.5. The roles of glutathione in development

An understanding of how GSH relates to the dynamics and regulation of development was provided in a study of a slime mold (*Physarum polycephalum*) (Allen, *et al.*, 1985). This slime mold takes on distinctive forms in culture, such as flagellate, plasmodium, sclerotium, and spore. Several reports show that glutathione (GSH), a major thiol-containing molecule, is involved in *Physarum* differentiation. For instance, as the plasmodium differentiates into spherules, the intracellular GSH concentration decreases dramatically. In fact, the decrease in GSH may change the oxidation-reduction state of the cell to induce spherulation of the plasmodium (Nations, *et al.*, 1987).

Recent studies have suggests the important roles of GSH in embryonic structures and the organ development. Beginning with fertilization of the oocyte until delivery the developing embryo encounters changing environmental

conditions such as varying levels of oxygen, which can give rise to reactive oxygen species (ROS). At this stage, high GSH concentrations have been observed for normal fertilization (Sutovsky and Schatten, 1997). Following successful fertilization, the zygote undergoes a series of cleavage divisions. With the dividing embryo maintaining the same approximate overall volume as the unfertilized oocyte, GSH concentrations drop in a near linear fashion from 1.2 pmoles/oocyte to around 0.12 pmoles/embryo at the blastocyst stage (Gardiner and Reed, 1994). The mechanism for this may involve ATP-dependent synthesis during oocyte maturation, which is switched off after fertilization. When GSH deficiency is pharmacologically induced by an inhibitor (buthionine sulfoximine, BSO) in newborn mammals, it leads to rapid multi-organ failure and death within a few days (Meister, 1994).

In plants, GSH also has long been evaluated for its function during seed development. Developing seeds are an important sink for sulfur in either oxidized or reduced form. Thus, sulfur nutrition of maternal plants may directly affect the delivery and metabolism of sulfur. The potential transport metabolites for reduced sulfur is GSH (Rennenberg and Filner, 1982). In plant cells, knocking out expression of GSH1, encoding the first enzyme of the committed pathway of GSH synthesis, causes lethality at the embryo stages (Cairns, *et al.*, 2006; Noctor, *et al.*, 2012), knockouts for GSH2, encoding glutathione synthetase, show a seedling-lethal phenotype (Pasternak, *et al.*, 2008). Moreover, several mutants, in which decreased GSH contents are caused by less severe mutation in the GSH1 gene, show failure in development of a root apical meristem (Vernoux, *et al.*, 2000). In other mutants, the developmental phenotypes are weak or absent, but alterations in environmental responses are observed.

2. *Dictyostelium discoideum*

2.1. An overview of *Dictyostelium discoideum*

The slime mold *Dictyostelium discoideum* is a well-established model organism to study cell biology. The life cycle of *Dictyostelium discoideum* comprises two phases. During the vegetative phase, it grows as a unicellular organism, feeding on bacteria and multiplying by binary fission. Upon starvation, cells stop growing and undergo a multicellular developmental cycle that ultimately leads to the formation of a fruiting body consisting of two distinct cells, vacuolated stalk and dormant spore cells. Finally, the fruiting body is allowed to disperse the spores which can survive under harsh environmental conditions and germinate under the optimal condition (Scheme 2).

The initial response of starvation, if the cell density is sufficiently high, is for the cells to collect in multicellular aggregates by chemotaxis in response to oscillatory cAMP pulses. The pulsatile release of cAMP leads to concentric or spiral-rings of amoebae, which is called hemispherical mounds up to 10^5 cells that become enclosed in a protein cellulose slime sheath to form tight aggregates. As the development cascade proceeds, a rise in the cAMP concentration to micro-molar levels occurs (Abe and Yanagisawa, 1983; Schnitzler, *et al.*, 1995). In this time, a protruding tip forms at the apes of each aggregates, and each aggregate then elongates to form finger-like structure or migrating slug, which is sensitive to heat, light, and humidity. cAMP and a substance called differentiation-inducing factor help to form different cell-types. Initial differentiation of randomly dispersed cells into pre-stalk and pre-spore cells is hardly distinguishable in the aggregate. However, the cells sort out chemotactically during tip formation and by the slug stage the pre-stalk cells occupy the anterior

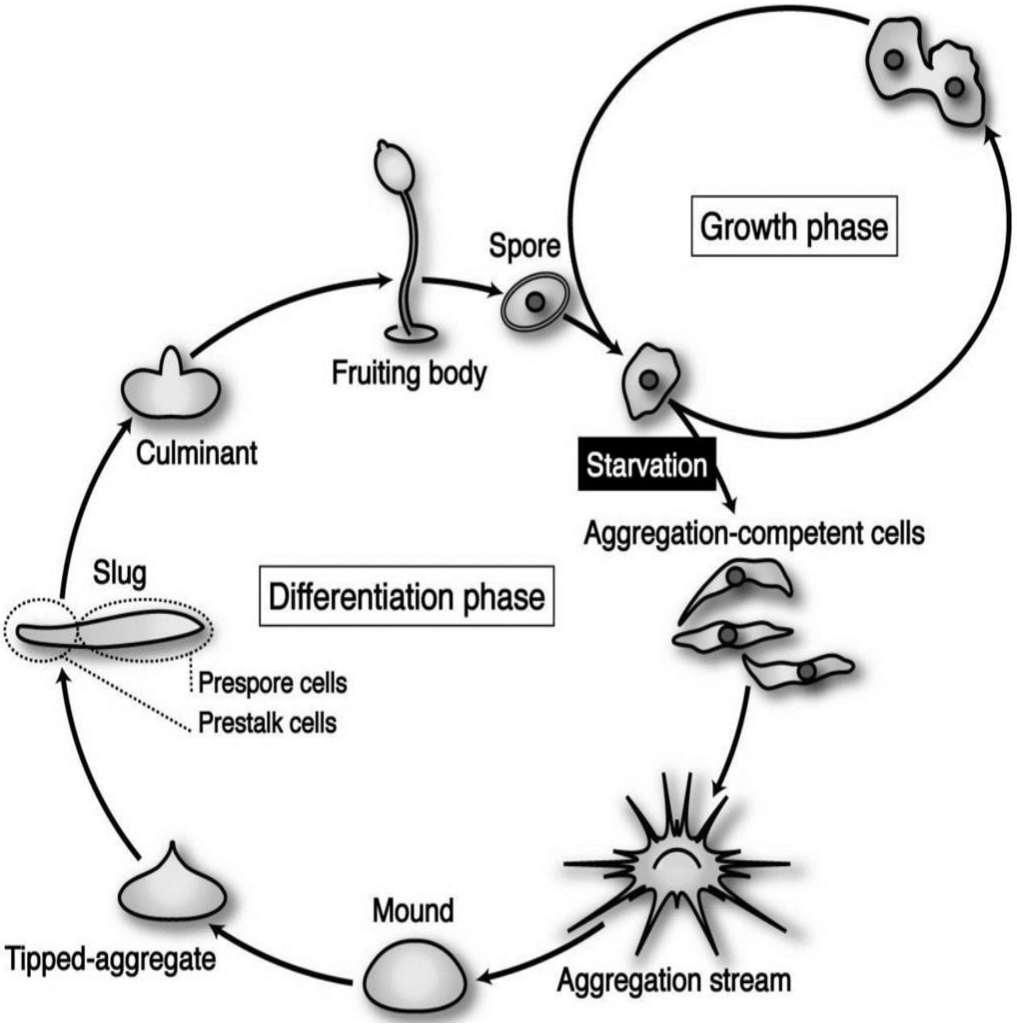

Scheme 2. *Dictyostelium discoideum* life cycle. The life cycle of *Dictyostelium discoideum* consists of distinct two different phase. Starvation triggers individual amoebae to develop into multicellular structure. Aggregate (8 h), slug (16 h), and a mature fruiting body (24 h) (Maeda, 2013).

20% with the pre-spore cells at the back of the slug (Loomis, 1993). The tip or pre-stalk cells behave as an organizer, which is orchestrating all subsequent movements of developing cells (MacWilliams, 1982). During culmination, pre-stalk cells penetrate through the pre-spore-cell mass and lift it off the substratum. Finally, cells mature into spore and stalk cells and form the final structure with a sorus atop a slender stalk (Devine, *et al.*, 1982).

The cells involved in the lifecycle undergo cell movement, chemotaxis, cell adhesion, cell-type determination, and pattern formation, which are essential for the establishment of multicellular organization, thus, are applicable to human cancer research. The simplicity of its lifecycle makes *D. discoideum* a valuable model organism to study genetic, cellular, and biochemical processes in other organisms. Also, The 34 Mb genome contains many genes predicted to encode 125,000 proteins that are homologous to those in higher eukaryotes and are missing in *S. cerevisiae*. The recent completion of the *Dictyostelium* genome sequence greatly facilitates biochemical and molecular genetic analysis (Felder, *et al.*, 2005).

2.2. The early events during development of *D. discoideum*

During the initial stage of development, a considerable number of genes are expressed at high rates (Kumagai, *et al.*, 1989; Louis, *et al.*, 1993; Mann and Firtel, 1989). These include the genes for the cAMP receptor (*carA*), for the Gα subunit 2 (*gpaB*) that is coupled with the receptor, for the activatable adenylyl cyclase (*acaA*), and for the secreted and internal cAMP phosphodiesterases (*pdsA* and *regA*) (Franke, *et al.*, 1991; Parent and Devreotes, 1996). The products of these genes function on the regulation of the chemotactic aggregation by generating an oscillatory network that relays extracellular cAMP signals and

regulating the levels of cAMP both inside and outside the cells (Gerisch, *et al.*, 1979). When certain cells secrete cAMP, the stimulated neighbor cells migrate toward cAMP in a head-to-tail manner and propagate the cAMP signal until an aggregate forms. They stick to each other in an EDTA-resistant manner as the consequence of expressing the genes, *csaA* and *lagC*, that encode the surface proteins gp80 and gp150, respectively (Harloff, *et al.*, 1989; Wang, *et al.*, 2000). The effects of cAMP pulses on the gene expression may be directly related. In addition, *Dictyostelium* cells degrade the extracellular cAMP by using an intricate removal system, ePDE, to prevent the loss of directional information and gene expression resulting from saturation of the receptors.

2.2.1. The cAR1-mediated cAMP signaling

During chemotactic aggregation, oscillatory cAMP signaling is controlled by a cAR1-mediated signal pathway that regulates the activation and inhibition of adenylyl cyclase (ACA), as well as the cyclical degradation of both intracellular and extracellular cAMP (Bader, *et al.*, 2007; Kriebel, *et al.*, 2003). The receptor, cAR1, is a seven trans-membrane domain glycoprotein. It is related to receptors in animals, plants and other simple eukaryotes and is coupled to trimeric GTP-binding proteins. In *D. discoideum*, the cAR1-controlled pathway leading to ACA activation involves the dissociation of heterotrimeric G protein subunits Gα2 and Gβγ, which in turn activate many transient responses, including the activation of ACA (Kriebel, *et al.*, 2003). cAR1 also controls the activity of guanylyl cyclase (GC) and phospholipase C (PLC), and modulation of the actin and myosin cytoskeleton, which are dependently of G proteins. Meanwhile, receptor phosphorylation, $Ca2^{+}$ mobilization, and ERK activation are events that are activated independently of G proteins (Milne and Devreotes, 1993; Segall, *et al.*, 1995; Snaar-Jagalska, *et al.*, 1988) (Scheme 3).

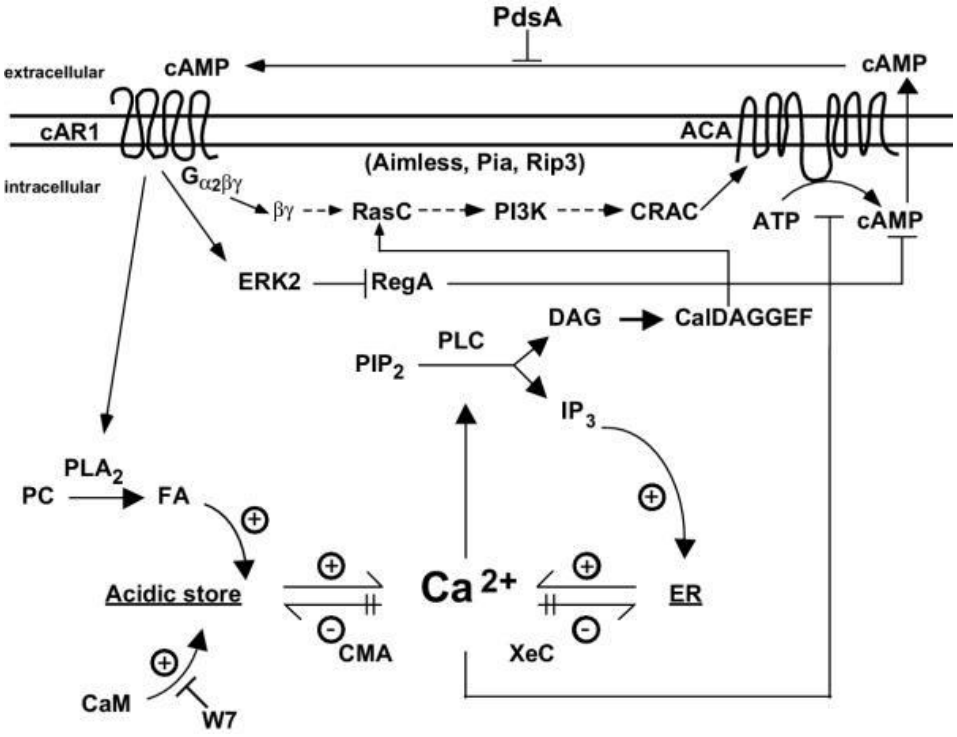

Scheme 3. The cAR1-mediated cAMP signaling in *D. discoideum*. Adenylyl cyclase (ACA) was shown to be activated by heterotrimeric G proteins (Gα2βγ), which is bound to cAR1. ERK2 inhibits RegA, a cytosolic phosphodiesterase. cAR1 also activates phospholipase A2 that liberates fatty acids (FA) and elicits $Ca2^{+}$-influx. cAMP released to the outside of the cell elicits feedback stimulation during oscillation. Extracellular phosphodiesterase (PdsA) provides for a low extracellular cAMP level allowing sensitive detection of the next wave (Malchow, *et al.*, 2004).

The amount of cAMP made by adenylyl cyclase is proportional to the level of the extracellular stimulus, and the amount of extracellular cAMP depends on how much intracellular cAMP was made (Dinauer, *et al.*, 1980).

The heterotrimeric G proteins coupled to the cAMP receptors are composed of α, β, and γ subunits. In *Dictyostelium*, G protein complexes may contain 1 of 11 α subunits coupled to a single βγ subunit (Lilly, *et al.*, 1993; Wu, *et al.*, 1995; Zhang, *et al.*, 2001). During aggregation, only Gα2 seems to be coupled to cAR1 to mediate all the cAMP-dependent responses (Kumagai, *et al.*, 1989; Sun and Devreotes, 1991). cAMP binding to cAR1 induces the exchange of GDP for GTP in the Gα2 subunit and the dissociation of Gα2 from Gβγ.

After cAMP binding on the receptor, there is an adaptive process; a constant level of cAMP causes one burst of synthesis and secretion and then halt. There is no loss of cAR1 from the cell surface. As with many sensory processes, the receptors quickly adapt within ~1-2 min. Thus, the extracellular cAMP is hydrolyzed by an extracellular phosphodiesterase (ePDE), allowing the receptors to deadapt and prepare to respond to the next cAMP pulse. In *Dictyostelium*, the alternation between activation and adaptation is essential for relaying the directional cAMP signal necessary for chemotaxis (Devreotes and Zigmond, 1988).

2.2.2. Chemotaxis in *D. discoideum*

Chemotaxis is the directed migration of cells in gradients of signaling molecules, an essential biological process that underlies morphogenesis during development, and the recruitment of immune cells to sites of infection. It is also an important component of pathological conditions, including metastasis and chronic inflammatory diseases. In *D. discoideum*, chemotaxis to cAMP is at the heart of this stage of the lifecycle.

The directed movement of cells during chemotaxis can conceptually be viewed as the integration of three separate processes. First, there is directional sensing, the capacity of cells to determine the direction of the concentration gradient. Second, cells elaborate periodic pseudopod extensions or membrane projections. These are the basic unit of motility, and in amoebae are produced at approximately one minute intervals. Third, there is polarization, or stable changes in morphology, and the localization of proteins to the front and back of cells. Polarization enhances migration by generating persistent movement in a specified direction (Franca-Koh, *et al.*, 2006).

Directional sensing

The best-studied indicator of directional sensing is the phospholipid, PIP3, which specifically accumulates at the front of a variety of cells when exposed to appropriate gradients. In *D. discoideum*, the enzymes, phosphatidylinositol that produces PIP3 by phosphorylating PIP2, and PTEN (phosphatase and tensin homologue deleted on chromosome ten) that catalyzes the reverse reaction coordinate chemotaxis within cells (Funamoto, *et al.*, 2002; Huang, *et al.*, 2003; Iijima, *et al.*, 2002). At the leading edge, where chemoattractant concentrations are highest, Ras is activated and PI3K is recruited from the cytoplasm (Sasaki, *et al.*, 2004). Conversely, PTEN falls off the plasma membrane at the front but remains strongly bound at the back. These events also occur in cells treated with inhibitors of actin polymerization, indicating that neither movement nor actin polymerization are required for directional sensing. In cells lacking PTEN, broadly distributed PIP3 promotes actin polymerization and pseudopod extension all around the perimeter, and chemotaxis is severely impaired (Iijima, *et al.*, 2002).

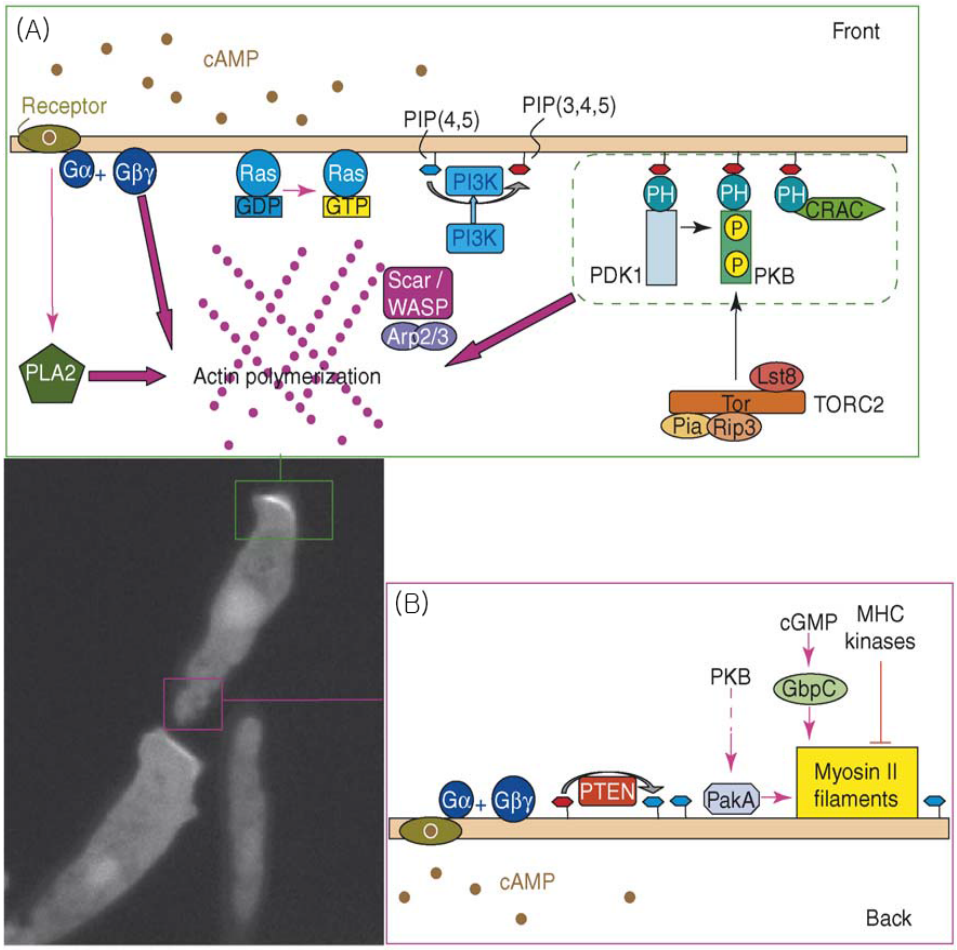

Scheme 4. Chemotaxis in *D. discoideum*. In a gradient, chemotactic cells persistently activate specific pathways at the front and back. At the front (A), Ras is activated and PI3K is recruited to the plasma membrane, leading to the accumulation of PIP3. PIP3 interacts with PH domain-containing proteins such as PDK1, PKB and CRAC. PKB is phosphorylated and activated by PDK1 and the TORC2 complex and is an important regulator of actin polymerization. At the back (B), PTEN remains membrane-bound and degrades PIP3, whereas myosin II is assembled into contractile filaments that suppress pseudopod formation and promote retraction of the cell's rear (Franca-Koh, *et al.*, 2006).

Pseudopod extensions

Cell movements and shape changes are driven largely by modulating of the actin cytoskeleton. At the leading edge, actin polymerization mediated by the Arp2–Arp3 complex produces a network of branched filaments that lead to pseudopod extension. Recent studies have examined several regulators of the Arp2–Arp3 complex, in particular the WASP (Wiskott–Aldrich syndrome protein) and Scar (suppressor of cAMP receptor) family of proteins. In *D. discoideum*, cells with lowered levels of WASP are unable to aggregate (Myers, *et al.*, 2005). Knockout of Scar moves more slowly but are able to chemotaxis and aggregate (Ibarra, *et al.*, 2006).

Regulation of the cytoskeleton at the back and sides are equally as important as the events occurring at the front. Thus, the focus is on preventing lateral extensions that point away from the direction of the gradient and supplying contractile force to retract the rear of the cell. For example, *D. discoideum* cells lacking the myosin II heavy chain (MHC) gene extend numerous lateral and even some vertical pseudopods, which correlates with the impaired recruitment of myosin II to the cortical cytoskeleton (Bosgraaf, *et al.*, 2002). Also, cGMP is a key regulator of this kinase, because mutants with decreased cGMP phosphodiesterase activity have increased myosin regulatory light chain (MLC) phosphorylation.

Polarization

The elongated cell morphologies of *D. discoideum* developing cells contribute to chemotaxis by facilitating faster migration and greater persistence in direction. Highly polarized cells, such as 7-hour-starved amoebae, maintain the same leading edge and turn towards the new direction, suggesting that the anterior

region is more sensitive to chemoattractants. By contrast, less-polarized cells, such as 5-hour-starved *D. discoideum*, respond by retracting existing pseudopods and extending new projections in the correct direction. This is driven by redistribution of PI3K, PTEN and PH-domain proteins. However, these components are relocalized much more rapidly when polarity is abolished by treating cells with pharmacological inhibitors of actin polymerization (latrunculin A) (Janetopoulos, *et al.*, 2004). This suggests that actin cytoskeleton dependent feedback loops at the front and back of the cell stabilize intracellular asymmetries.

2.3. Cell differentiation in *D. discoideum*

2.3.1. Control of cell-type induction

After the cells have aggregated, they form the hemispherical mound. Mounds are characterised by rotating waves of cAMP that direct the counter-rotational periodic movement of the cells. Cells start to differentiate into pre-spore and pre-stalk cells during aggregation, on the basis of physiological biases like nutritional state and cell cycle position at the time of starvation already present in the population before aggregation (Araki, *et al.*, 1997; Huang and Pears, 1999). The emerging cell types initially form a 'salt and pepper' pattern in the mound. Some pre-stalk cells then sort out to form the tip and the slug tip guides the movement of all other cells thus acting as an organiser. The tip's action as an organizer can be mimicked by the periodic injection of cAMP pulses of the right frequency and duration (Dormann and Weijer, 2001), which is in agreement with the fact that pre-stalk cells express ACA and the extracellular cAMP phosphodiesterase pdeA (Verkerke-van Wijk, *et al.*, 2001; Weening, *et al.*, 2003).

In slugs, cells in the tip often rotate perpendicularly to the direction of slug

migration, especially when it is lifted from the substrate. In the posterior part of the slug, the cells move forward periodically and all cells move on average with the speed of the whole slug. It has been shown that the assumptions of cAMP wave propagation. Moreover, induction of pre-stalk and pre-spore cells is thought to results from a complex interaction of cAMP and the pre-stalk/stalk-inducing factor, DIF, a chlorinated hexaphenone (Morris, *et al.*, 1987). Generally, cAMP induces pre-spore-specific gene expression. DIF is antagonistic toward pre-spore cell differentiation and is required for the induction of the pstB subclass of pre-stalk genes. DIF-mediated pstB cell differentiation is antagonized by extracellular cAMP (Berks and Kay, 1990). By contrast, pstA and pstO cell differentiation requires both DIF- and cAMP-mediated responses.

2.3.2. Cell fate and patterning

There are good evidences that the initial choice of cell type is biased by the conditions of the cells when starvation is imposed. Well-nourished cells may be preferentially differentiated into spores, whereas poorly fed cells may be to die in the production of stalk when cells of the two populations are mixed and developed (Inouye and Takeuchi, 1982). Furthermore, when cells of the one population are starved alone, the well-nourished cells aggregate several hours faster than cells grown in limiting nutrients (Forman and Garrod, 1977). There is always heterogeneity in the population, whether genetic, temporal, or nutritional, and this heterogeneity affects the determination of cell fate. These cell biases toward pre-stalk or pre-spore formation were expressed in the absence of the cell contact and were not due to intercellular communication, but rather to a cell-autonomous effect derived from the position in the cell cycle (Gomer and Firtel, 1987; Wood, *et al.*, 1996). Wood *et al*. had been isolated a mutant with an abnormally high percentage of stalk cells called *rtoA*, which codes for a novel

protein expressed during vegetative growth and then again after aggregation. This effect of the mutation is to remove the dependency of pre-stalk or pre-spore differentiation on cell cycle position. This increases the frequency of pre-stalk cells (Wood, *et al.*, 1996).

It is also known that amoebae in the 'low Ca^{2+}' class exhibit a pre-spore tendency and those in the 'high Ca^{2+}' class show a pre-stalk tendency (Azhar, *et al.*, 2001).

cAMP-dependent protein kinase, PKA regulates multiple pathways at key time including aggregation, cell-type differentiation, and terminal differentiation (Mann and Firtel, 1991; Mann and Firtel, 1993). PKA is essential for pre-spore cell differentiation and required for maximal and efficient pre-stalk cell differentiation (Hopper, *et al.*, 1993; Williams, *et al.*, 1993). In suspension culture, *pka* null cells are unable to induce pre-spore cell differentiation in response to cAMP and express pre-stalk cell differentiation at very low levels.

The serine/threonine kinase, GSK3, is also required for spatial patterning and cell fate decisions in *D. discoideum* (Harwood, *et al.*, 1995). *gsk3* null cells preferentially differentiate into the basal disk at the expense of pre-spore cells. Recent studies indicate that GSK3 lies downstream from cAMP receptor, cAR3 (Plyte, *et al.*, 1999). In addition to being positively regulated by cAR3, GSK3 may be negatively regulated by cAR2 and cAR4 (Ginsburg and Kimmel, 1997). cAR2 is specially expressed in the pre-stalk cells, and *car2* null cells arrest at the mound stage and exhibit aberrant cell-type-specific gene expression. *car4* null cells complete development, but there is a delay at culmination and the slug and fruiting body are quite abnormal.

2.3.3. Subdivision of the multicellular structures

In *D. discoideum*, the cells in the mound, slug, and fruiting body can be

distinguished into different types on the basis of morphology and biochemical markers as mentioned above (Scheme 5).

Two principal classes of cells develop from the aggregate cells – pre-spore cells (psp) destined to become spores and pre-stalk cells (pst) destined to form stalks. About 80% of the cells in the aggregate will eventually become spores, the remaining 20% become the stalk and attachment/basal disc.

The pre-stalk cells can be divided into several distinct cell types:

1) pst A cells

   These occur at the tip of the mound and slug, occupying the anterior-most 1/3 of the pre-stalk region (accounting for 5-10% of the total cells). PstA cells have active promoters for the ecmA gene, since this gene encodes an extracellular matrix protein. These cells originally form in random positions in the very early mound but move to the tip during cell-sorting. PstA cells are capable of transdifferentiating into pstO cells.

2) pst O cells

   These occur in the anterior of the mound and slug behind the pstA cells, accounting for 5-15% of the cells. They also form originally in random positions within the mound. They are capable of undergoing transdifferentiation into either pstA cells or ALC cells.

3) pst B cells

   These initially form scattered around the mound but sort to the base in the slug and form the inner basal disc. They express the ecmB extracellular matrix gene.

4) pst AB cells

   These develop from pstA cells when these cells enter the stalk tube and

form a core inside the tip of the mound and slug. These cells express both ecmA and ecmB extracellular matrix genes and are destined to become stalk cells.

Non-pre-stalk cell types:

5) psp cells (pre-spore cells)

   These are destined to become spores, though they may transdifferentiate into ALC cells.

6) ALC (anterior-like cells)

   These are intermingled, as small groups, with psp cells and cluster to form the rearguard cells in the slug and culminant. One subtype of ALC cells are the pstO/ALC cells (ALC/pstO cells) which have active pstO-specific promoters and interchange with pstO cells in the pre-stalk. Other cell types include ALC/pstA, ALC/pstAB, ALC/pstB cells, according to the cells they most closely resemble biochemically. It appears that cell type is determined by position within the mound or slug and that cells crossing region boundaries may transform into the same type as their neighbors.

Other cell types:

7) Tip organizer cells

   These are pstA cells at the very tip. They possibly act as pacemaker cells by setting the frequency and direction of the cAMP waves that direct the other cells in the mound and slug.

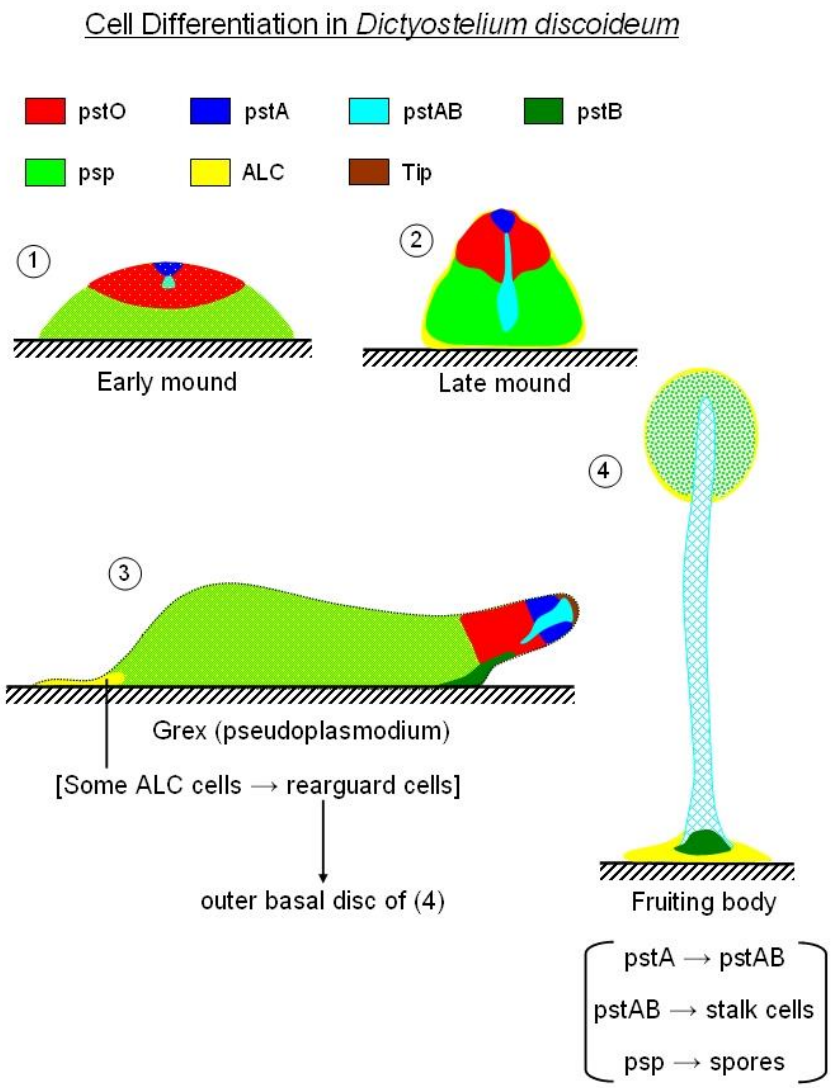

Scheme 5. Subdivision of cell-types in multicellular structures. In *D. discoideum*, the cells in the mound, slug, and fruiting body can be distinguished into different types on the basis of morphology and biochemical markers (http://cronodon.com/BioTech/Dictyostelium.html).

2.3.4. Terminal differentiation (Culmination)

During early development, the programming is built into the cells, however, during the final stage of development, terminal differentiation is rigorously controlled by signals from other cells, acting through cAMP and the receptor system to promote maturation of the precursor cells. During this process, which is known as culmination, slug stops migrating and rounds up, with the main body of pre-stalk cells on top and another group on the substratum. These bottom cells eventually form the basal disc of stalk cells that support to stabilize the fruiting body. Another pre-stalk cells on the top first lay down cellulose on the existing stalk tube, then enter into it, are vacuolated and die. The pre-spore cells are carried aloft by the growing stalk and mature quite shortly. Maturation proceeds in a wave from the boundary with the overlying pre-stalk tissue, which suggest a localized inductive signal (Richardson, *et al.*, 1994). A wide variety of experimental data indicates that culmination and terminal differentiation of stalk and spore depend on PKA. In addition, ammonia is producing as a by-product of protein catabolism within developing cells and a decrease in its concentration is necessary to trigger culmination (Davies, *et al.*, 1993). Also, the signals triggering the maturation of spore and stalk cells probably include the partially characterized peptide factors SDF1 and SDF2 (Anjard, *et al.*, 1998; Anjard, *et al.*, 1997). Both factors induce extremely rapid maturation of pre-spore cells in monolayer culture and SDF1 also stimulates stalk cell formation (Anjard, *et al.*, 1998).

3. Aims of this study

Glutathione (GSH, γ-glutamyl-L-cysteinylglycine) serves as a cell's reservoir of non-protein thiol and is a critical determinant of diverse cellular processes including cell proliferation, differentiation, and apoptosis (Aw, 2003; Jurgensen, *et al.*, 2001; Meister and Anderson, 1983). Since GSH plays important roles in redox regulation, detoxification, immune system, and cellular signaling (Ghezzi, 2011; Janaky, *et al.*, 1999; Ketterer, *et al.*, 1983; Meister and Anderson, 1983), the precise understanding of regulatory mechanism of GSH is particular.

In cell, GSH biosynthesis is accomplished by two ATP-dependent enzymatic reactions (Meister and Anderson, 1983). First, L-glutamic acid and L-cysteine are condensed by γ-glutamylcysteine synthetase (GCS) as the rate-limiting step. And then, glycine is added to the dipeptide by glutathione synthetase (GSS). Typically, GCS activity is feedback-inhibited by GSH (Meister and Anderson, 1983), which maintains cellular redox homeostasis. To date, our group have demonstrated that GSH is required for most of developmental stages of *D. discoideum* from onset (aggregation) to completion (fructification) (Choi, *et al.*, 2006; Kim, *et al.*, 2005; Kim, *et al.*, 2014). For instance, GCS null cells failed to develop and their developmental status was determined by exogenously added GSH levels (Kim, *et al.*, 2005). Moreover, GCS null cells showed pre-stalk cell bias in chimeras with WT cells, suggesting that GSH level influences cell fate (Kim, *et al.*, 2005). Recently, GSH action mechanism in the transition from growth to development through YakA signaling was discovered using GCS null cells (Kim, *et al.*, 2014; Souza, *et al.*, 1998). Meanwhile, it has been ignored the possibilities of regulatory mechanism through GSS, the final step enzyme in GSH biosynthesis, and its gene (*gshB*).

In this study, I suggest a novel mechanism by GSH in the up-regulation of cAR1-mediated cAMP signaling using *gshB* overexpressing (*gshB*^{oe}) cells. Since cAR1-mediated cAMP signaling is essential for chemotactic aggregation during early development and affects cell differentiation during terminal development as well in *D. discoideum*, the underlying mechanism of cAR1-mediated cAMP signaling has been investigated through genetic and molecular research. Thus, the findings shown in this study will provide new and unexpected insights of the relationship between GSH and cAMP signal transduction pathway, both which govern the development of *D. discoideum*. Especially, these results suggest the indispensable role of *gshB* in the modulation of G protein alpha 2 (Gα2) involved with cAR1-mediated cAMP signaling during development of *D. discoideum* for the first time.

II. MATERIALS AND METHODS

1. Chemicals used in this study

Enzymes used in DNA manipulations were purchased from Koscochem (Korea), Roche Molecular Biochemicals, or Promega Life Science. Nylon membrane, nitrocellulose membranes, and Rapid-Hyb buffer were purchased from GE Healthcare. G418 and GSH were obtained from Duchefa. cAMP Biotrak EIA System was purchased from Amersham Bioscience. Monobromobimane (mBBr), N-ethylmaleimide (NEM), methanesulfonic acid, methanol, trifluoroacetic acid (TFA), tetramethylrhodamine-5-(and 6)-isothiocyanate (TRITC)-conjugated phallodin and most of chemicals were purchased from Sigma-Aldrich. Blasticidin and 4-morpholinepropanesulfonic acid (MOPS) were purchased from ICN. All other chemicals used were of the highest quality generally available.

2. *D. discoideum* culture and development

Dictyostelium discoideum Wild type (WT) and mutant cells were grown axenically with shaking at 150 rpm and 22℃ in HL5 medium containing glucose (ForMedium, UK). To induce development, growing cells were harvested by centrifugation at 500 *g* for 5 min at 4℃ and washed twice with KK2 buffer (16.5 mM KH_2PO_4, 3.8mM K_2HPO_4, pH 6.2) at a density of 5×10^7 cells/ml and then deposited on 1.5% KK2 agar plates (Sussman, 1987). Cells on agar plates were incubated at 22℃ for the desired time.

For a quantitative sporulation assay, cells were cultured at a density of 1×10^8 cells/ml, allowed to develop for 2 days and then harvested. Spores were counted using a hemacytometer.

For the streaming assay, cells were resuspended at a low density of 2×10^5

cells/cm^2 in PBM (20 mM KH_2PO4, 1 mM $MgCl_2$, 0.01 mM $CaCl_2$, pH 6.1 with KOH) and developed on agar plates at 22℃ for 16 h in submerged monolayer culture. The images of cell streaming were taken with a Zeiss Axiovert 200M inverted microscope with a 20 × objective.

3. Generation of overexpression and/or knockdown strains

All primers used in this study are summarized in Table 2. The *Dictyostelium discoideum* KAx3 strain was used as the wild-type (WT) strain. All mutant strains were derived from WT cells. The generation of the *carA*-overexpressing cells (*carA*^{oe}) has been previously described in (Kim, *et al.*, 2014). To constitutively overexpress *gcsA*, *gshB* or *gα2* (*gcsA*^{oe}, *gshB*^{oe} or *gpaB*^{oe}, respectively) in *D. discoideum*, corresponding full-length gDNA strands were ligated into a pTX-FLAG vector. To generate the *gshB* knockdown strain (*gshB*^{as}), a full-length gDNA strand was inserted into a pTX-FLAG vector in the antisense orientation. Furthermore, to silence *gpaB* expression in both KAx3 and *gshB*^{oe} cells (*gpaB*^{as} and *gpaB*^{as}/*gshB*^{oe}, respectively), a full-length gDNA strand was inserted in the antisense orientation into the *Bam*HI/*Xho*I site of a pDBsrXP-green fluorescence protein (GFP) vector to delete a GFP fragment and avoid overlapping with a specific marker in the pTX-FLAG vector in *gshB*^{oe} cells. The resulting constructs were introduced by electroporation (Pang, *et al.*, 1999). Cells transformed with the pTX-FLAG or pDBsrXP vector were selected with 10 μg/ml G418 or blasticidin S, respectively.

Table 1. *E. coli* and *D. discoideum* strains used in this study

Strains	Genotype or description	Reference or sources
E. coli DH5α	*F-ΔlacU169(f80lacZDM15)endA1 rec1hsdR17 deoR supE44 thi-1 λ-avrA96 elA1*	Hanahan, 1983
KAx3	Axenic wild-type strain	Firtel, 1997
gcsA^{oe}	KAx3:[pTX FLAG-*gcsA*], neo^{r} GCS-expressing KAx3	This study
gshB^{oe}	KAx3:[pTX FLAG-*gshB*], neo^{r} GSS-expressing KAx3	This study
gshB^{as}	KAx3:[pTX FLAG-*gshB* antisense], neo^{r} GSS-knockdown KAx3	This study
carA^{oe}	KAx3:[EXP4(+)-*carA*], neo^{r} cAR1-expressing KAx3	Kim, 2014
gpaB^{oe}	KAx3:[pTX FLAG-*gα2*], neo^{r} Gα2-expressing KAx3	This study
gpaB^{as}/KAx3	KAx3:[pDBsrXP-*gα2* antisense], neo^{r} Gα2-knockdown KAx3	This study
gpaB^{as}/*gshB*^{oe}	GSS^{OE}:[pDBsrXP-*gα2* antisense], neo^{r} Gα2-knockdown *gshB*^{oe}	This study
Gα2-GFP/KAx3	KAx3:[pDBsrXP-gα2-GFP], bs^{r} Gα2-GFP expressing KAx3	This study
Gα2-GFP/*gshB*^{oe}	GSS^{OE}:[pDBsrXP-gα2-GFP], bs^{r} Gα2-GFP expressing *gshB*^{oe}	This study

Table 2. Plasmids and constructs used in this study

Plasmids	Description	References or sources
pGEM-Teasy	PCR cloning vector	Promega
Exp4(+)	Expression vector for *Dictyostelium*	Firtel, 1997
pTX-FLAG	FLAG-tagged protein expression vector	Egelhoff. 2000
pDBsrXP-GFP	GFP-tagged protein expression vector	Wolfgang Nellen, 2010
pGEM-Teasy-*gshB*	pGEM-Teasy vector containing *gshB* ORF	This study
pGEM-Teasy-*gpaB*	pGEM-Teasy vector containing *gpaB* ORF	This study
pTX-FLAG-*gshB*	pTX-FLAG vector fused with *gshB* ORF in frame	This study
pTX-FLAG-*gpaB*	pTX-FLAG vector fused with *gpaB* ORF in frame	This study
pTX-FLAG-$gshB^{as}$	pTX-FLAG vector fused with *gshB* ORF in antisense	This study
pDBsrXP-$gpaB^{as}$	pDBsrXP vector fused with *gpaB* ORF in antisense	This study
pDBsrXP-Gα2-GFP	pDBsrXP vector fused with *gα2*-GFP	This study

4. RNA extraction and northern blot analysis

Total RNA was isolated by using TRIzol reagent (Invitrogen) according to the manufacturer's instructions and solubilized in formamide (Sigma-Aldrich) (Feinberg and Vogelstein, 1983). For northern blot analysis, the RNA (20 μg) samples were separated using gel electrophoresis in a 1% agarose gel containing 0.22 M formaldehyde (Sigma-Aldrich) and then transferred to Hybond-N+ nylon membrane (GE Healthcare). Probes were generated by PCR and labeled with [α-^{32}P]-dATP. The used oligonucleotide sequences are described in Table S1. The blot was pre-hybridized in Rapid-Hyb buffer (GE Healthcare) for 1h and then hybridized with probe for 2h. The blot was washed twice with SSC buffer (0.1% SDS, 0.3M NaCl, 30 mM trisodium citrate) for 5 min at 65℃. The signal was visualized using a BAS-2500 scanner (Fujifilm).

5. Measurement of intracellular GSH level

Intracellular GSH concentration was determined according to a method described by Newton and Fahey with some modifications (Newton and Fahey, 1995). Prepared cells were extracted and reacted with 50% aqueous acetonitrile containing 50 mM HEPES (pH 8.0), 2 mM EDTA and 2 mM monobromobimane (mBBr). After incubation at 60℃ for 15 min, the samples were acidified with 5 μl of 5 N methanesulfonic acid. Cell debris was removed from the crude extract by centrifugation and the resulting supernatant (10 μl) was injected into an HPLC column (ZORBAX SB-C18 column). Control sample was treated with 5 mM N-ethylmaleimide (NEM) and incubated at 50℃ for 10 min prior to the derivation to protect thiol group from being labelled with mBBr. HPLC was performed using a Waters system equipped with a Hewlett-Packard 1050 series fluorescence

detector. Thiol compounds derived from mBBR was detected with excitation and emission at 370 and 480 nm, respectively. The mobile phase consisted of buffer A (methanol, HPLC grade) and buffer B (0.1% trifluoroacetic acid). The proportion of buffer A in the continuous gradients was as follows; 15% at 0 - 2 min, 25% at 30 min, 100% at 34 min, 15% at 37 min and 15% at 40 min.

6. F-actin staining assay

For an F-actin staining assay, cells were washed twice with PBM buffer (20 mM KH_2PO_4, 10 μM $CaCl_2$, 1 mM $MgCl_2$, pH 6.1 with KOH) and then starved for 5 - 6 h. Cells were fixed (3.7% formaldehyde in PBS for 5 min) and permeabilized (0.5 % Triton X-100 in PBS). After then, cells were stained with 3 μg/ml of tetramethylrhodamine B isothiocyanate-phalloidin (TRITC-phalloidin) for 1 h in the dark. F-actin distribution images were captured with a Zeiss Axiovert 200M inverted microscope with a 40 × objective.

An *In vivo* F-actin polymerization was performed as previously described in (Zigmond, *et al.*, 1997), with some adjustments. A total of 1×10^7 cells was starved on KK2 plate for 5-6 h. Cells were collected and resuspended to 2 ml PBM. After cells were stimulated with 1 μM cAMP, 100 μl samples were collected at 0, 5, 10, 20, 30, 50, 80, 100 and 150 s and mixed with 500 μl of actin fixative buffer (10 mM PIPES pH 6.8, 20 mM KH_2PO_4, 5 mM EGTA, 0.5% Triton X-100, 3.7% formaldehyde, 2 μg/ml TRITC-Phalloidin). The samples were incubated for 1 h in dark and centrifuged at 1300 rpm for 10 min at 4℃. Pellet cells were extracted with 1 ml of methanol and incubated at 4℃ overnight on a rotatory shaker. Fluorescence was measured in 540ex/575em.

7. Neutral red and histochemical staining

For neutral red staining, exponentially growing cells were collected, washed twice in KK2 buffer and resuspended at a density of 1×10^7 cells/ml. Cells were stained with KK2 buffer containing 0.03% neutral red for 5 min at RT. The stained cells were allowed to develop in the dark and photographed with an Axiolab microscope (Zeiss).

To observe the pre-spore cell region during cell differentiation, *pspA/lacZ* constructs were introduced into KAx3 or mutant cells. The cells were allowed to develop on nitrocellulose filters. Developing structures were fixed with Z buffer (60 mM Na_2HPO_4, 40 mM $NaHPO_4$, 10 mM KCl, 1mM $MgSO_4$, 2 mM $MgCl_2$) containing 1% glutaraldehyde and permeabilized with Z buffer having 0.1% NP40. After washing twice with Z buffer, cells stained with X-gal, as previously described in (Dingermann, *et al.*, 1989).

To quantitate different cell types (pre-spore or pre-stalk cells), aggregates developing on agar plates were dissociated in buffer (20 mM Na_2HPO_4/KH_2PO_4, 20 mM EDTA, pH 7.0). Dissociated cells were fixed and resuspended at a density of 1×10^7 cells/ml in staining solution. After incubation, the number of stained cells was counted by using a hemacytometer.

8. Quantitative RT-PCR

cDNA was synthesized from 1 µg of total RNA using a superscript III reverse transcriptase kit (Promega, USA). One microliter of cDNA was used as template for qRT-PCRs in a 20 µL reaction using SYBR Premix Ex Taq (TaKaRa, Japan) and *rnlA* was used as a control. Fluorescence was detected on an Applied Biosystems 7500 (Applied Biosystems, USA) real-time PCR system, The qRT-

PCR samples for each gene at indicated time point were done in triplicate and cycle threshold values generated were averaged. All the qRT-PCR data were analyzed as described in (Schmittgen, *et al*., 2008).

9. Measurement of intracellular cAMP level

To measure intracellular cAMP levels during early development, vegetative cells were washed twice with KK2 buffer, resuspended in KK2 buffer at a density of 1×10^7 cells/ml and shaken at 150 rpm at 22℃. After 2 h of development, cAMP stimulation was performed by the adding of 30 nM cAMP every 6 min for 4 h, followed by the addition of 300 μM cAMP after 2 h. Pulsed cells were centrifuged at 500 g for 5 min at 4℃ and resuspended at a density of 1×10^7 cells/ml. A total of 100 μl of the suspension was added to 100 μl of 3.5 % perchloric acid. After neutralization with 50 μl of 50% saturated $KHCO_3$, cellular cAMP content was measured using a cAMP Biotrak EIA System (Amersham Bioscience, UK).

10. GFP fluorescence microscopy

For Gα2-GFP fusion expression, full-length *gpaB* gDNA was inserted into the C-terminal cloning site of a pDBsrXP-GFP vector. The resulting constructs were into KAx3 and *gshB*^{oe} cells by electroporation. To monitor the localization of Gα2-GFP responses to cAMP stimulation, the cells were developed until they reached the chemotaxis-competent stage by providing exogenous pulses of 30 nM cAMP at 6 min intervals in KK2 as previously described (Janetopoulos, *et al.*, 2001). The pulsed cells were then applied to glass coverslips and observed for 30 s after 1 μl cAMP stimulation. Fluorescence was visualized with a Zeiss

LSM700 confocal fluorescence microscope using a 100 × oil immersion objective.

11. Cell fate choice

To examine the cell fate determination of GFP-labeled strains, each strain was transformed with a pDbsrXP-GFP vector and allowed to develop in chimera. For chimeric development, the GFP-marked cells were mixed with unmarked KAx3 cells at a 1:3 ratio at a final density of 5×10^7 cells/ml, and incubated the mixtures for 16 h in the dark. Microscopy was performed using Zeiss Axiovert 200M inverted microscope with a 10 × objective.

III. RESULTS

1. Effects of intracellular GSH level on development of *D. discoideum*

1. 1. Generation of mutant cells having high or low GSH contents in *D. discoideum*

To elucidate regulatory mechanisms of GSH, which affects development in *D. discoideum*, two genes sequentially encoding GSH biosynthesis enzymes; i.e., *gcsA* (GCS) and *gshB* (GSS), were overexpressed in KAx3 cells using the actin promoter ($gcsA^{oe}$ and $gshB^{oe}$, respectively), and *gshB* was knocked down using antisense RNA inhibition ($gshB^{as}$; Fig. 1.1. A - C). At starvation (0 h), the levels of GSH in $gcsA^{oe}$ and $gshB^{oe}$ cells were increased by approximately 18% and 21%, respectively, compared to KAx3 cells, whereas the GSH level in $gshB^{as}$ cells was decreased by approximately 29% (Fig. 1.2.). However, at 16 h after starvation, no significant differences were observed in the GSH levels of $gcsA^{oe}$ and $gshB^{as}$ cells compared to those of KAx3 cells. It was found that there is an approximate twofold increase in GSH content in only $gshB^{oe}$ cells. Therefore, the possibility that *gshB* expression increases *gcsA* expression was examined. Northern blot analysis showed that *gshB* expression and *gcsA* expression did not affect each other (Fig. 1.1.D). These results suggest that *gshB* overexpression increases intracellular GSH levels in both the early and late development of *D. discoideum*, regardless of *gcsA* expression.

1. 2. An increase of intracellular GSH level inhibits *Dictyostelium* development

Next, the effect of intracellular GSH levels on developmental morphology was examined by using the mutant cells (Fig. 1.3.A). $gcsA^{oe}$ cells exhibited a delay

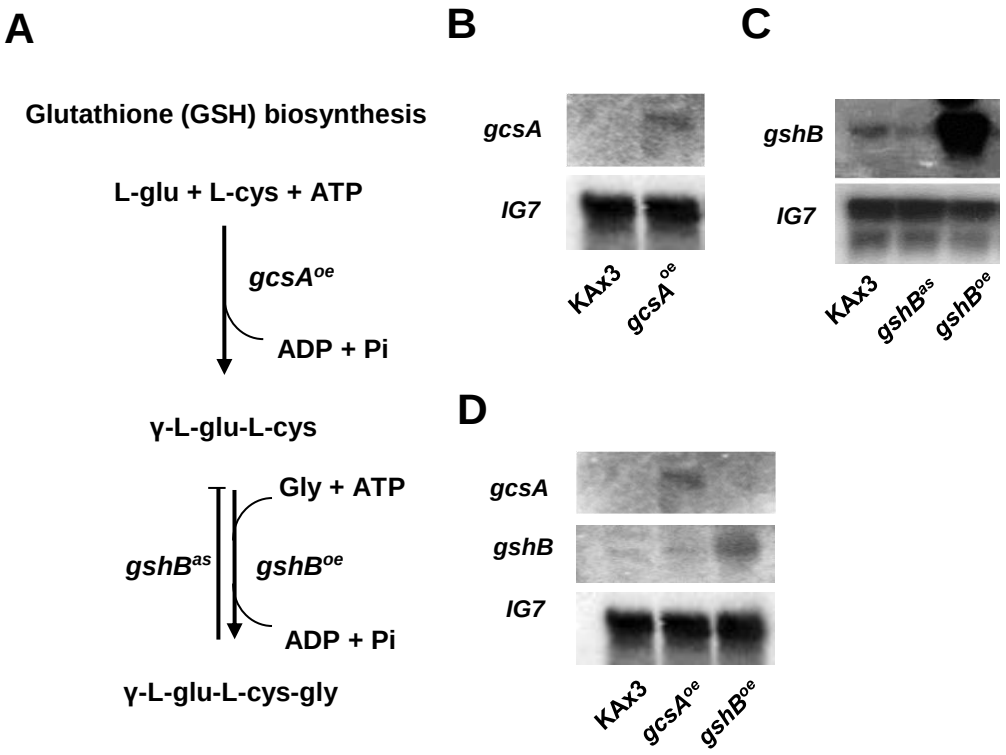

Fig. 1.1. Generation of *gcsA*^{oe}, *gshB*^{oe}, and *gshB*^{as} mutant cells. (A) A model showing production of mutant cells for the modulation of GSH biosynthesis. Confirmation of the production of *gcsA*^{oe}, *gshB*^{oe}, and *gshB*^{as} mutant strains in *D. discoideum*. The productions of *gcsA*^{oe} (B), *gshB*^{as} and *gshB*^{oe} (C) mutants were confirmed by northern blot analysis. (D) Analysis of *gcsA* and *gshB* expression level in *gcsA*^{oe} and *gshB*^{oe} cells. The overexpression of *gcsA* and *gshB* does not affect the transcript levels of each other. *gcsA*, γ-glutamylcysteine synthetase (GCS); *gshB*, encoding GSH synthetase (GSS); *IG7*, a loading control.

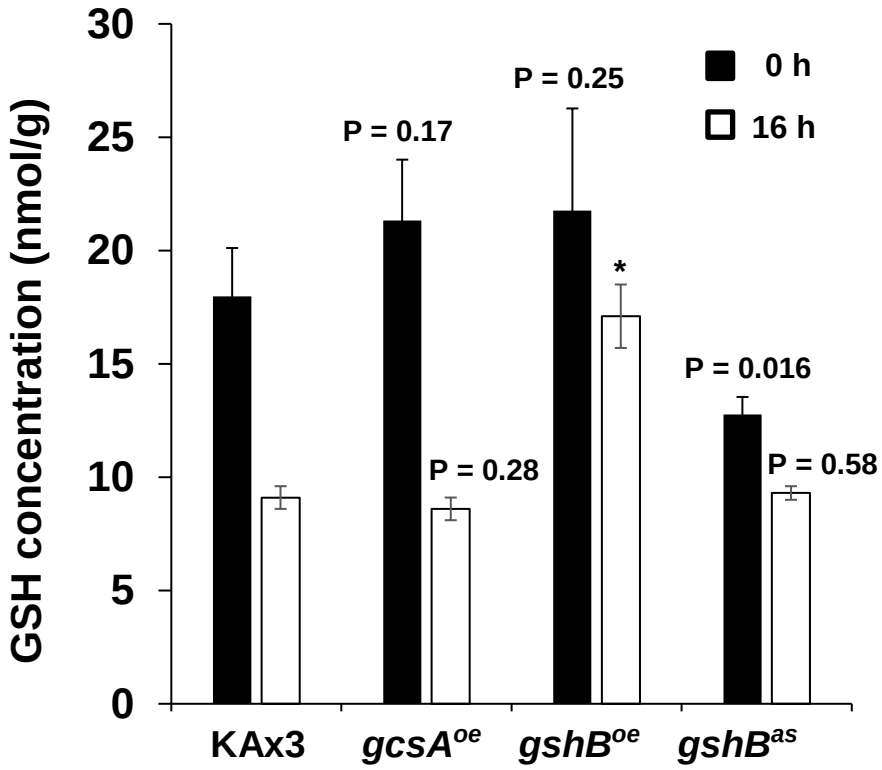

Fig. 1.2. Intracellular GSH concentrations in KAx3, *gcsA*^{oe}, *gshB*^{oe}, and *gshB*^{as} cells. Cells were harvested at two different stages during development (at 0 h and 16 h after starvation). *gshB*^{oe} cells have high GSH levels both in early and late development. Data represent the means and SEM of at least three independent experiments. *$P < 0.001$, Student's *t*-test.

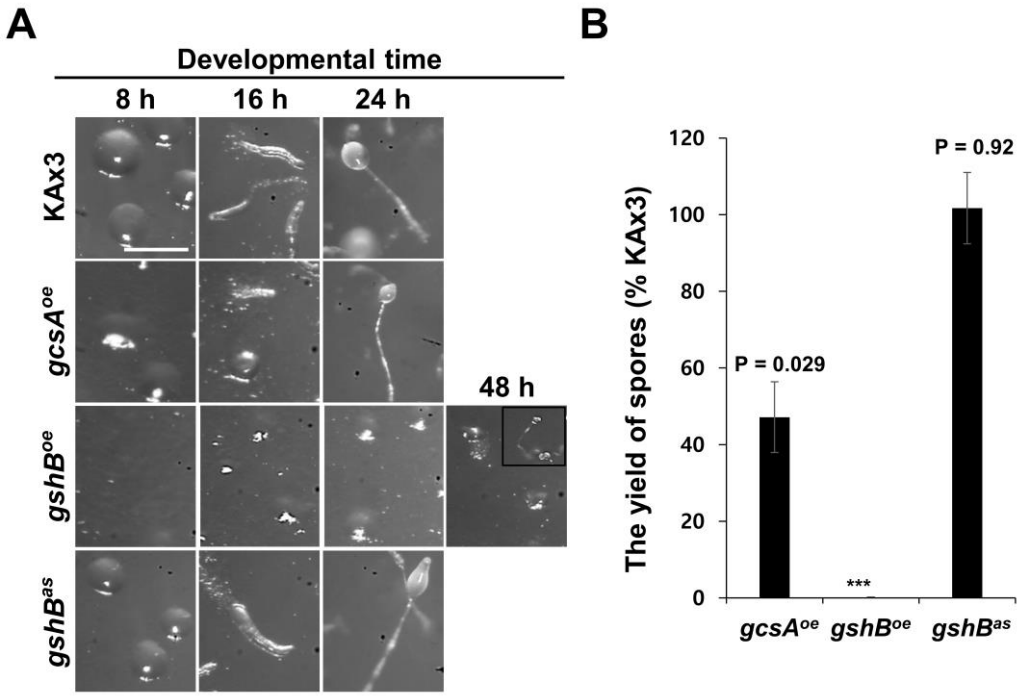

Fig. 1.3. Effects of intracellular GSH levels on developmental morphology. (A) Effects of high levels of GSH on developmental morphology. Cells were developed on nonnutrient agar and photographed at the indicated times. Most of *gshB*^{oe} cells were arrested at the mound stage by 48 h. (Scale bar: 0.5 mm.) (B) Effects of high levels of GSH on sporulation. *gshB*^{oe} cells showed severe defects in spore formation. Data represent the means and SEM of at least three independent experiments. ***$P < 0.0001$, Student's *t*-test.

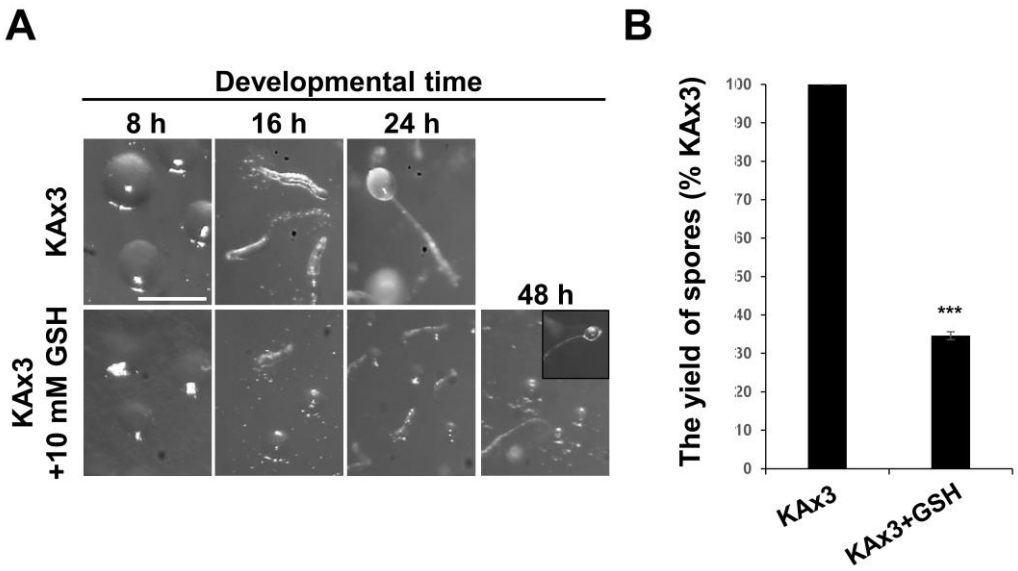

Fig. 1.4. High level of GSH inhibits normal multicellular development. (A) Developmental morphology of KAx3 cells pre-cultured with exogenously added 10 mM GSH. Cells were starved on nonnutrient agar and photographed at the indicated times. 10 mM GSH-treated KAx3 cells show the delayed development by 48 h. (Scale bar: 0.5 mm.) (B) Spore formation of 10 mM GSH-treated KAx3 cells. The spore yield of KAx3 cells treated with 10 mM of exogenous GSH is significantly decreased by 66 % relative to untreated KAx3 cells. Data represent the means and SEM of at least three independent experiments. ***$P < 0.0001$, Student's *t*-test.

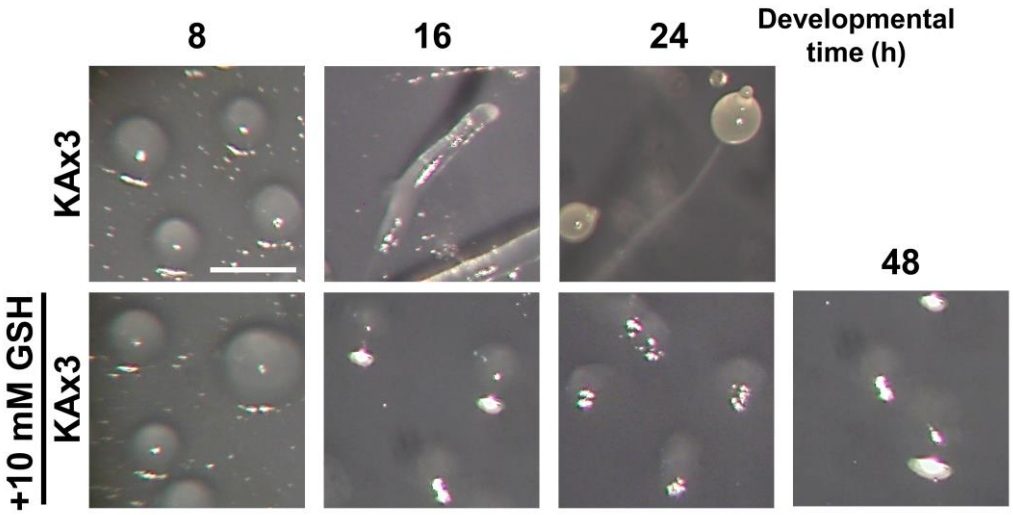

Fig. 1.5. The excess of GSH inhibits development after mound formation. KAx3 cells were allowed to develop on a nitrocellulose filter until the mound stage, and the filter was transferred to agar plate containing 10 mM GSH. (Scale bar: 0.3 mm.)

in aggregation and slug formation, although they formed a mature fruiting body, whereas *gshB*^{as} cells normally developed from tight aggregates (8 h), into slugs (16 h) and fruiting bodies (24 h). In addition, most of the *gshB*^{oe} cells showed severe developmental defects and were arrested at the mound stage up to 48 h. Spore formation was significantly decreased in *gcsA*^{oe} and *gshB*^{oe} cells by 53% and 99.82% compared to the KAx3 cells, respectively (Fig. 1.3.B). Moreover, in KAx3 cells, addition of 10 mM GSH led to the defects, such as the developmental delays and the reduced spore formation (by 66% compared to KAx3 cells), which were similar to those characteristic of *gcsA*^{oe} and *gshB*^{oe} cells (Fig. 1.4. A and B). Therefore, to test whether the excess GSH still inhibits developmental processes after mound formation, KAx3 cells were allowed to develop until the tight aggregate stage (mound stage) on a nitrocellulose filter, and then the filter was transferred to agar plate containing 10 mM GSH. As the results, the development was completely blocked and the cells remained as loose aggregates for a prolonged period (Fig. 1.5). These results indicate that excessive increases in GSH levels inhibit normal development in *Dictyostelium*, implying that regulation of intracellular GSH concentration is mightily important in *Dictyostelium* development.

2. Developmental properties of *gshB*^{oe} cells

2. 1. Effects of high GSH level on aggregation processes

To obtain detailed information about the effects of increased GSH levels on both early and late stages of development in *D. discoideum*, I focused on the physiological phenotype of *gshB*^{oe} cells. First, the chemotactic aggregation of developing cells at a low cell density of 2×10^5 (cells/cm^2) in submerged culture was examined. KAx3 cells formed an elongated stream moving towards the

aggregation center in a head-to-tail manner, whereas *gshB*^{oe} cells were not able to form aggregates and streams (Fig. 2.1.A). The organization of the actin cytoskeleton in chemotactic responses to cAMP is important in stream formation during aggregation stage (Chen, *et al.*, 2003). At 5–6 h after the onset of starvation, KAx3 cells were well-polarized and exhibited a strong F-actin assembly at the leading edge, as well as assembly at the posterior zone. However, *gshB*^{oe} cells exhibited multiple pseudopodia, indicating a lack of axial polarity (Fig. 2.1.B and Fig. 2.2. A and B). To understand the polarity of *gshB*^{oe} cells in more detail, an *in vivo* F-actin polymerization in response to cAMP stimulation was tested in KAx3 and *gshB*^{oe} cells (Fig. 2.3.A). In KAx3 cells, F-actin levels were rapidly increased 1.5-fold within approximately 10 s after cAMP stimulation, whereas *gshB*^{oe} cells exhibited a 1.3-fold increase in their F-actin levels within 10 s after cAMP stimulation, followed by two additional peaks (at 20 and 100 s, respectively), indicating that *gshB*^{oe} cells had the abnormal fluctuating pattern in F-actin polymerization. The average level of F-actin did not show significantly differences between KAx3 and *gshB*^{oe} cells (Fig. 2.3.B).

Regarding *Dictyostelium* development, it has previously been reported that developmental cell fate is dependent on the growth conditions (Gomer and Firtel, 1987). Therefore, the chemotactic aggregation of *gcsA*^{oe} and *gshB*^{as} cells having higher and lower GSH levels at the initiation of starvation was also investigated. When cells were allowed to develop at a low cell density, *gcsA*^{oe} cells exhibited increased pseudopodia and they did not form cell streaming as *gshB*^{oe} cells did. However, *gshB*^{as} cells produced cell streaming and showed normal cell polarity (Fig. 2.1. and Fig. 2.2.).

2. 2. Effects of high GSH level on cell differentiation

The coordinated cell movement driven by cAMP signaling also plays important roles in morphogenesis and cell differentiation during *Dictyostelium* development (Bretschneider, *et al.*, 1997; Chisholm and Firtel, 2004; Dormann, *et al.*, 1998; Rietdorf, *et al.*, 1996). Therefore, cell-type proportioning and pattern formation in *gshB*^{oe} cells were investigated. Generally, cell differentiation can be apparently observed in a slug comprised of the anterior pre-stalk cells and the posterior pre-spore cells (Fig. 2.4. A and B.). In particular, pre-stalk cells are sorted at the apex of the mound before the formation of the slug tip (Traynor, *et al.*, 1992). Because *gshB*^{oe} cells were arrested at the mound stage as described above (Fig 1.3.A), cell-type proportioning in the mound of KAx3 and *gshB*^{oe} cells was examined. In KAx3 mounds, pre-stalk cells were localized at the apex (Fig. 2.4.A. *white box in top*), whereas in *gshB*^{oe} mounds, pre-stalk cells were scattered, and their expression seemed to be increased than those in KAx3 cells (Fig. 2.4.A.). Whereas, the pre-spore cells in *gshB*^{oe} mounds were scarcely detectable (Fig. 2.4.B). The expression patterns of developmental-specific marker genes in *gshB*^{oe} cells revealed these phenotypic defects, such as a delay of aggregation (*cadA*, *csaA*, and *lagC*), an increased expression of a pre-stalk-specific gene (*ecmA* but not *ecmB*) and little or no expression of pre-spore-specific genes (*pspA*, and *cotC*; Fig. 2.5.).

The intracellular GSH levels at the transition from growth to starvation also influences cell-type differentiation during late development (Fig. 1.2.). The slugs of *gcsA*^{oe} cells displayed enlarged pre-stalk regions and smaller pre-spore regions, as the mound of *gshB*^{oe} cells did. In contrast, the slugs of *gshB*^{as} cells were comprised smaller pre-stalk regions and larger pre-spore regions (Fig. 2.4. A and B).

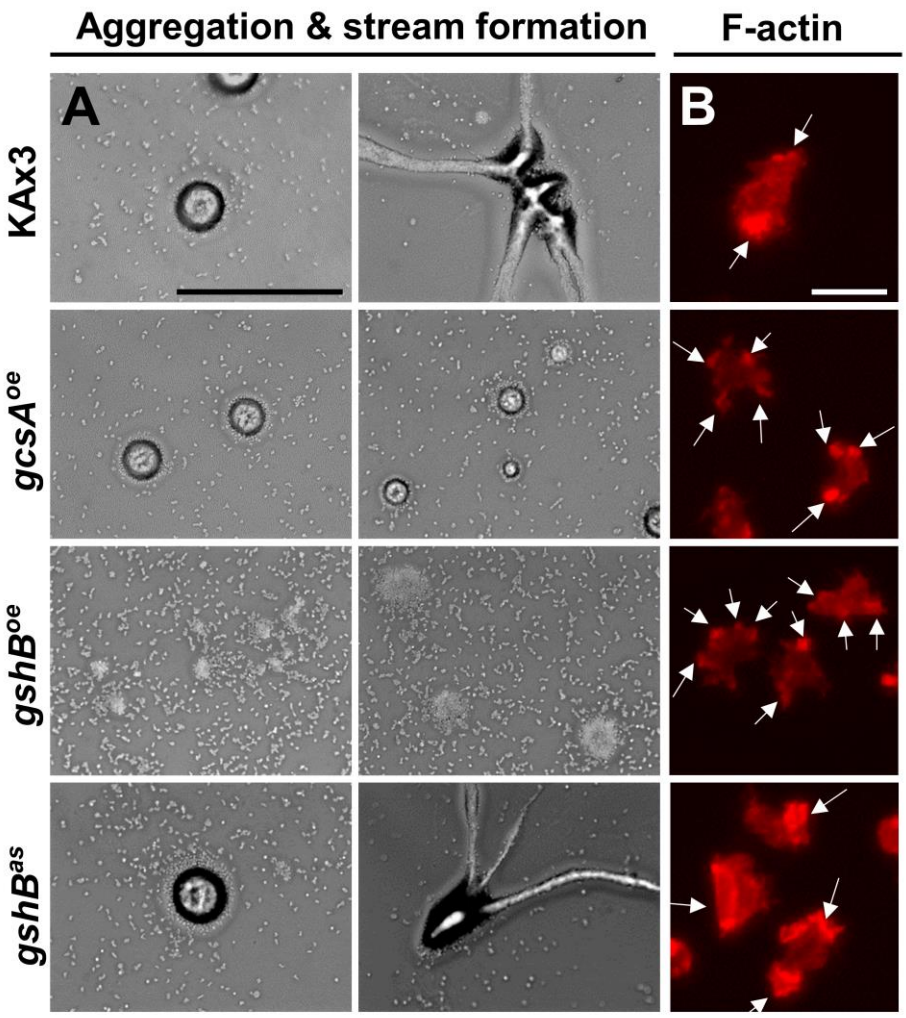

Fig. 2.1. The phenotypes of KAx3, *gcsA*^{oe}, *gshB*^{oe}, and *gshB*^{as} cells during early development. Aggregation and stream formation (A) and cell polarity (B**)** in KAx3, *gcsA*^{oe}, *gshB*^{oe}, and *gshB*^{as} cells during early development. The arrows in *B* indicate the F-actin based pseudopod. (Scale bars: 0.5 mm in A, 10 μm in B.)

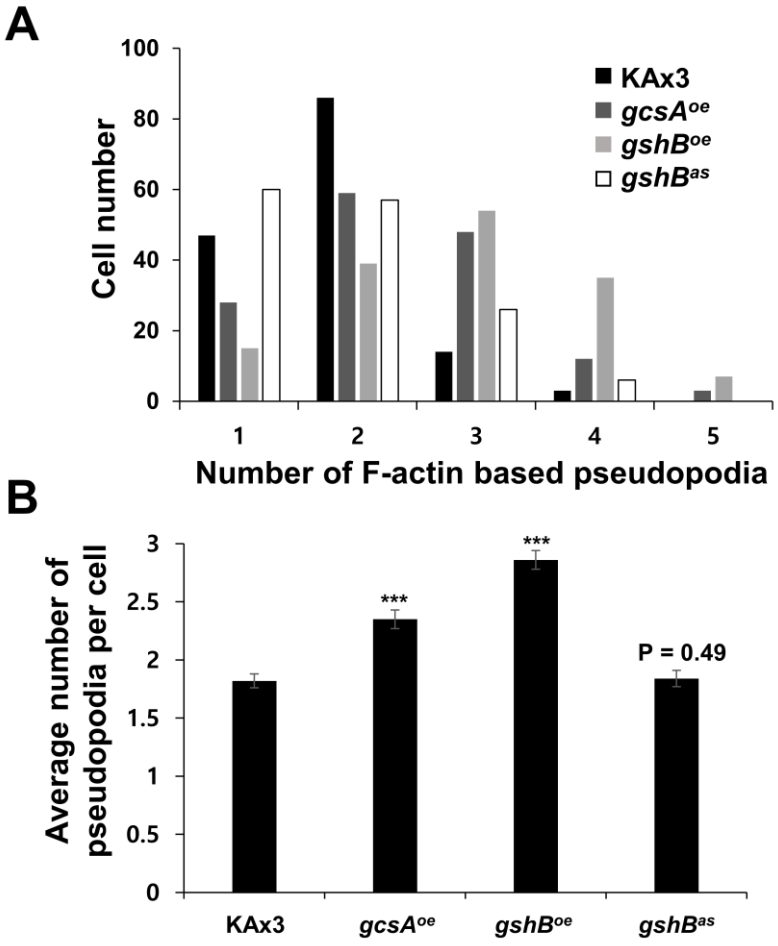

Fig. 2.2. Analysis of F-actin based pseudopodia formation in KAx3, *gcsA*^{oe}, *gshB*^{oe}, and *gshB*^{as} cells during aggregation. (A and B) The average numbers of F-actin based pseudopodia per cell were measured by counting from at least 150 cells. ***$P < 0.0001$, Student's *t*-test.

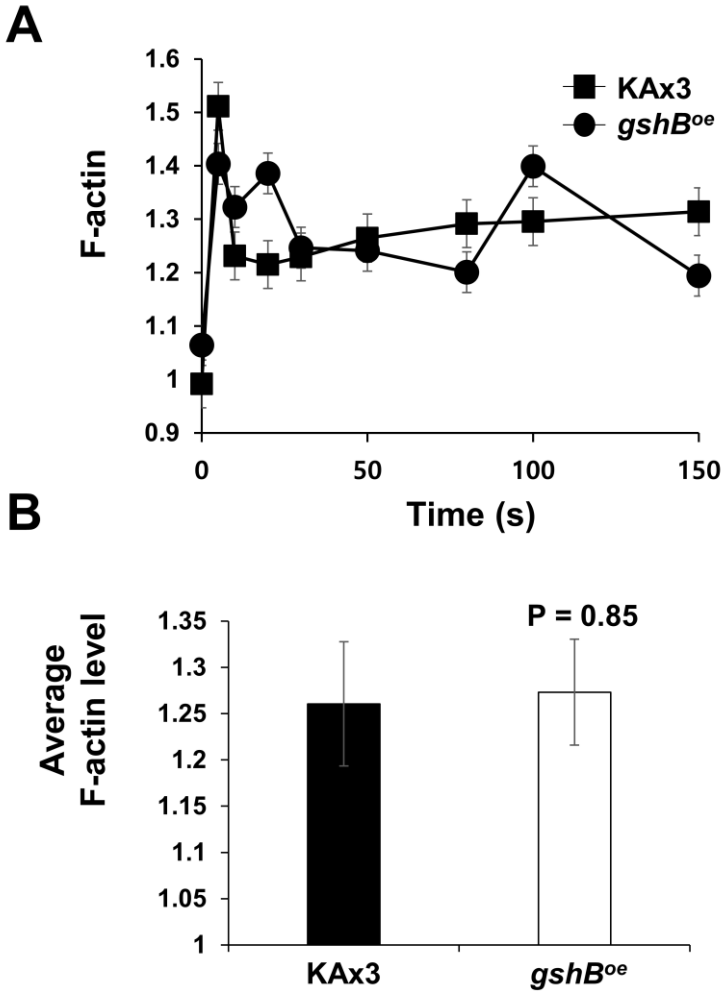

Fig. 2.3. *In vivo* F-actin polymerization assay in response to cAMP in KAx3 and *gshB*^{oe} cells. F-actin polymerization (A) and the average level of F-actin (B) in KAx3 and *gshB*^{oe} cells during early development. Error bars in A and B represent SEM calculated from at least three independent experiments, using Student's *t*-test.

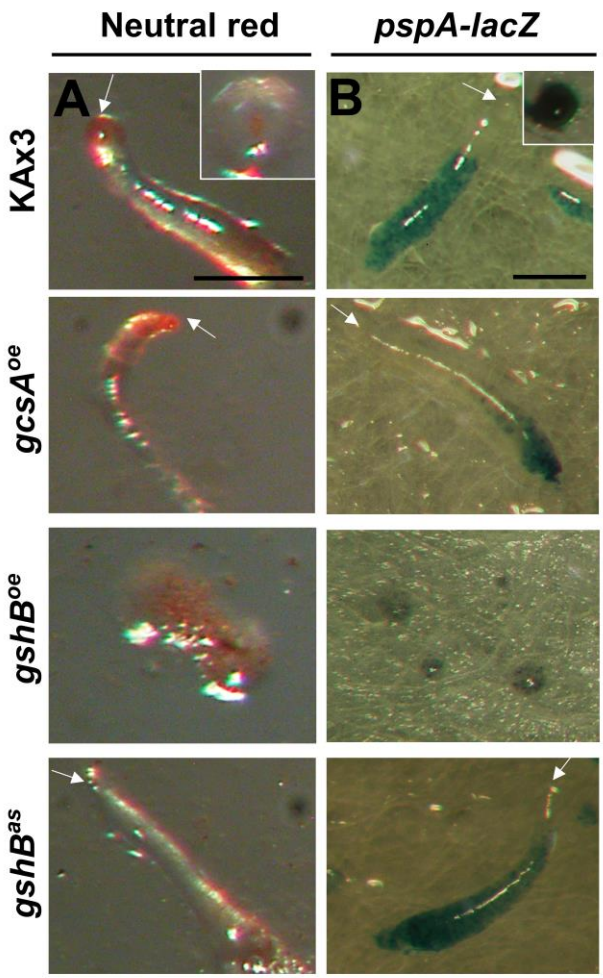

Fig. 2.4. Cell differentiation in KAx3, *gcsA*^{oe}, *gshB*^{oe}, and *gshB*^{as} slug or mound during late development. Cells were stained with neutral red, a vital dye which specifically stains pre-stalk cells, and then developed (A), or cells expressing pspA specific markers were developed, fixed and stained for lacZ β-galactosidase activity (B). (Scale bars: 0.5 mm in A and B.)

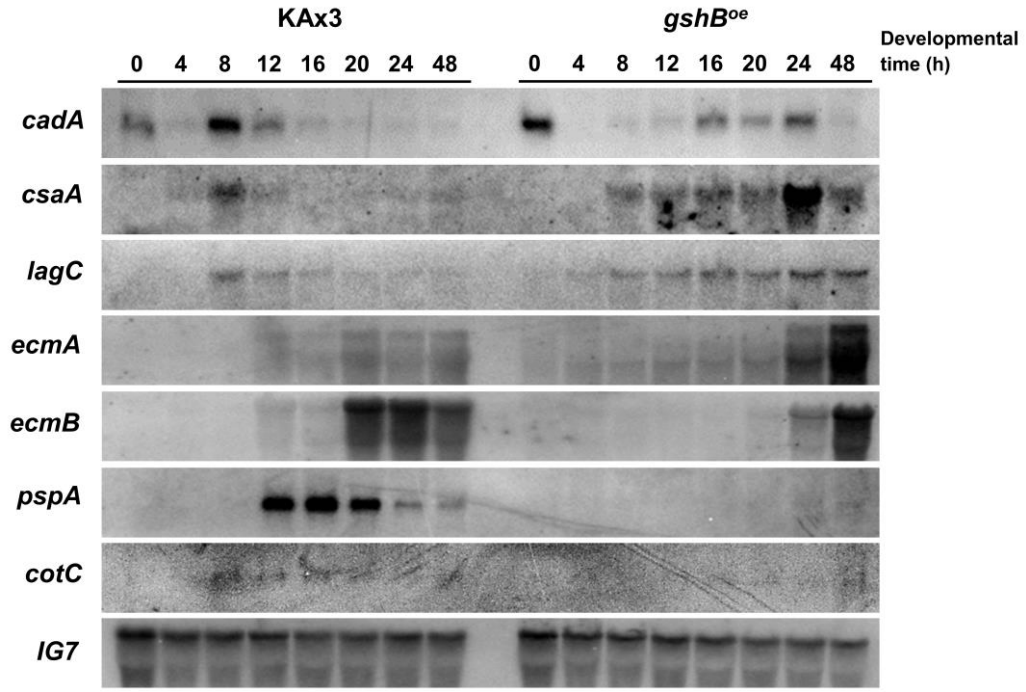

Fig. 2.5. The mRNA expression patterns of the developmental markers in KAx3 and *gshB*^{oe} cells. KAx3 and *gshB*^{oe} cells were allowed to develop on non-nutrient KK_2 plates and were harvested at the indicated times during development. Northern blots were performed using fragments of the indicated developmental marker genes as hybridization probes. *cadA* and *csaA*, aggregation-specific; *lagC*, post-aggregative-specific; *ecmA* and *ecmB*, pre-stalk-specific; *pspA* and *cotC*, pre-spore-specific genes; *IG7*, a loading control.

2. 3. Effects of high GSH level on the regulation of cAR1-mediated cAMP signaling

Based on these results, we determined the expression pattern of the essential components of the cAMP signaling pathway (*carA*/cAR1/cAMP receptor 1, *gpaB*/Gα2/G protein alpha subunit 2, *gpbA*/Gβ/G protein beta subunit and *acaA*/ACA/adenylyl cyclase A), which are developmental regulators (Parent and Devreotes, 1996). In *gshB*^{oe} cells, the expression level of *carA* and *gpaB* was upregulated after starvation and showed significant increases relative to that in KAx3 cells, especially after 8 h of development (Fig. 2.6). Similarly, the expression levels of *gpbA* and *acaA* were upregulated for 4-20 h of development. Because *gshB*^{oe} cells showed increased expression levels of genes related to cAMP signaling, the intracellular cAMP levels during early development were also measured. In *gshB*^{oe} cells, the intracellular cAMP concentrations were approximately 4.5-fold higher than those of KAx3 cells at 8 h after the onset of development, which was consistent with the expression patterns of *carA* and *gpaB* (Fig. 2.7). When cells are deposited on non-nutrient agar, KAx3 cells exhibit chemotactic behavior in response to cAMP and initiate aggregation after 6-8 h of development (Parent and Devreotes, 1996). Therefore, the above results (Fig. 2.6. and Fig. 2.7.) suggest that the intracellular GSH concentration induced by *gshB* overexpression caused an abnormal increase in the intracellular cAMP content, leading to deficiencies in cAMP-mediated aggregation, stream formation and F-actin polymerization.

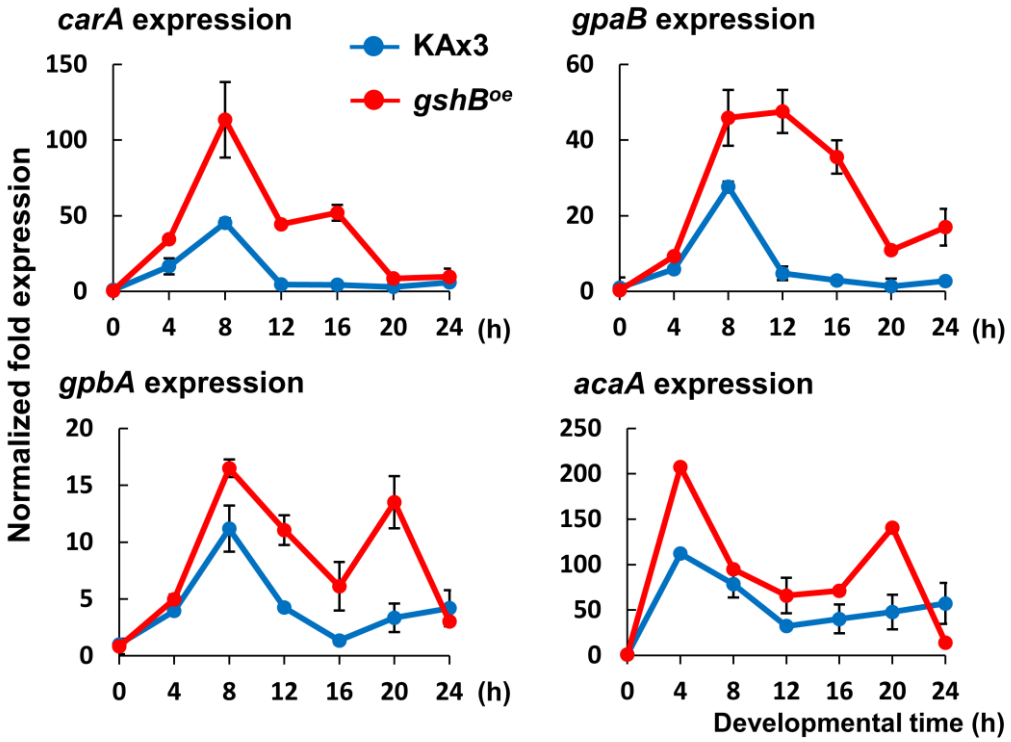

Fig. 2.6. Transcriptional regulation of key components related to cAMP signaling pathway in *gshB*^{oe} cells. *carA*, cAMP receptor 1 (cAR1); *gα2*, G-protein alpha 2 (Gα2); *gβ*, G-protein beta (Gβ); *acaA*, adenylyl cyclase A (ACA); *carB*, cAMP receptor 2 (cAR2); *acgA*, adenylyl cyclase G of germination stage (ACG). *rnlA* was used as a control. Error bars represent SEMs calculated from at least three independent experiments using Student's *t*-test.

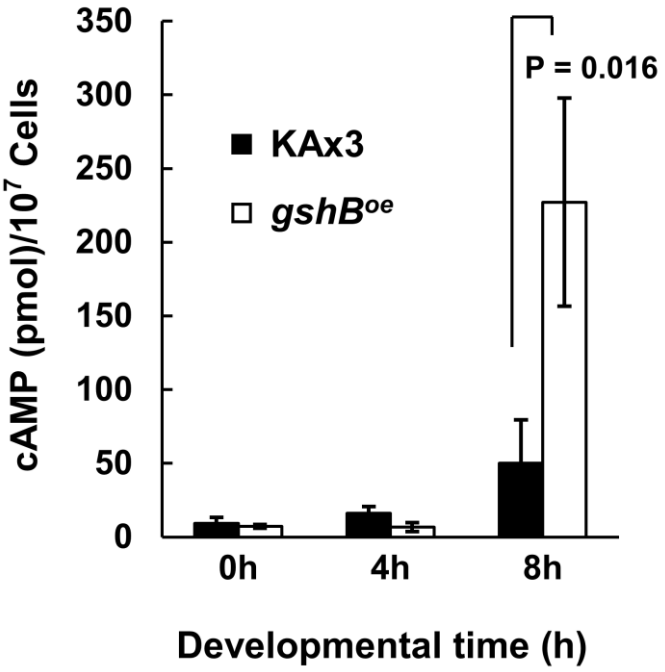

Fig. 2.7. Intracellular cAMP levels in *gshB*^{oe} cells during early development. At 8 h after the onset of starvation, cAMP levels in *gshB*^{oe} cells were significantly increased (approximately 4.5-fold greater than those in KAx3 cells). Error bars represent SEMs calculated from at least three independent experiments using Student's *t*-test.

3. The role of *gshB* overexpression in the regulation of *gpaB* expression

3. 1. Developmental properties of *gpaB*^{oe} cells

To investigate which step(s) of cAR1-mediated cAMP signaling cause the defective phenotype of *gshB*^{oe} cells, *carA* and *gα2*, encoding upstream components for cAMP detection and cAMP biosynthesis respectively, were constitutively expressed (Kim, *et al.*, 2014) (Fig. 3.1.A). The effects of each overexpression on developmental morphology were distinguishable. *carA*-overexpressing cells (*carA*^{oe}) developed normally into fruiting bodies, but *gpaB*-overexpressing cells (*gpaB*^{oe}) displayed similar phenotypic defects to those of *gshB*^{oe} cells. *gpaB*^{oe} cells displayed a mound-arrest phenotype and failed to produce spores (0.85% of KAx3 cells; Fig. 3.1. B and C). In addition, the intracellular cAMP concentrations of *gpaB*^{oe} cells were approximately 4.6-fold higher than those of KAx3 cells at 8 h after the onset of starvation (Fig. 3.2.). These results suggest that the developmental defects associated with *gshB*^{oe} cells may be due to the overexpression of *gpaB* in cAR1-mediated cAMP signaling.

3. 2. Effects of *gpaB* overexpression on aggregation processes

Based on the previous findings, the phenotypes of *gpaB*^{oe} cells were investigated in depth. When cells were allowed to develop at a low density of 2 × 10^5 cells/cm^2 in submerged culture, *gpaB*^{oe} cells were not able to form streams (Fig. 3.3.A). In addition, *gpaB*^{oe} cells showed defects in the cell polarity, displaying the excessive formation of pseudopodia (Fig. 3.3.B and 3.4. A and B). *carA*^{oe} cells also showed defects in stream formation and cell polarity (Fig. 3.3. and 3.4.). Next, the F-actin polymerization upon cAMP stimulation was

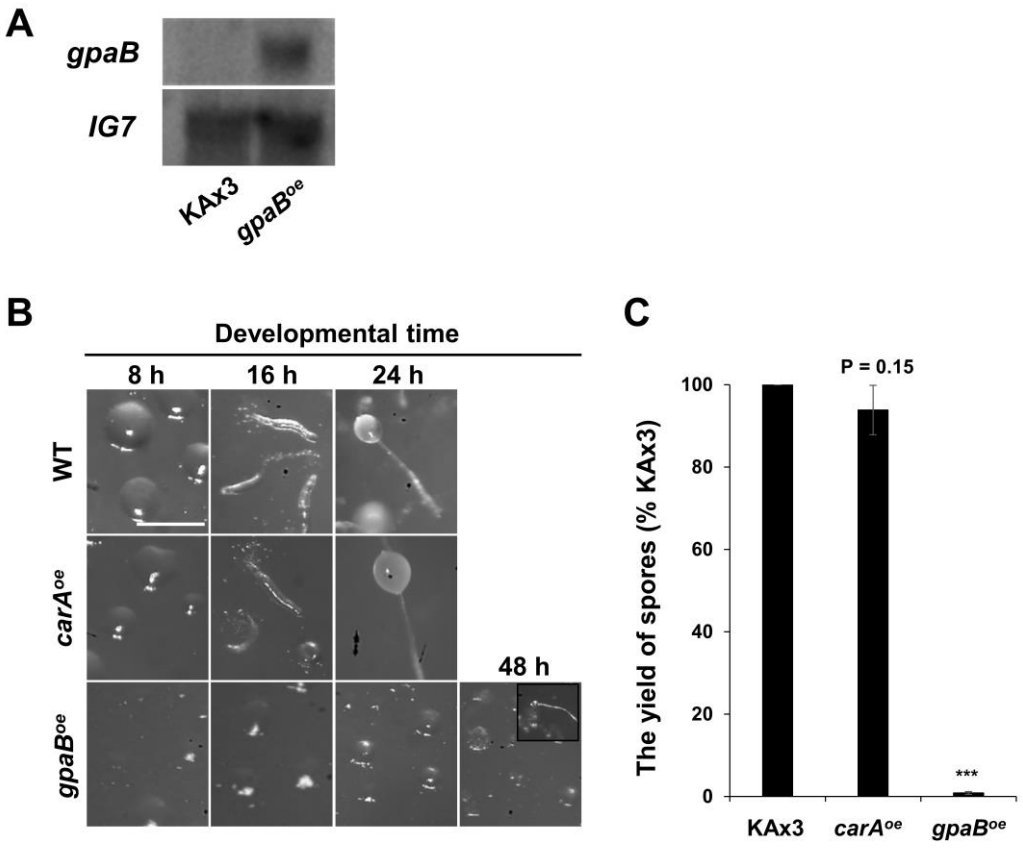

Fig. 3.1. Effects of the overexpression of *carA* and *gpaB* on developmental morphology. (A) Confirmation of the production of *gpaB*^{oe} mutant cells in *D. discoideum*. Overexpression of *gpaB* in Kax3 cells was analyzed by northern blot analysis. *gα2*, G-protein subunit alpha 2 (Gα2); *IG7*, a loading control. Effects of the overexpression of *carA* and *gpaB* on developmental morphology (B) and spore formation (C). Error bars in C represent SEM calculated from at least three independent experiments. ***$P < 0.0001$, Student t test. (Scale bar: 0.5 mm.)

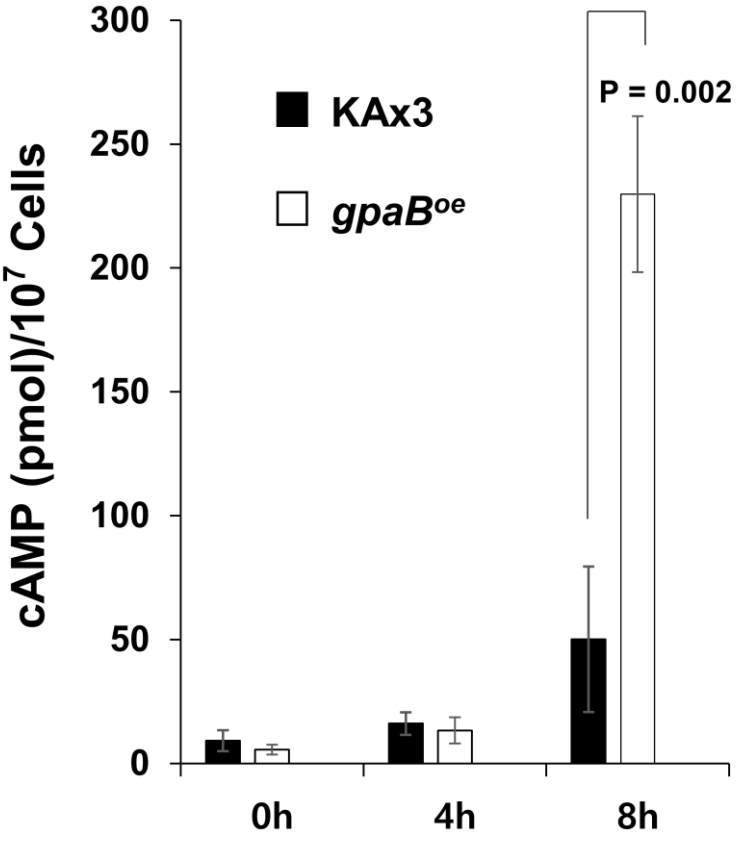

Fig. 3.2. Intracellular cAMP levels in KAx3 and *gpaB*^{oe} cells during early development. The cAMP level in *gpaB*^{oe} cells also exhibited remarkable increase at 8 h after the onset of starvation, as *gshB*^{oe} cells did.

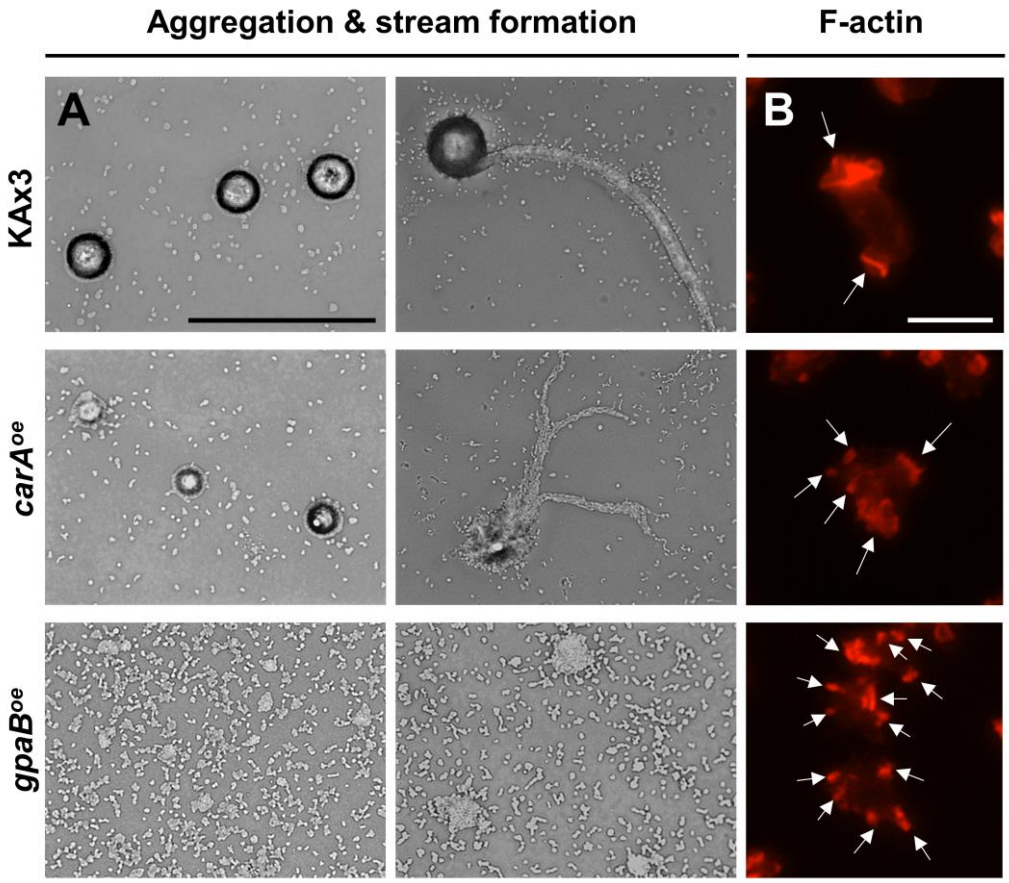

Fig. 3.3. The phenotypes of KAx3, *carA*^{oe} and *gpaB*^{oe} cells during early development. Aggregation and stream formation (A) and cell polarity (B**)** in KAx3, *carA*^{oe} and *gpaB*^{oe} cells during early development. *gpaB*^{oe} cells show phenocopies of *gshB*^{oe} cells. The arrows in *B* indicate the F-actin based pseudopod. (Scale bars: 0.5 mm in A, 10 μm in B.)

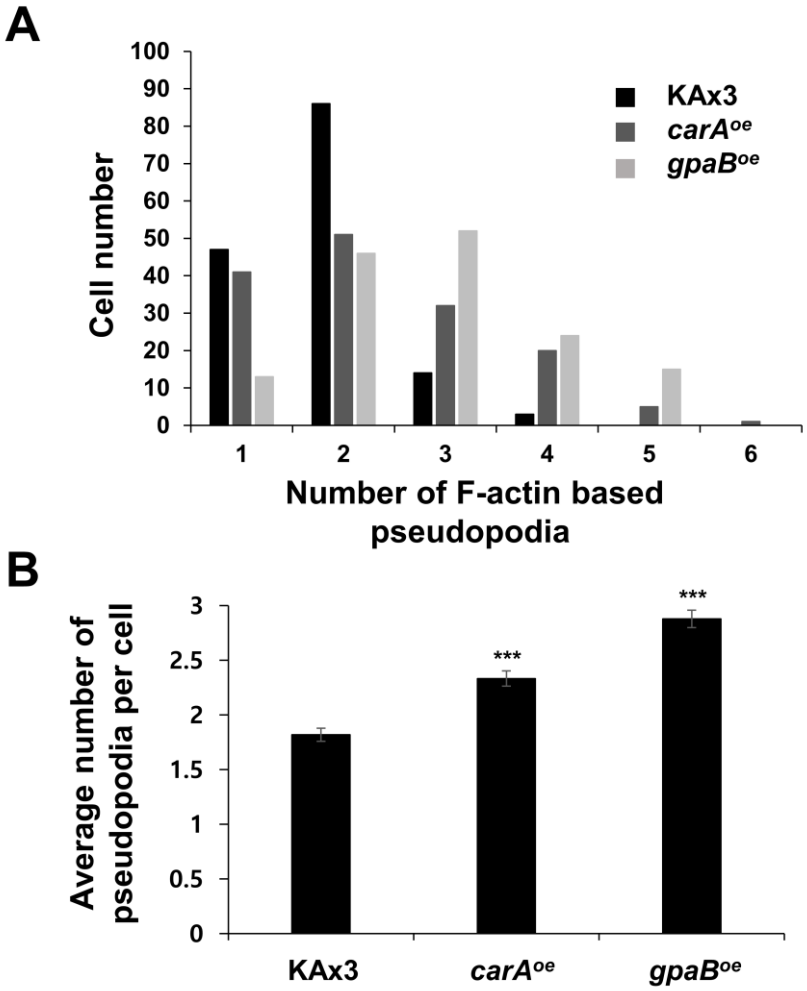

Fig. 3.4. Analysis of F-actin based pseudopodia formation in KAx3, *carA*^{oe} and *gpaB*^{oe} cells during aggregation. (A and B) The average numbers of F-actin based pseudopodia per cell were measured by counting from at least 150 cells. *gpaB*^{oe} cells have a defect in the suppression of the excessive F-actin based pseudopod formation ***$P < 0.0001$, Student t test.

examined in *gpaB*^{oe} cells. Their F-actin levels increased 1.2-fold within 10 s after cAMP pulse, followed by two additional peaks at 20 and 80 s, respectively (Fig. 3.5.A). During the time, the average level of F-actin did not display significantly differences between KAx3 and *gpaB*^{oe} cells (Fig. 3.5.B). These results suggest that *gpaB*^{oe} cells also have an abnormal pattern of F-actin polymerization.

3. 3. Effects of *gpaB* overexpression on cell differentiation

Because *gpaB*^{oe} cells were arrested at the mound stage, cell-type proportioning was observed in *gpaB*^{oe} mounds. In their aberrant mounds, *gpaB*^{oe} cells were strongly stained with neutral red (Fig. 3.6.A), but poorly stained for the *pspA-lacZ* marker (Fig. 3.6.B). However, in the slug of *carA*^{oe} cells, the pre-stalk cells and the pre-spore cells were normally expressed (Fig. 3.6. A and B). These data suggest that *gshB*^{oe} and *gpaB*^{oe} cells exhibit similar phenotypic defects with respect to cell-type differentiation. Therefore, to quantitate different cell types, the number of stained cells was also counted after disaggregation of the mounds of KAx3, *gshB*^{oe} and *gpaB*^{oe} cells (Fig. 3.7.). As the result, the number of pre-stalk cells was significantly increase in *gshB*^{oe} and *gpaB*^{oe} mounds (87.04 ± 1.15% and 87.38 ± 0.84%, respectively) relative to that in KAx3 mounds (20.26 ± 0.39%). Conversely, the number of pre-spore cells remarkably decreased in *gshB*^{oe} and *gpaB*^{oe} mounds (0.011 ± 0.001% and 0.012 ± 0.001%, respectively) relative to that in KAx3 mounds (72.82 ± 0.41%). Northern blot analysis confirmed the above defects, such as a delay of aggregation (*cadA*, *csaA* and *lagC*), the elevated expression of pre-stalk-specific genes (*ecmA* and *ecmB*), and the decreased expression of pre-spore-specific genes (*pspA* and *cotC*; Fig. 3.8.). Taken together, these data indicate that *gpaB*^{oe} cells exhibit phenocopies of *gshB*^{oe} cells in cell-type differentiation.

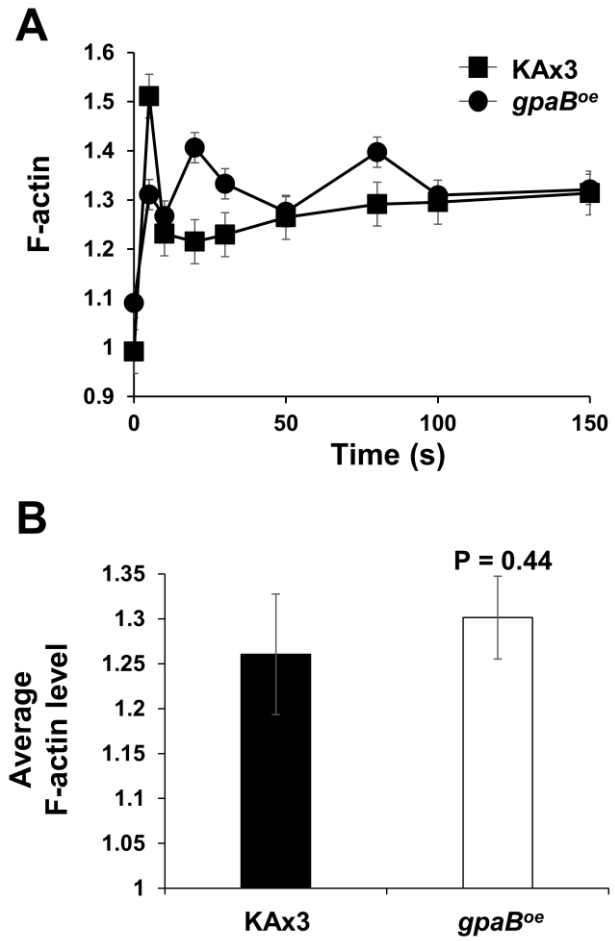

Fig. 3.5. *In vivo* F-actin polymerization assay in response to cAMP in KAx3 and *gpaB*^{oe} cells. F-actin polymerization (A) and the average level of F-actin (B) in KAx3 and *gpaB*^{oe} cells during early development. *gpaB*^{oe} cells show shallow and frequent peaks in F-actin level. Error bars in A and B represent SEM calculated from at least three independent experiments, using Student's *t*-test.

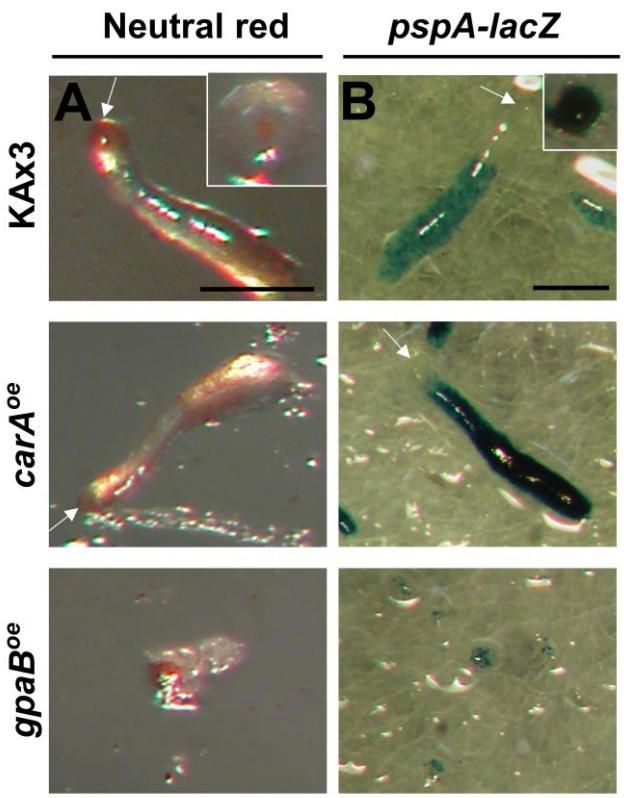

Fig. 3.6. Cell differentiation of KAx3, *carA*^{oe} and *gpaB*^{oe} slug or mound during late development. Cells were stained with neutral red, a vital dye which specifically stains pre-stalk cells, and then developed (A), or cells expressing *pspA* specific markers were allowed to develop, fix and stain for *lacZ* β-galactosidase activity (B). *gpaB*^{oe} cells exhibit the increased pre-stalk differentiation and the decreased pre-spore differentiation, like *gshB*^{oe} cells. (Scale bars: 0.5 mm in A and B.)

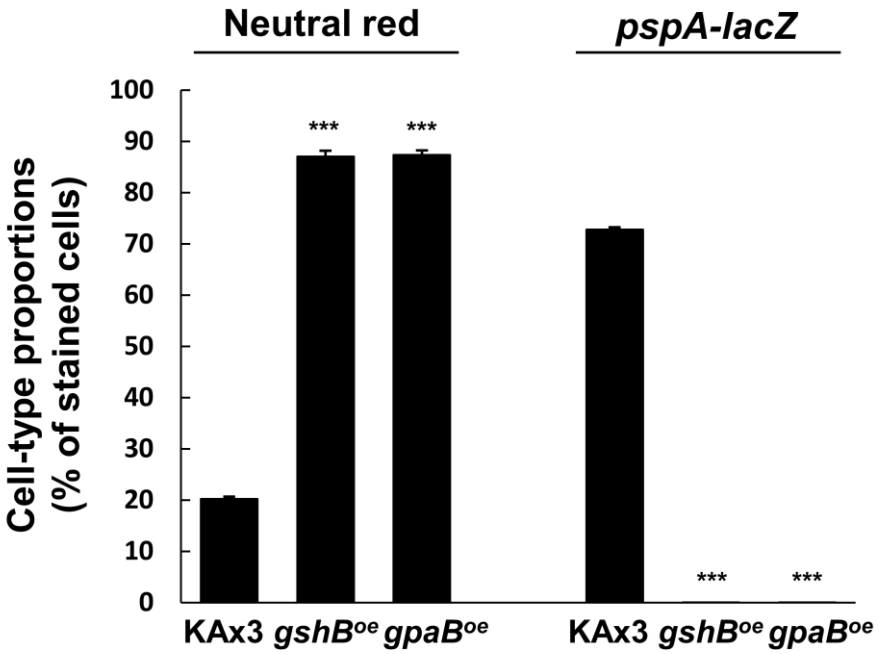

Fig. 3.7. *gshB*^{oe} and *gpaB*^{oe} cells exhibit similar defects in cell-type differentiation. Cell-type porportions in KAx3, *gshB*^{oe} and *gpaB*^{oe} mounds. Aggregates were dissociated, fixed and stained. The number of stained cells was counted by using a hemacytometer. Error bars indicate SEMs calculated from at least three independent experiments. ***$P < 0.0001$, Student's *t*-test

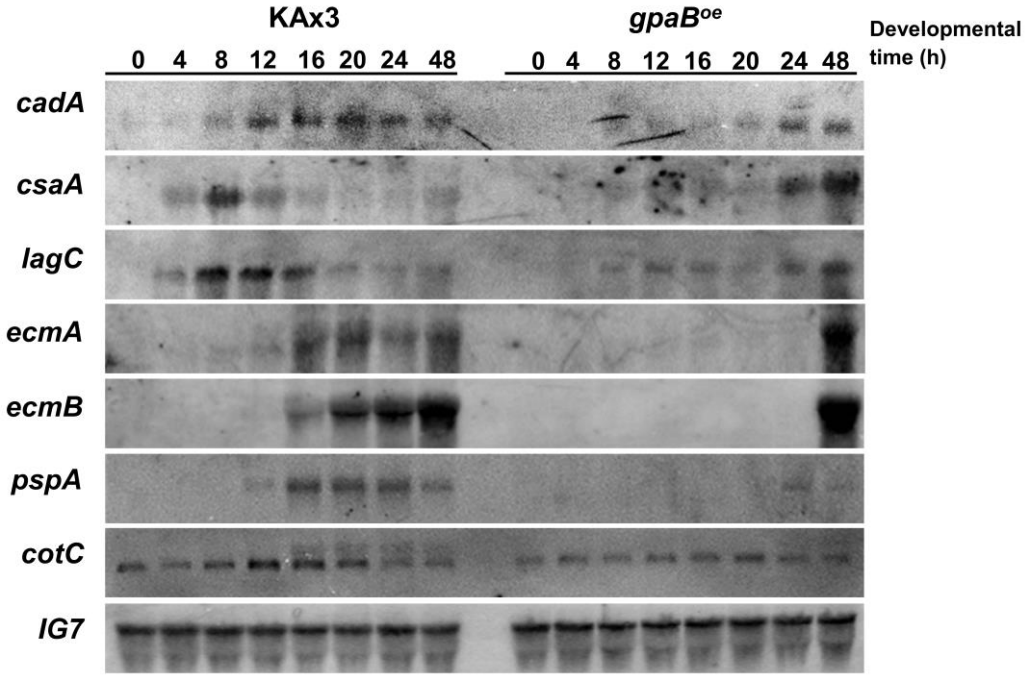

Fig. 3.8. The mRNA expression patterns of the developmental markers in KAx3 and *gpaB*^{oe} cells. KAx3 and *gpaB*^{oe} cells were allowed to develop on non-nutrient KK_2 plates and were harvested at the indicated times during development. Northern blots were performed using fragments of the indicated developmental marker genes as hybridization probes. *cadA* and *csaA*, aggregation-specific; *lagC*, post-aggregative-specific; *ecmA* and *ecmB*, pre-stalk-specific; *pspA* and *cotC*, pre-spore-specific genes; *IG7*, a loading control.

3. 4. The relationship between the expression of *gshB* and *gpaB*

3. 4. 1. *gpaB* knockdown can rescue the phenotypic defects in *gshB*^{oe} cells

To determine whether silencing of *gpaB* rescues the defects caused by *gshB* overexpression, *gpaB* knockdown strains in KAx3 and *gshB*^{oe} cells (*gpaB*^{as} and *gpaB*^{as}/*gshB*^{oe} cells, respectively) were generated using antisense RNA inhibition (Fig. 3.9.A) and the *gpaB* expression level was slightly lower in *gpaB*^{as} and *gpaB*^{as}/*gshB*^{oe} cells (0.86-fold and 0.84-fold, respectively) than that in KAx3 cells (Fig. 3.9. B and C). During development, *gpaB*^{as} cells formed aggregates, slugs, and fruiting bodies. Interestingly, *gpaB* knockdown in *gshB*^{oe} cells (*gpaB*^{as}/*gshB*^{oe}) partially rescued the defects of *gshB*^{oe} cells. *gpaB*^{as}/*gshB*^{oe} cells produced fruiting bodies with smaller sori than that of *gpaB*^{as} cells, but their sporulation was increased by 68% compared to that of *gshB*^{oe} cells (Fig. 3.10. A and B).

It is well known that Gα2 plays a crucial role in chemotaxis (Okaichi, *et al.*, 1992; Parent, *et al.*, 1998). Therefore, the effect of *gpaB* knockdown on chemotactic aggregation was also investigated. When cells developed at a low cell density, *gpaB*^{as} cells formed long streams towards the aggregation center, as KAx3 cells did. Furthermore, the defects in cell streaming and cell polarity characteristic of *gshB*^{oe} cells were partially restored by *gpaB* knockdown (Fig. 3.11. and Fig. 3. 12.). Expression profiles of the developmental-specific genes in *gshB*^{oe} cells were also rescued by *gpaB* knockdown (Fig. 3.13.). I supposed that in *gshB*^{oe} cells, increases of free Gα2 caused by induction of *gpaB* expression may facilitate Gα2 activation, resulting in the production of higher levels of cAMP. Therefore, the above results suggest that the developmental defects associated with *gshB*^{oe} cells may be caused by *gpaB* expression and high

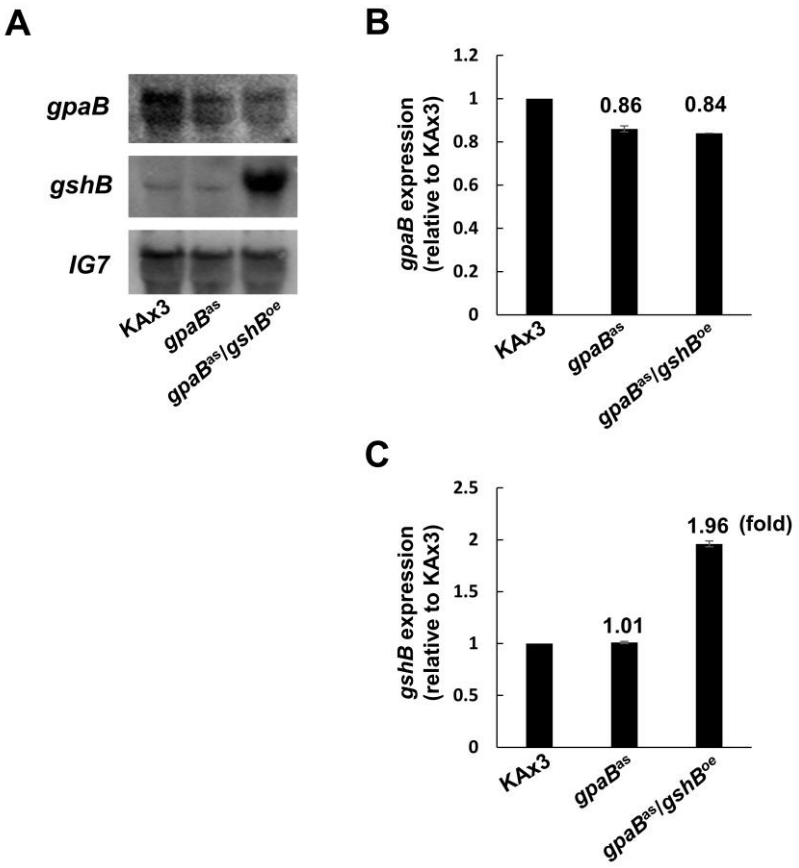

Fig. 3.9. Expression of *gpaB* and *gshB* in *gpaB*-antisense strains. (A) Northern blot analysis of *gpaB* and *gshB* expression in Kax3, *gpaB*^{as} and *gpaB*^{as}/*gshB*^{oe} cells. *gpaB* expression levels (B) and *gshB* expression levels (C) were normalized to *IG7*. Fold change in mRNA expression is relative to Kax3. *gshB*, GSH synthetase (GSS); *gpaB*, G-protein subunit alpha 2 (Gα2); *IG7*, a loading control. Data represent the mean and SEM of at least three independent experiments.

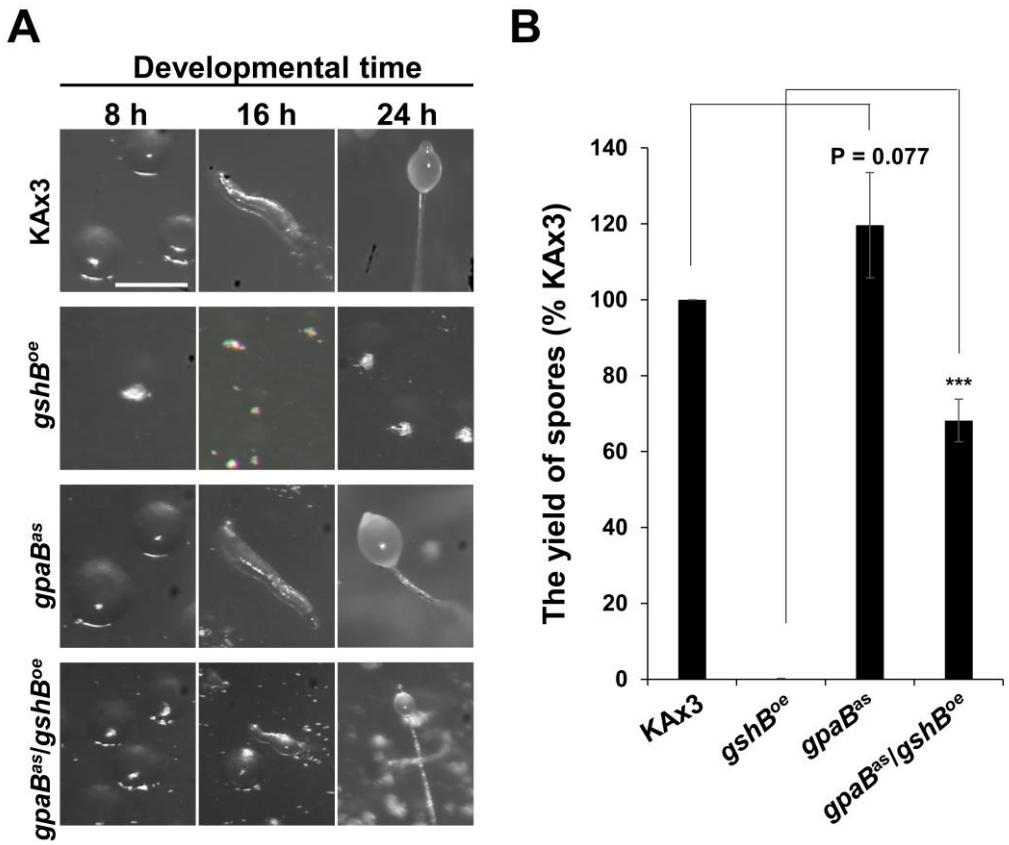

Fig. 3.10. *gpaB* knockdown can partially rescue the phenotypic defects of *gshB*^{oe} cells. Effects of *gpaB* knockdown in KAx3 and *gshB*^{oe} cells on developmental morphology (A) and spore formation (B). Contrary to the mound-arrest phenotype in *gshB*^{oe} cells, *gpaB*^{as}/*gshB*^{oe} cells can complete development. *gpaB* knockdown in KAx3 and *gshB*^{oe} cells increases the spore yields about 120 % and 68 % respectively. ***$P < 0.0001$, Student's *t*-test. (Scale bars: 0.5 mm.)

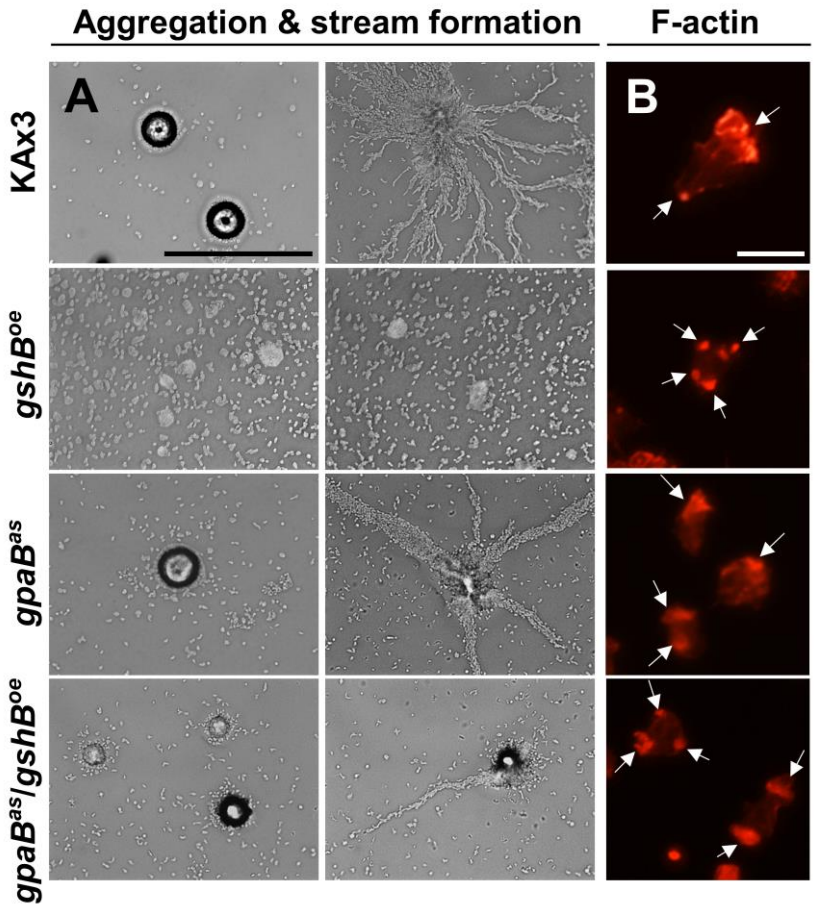

Fig. 3.11. The phenotypes of KAx3, *gshB*^{oe}, *gpaB*^{as} and *gpaB*^{as}/*gshB*^{oe} cells during early development. Aggregation and stream formation (A) and cell polarity (B**)** in KAx3, *gshB*^{oe}, *gpaB*^{as} and *gpaB*^{as}/*gshB*^{oe} cells during early development. *gpaB*^{as}/*gshB*^{oe} cells can form more tight aggregation and more improved streaming than *gshB*^{oe} cells did. Also, F-actin staining shows the partial recovery of the polarity of *gpaB*^{as}/*gshB*^{oe} cells compared with *gshB*^{oe} cells. The arrows in *B* indicate the F-actin based pseudopod. (Scale bars: 0.5 mm in A, 10 μm in B.)

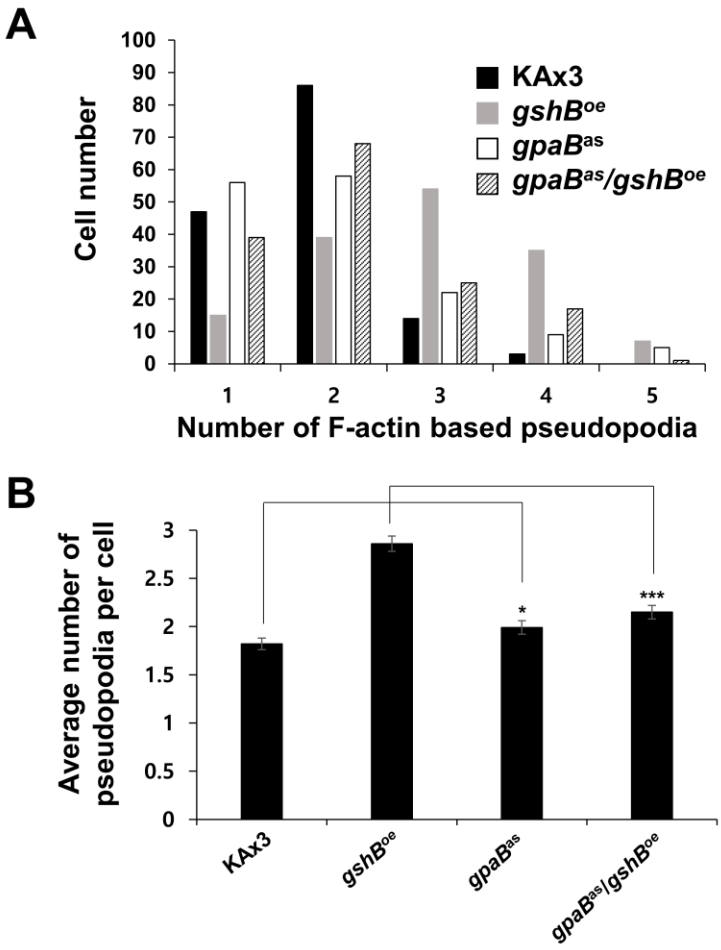

Fig. 3.12. Analysis of F-actin based pseudopodia formation in KAx3, *gshB*^{oe}, *gpaB*^{as} and *gpaB*^{as}/*gshB*^{oe} cells during aggregation. (A and B) The average numbers of F-actin based pseudopodia per cell were measured by counting from at least 150 cells. *gpaB*^{as}/*gshB*^{oe} cells show a partially rescued phenotype in the excessive F-actin based pseudopod formation of *gshB*^{oe} cells. *$P < 0.001$, ***$P < 0.0001$, Student's *t*-test.

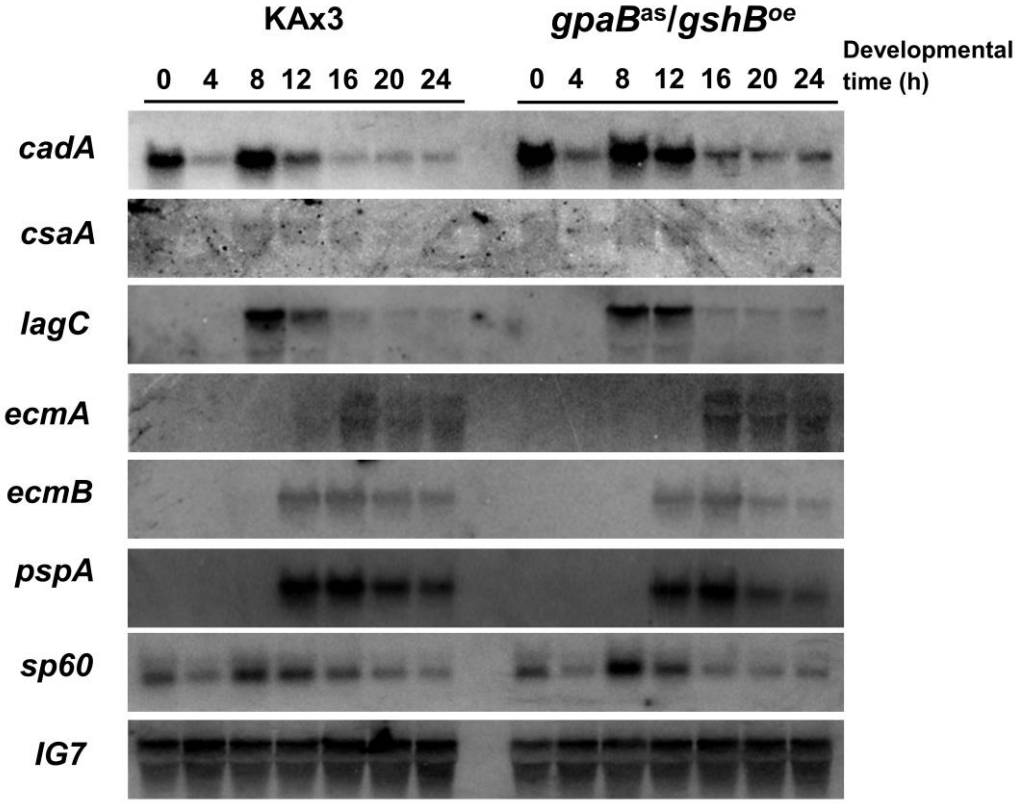

Fig. 3.13. The mRNA expression patterns of the developmental markers in KAx3 and *gpaB*^{as}/*gshB*^{oe} cells. KAx3 and *gpaB*^{as}/*gshB*^{oe} cells were allowed to develop on non-nutrient KK_2 plates and were harvested at the indicated times during development. Northern blots were performed using fragments of the indicated developmental marker genes as hybridization probes. *cadA* and *csaA*, aggregation-specific; *lagC*, post-aggregative-specific; *ecmA* and *ecmB*, pre-stalk-specific; *pspA* and *cotC*, pre-spore-specific genes; *IG7*, a loading control.

intracellular cAMP concentrations.

4. The effect of *gshB* overexpression on the regulation of Gα2 localization

It has been reported that heterotrimeric G proteins (Gα2βγ) cycle between the cytosol and plasma membrane (Elzie, *et al.*, 2009). Upon binding of cAMP to cAR1, they are recruited to the plasma membrane to participate in downstream signaling cascades, including ACA activation and actin cytoskeleton modulation (Elzie, *et al.*, 2009; Iijima and Devreotes, 2002; Iijima, *et al.*, 2002; Janetopoulos, *et al.*, 2001; Kortholt, *et al.*, 2011; Parent, *et al.*, 1998; Xu, *et al.*, 2005; Zigmond, *et al.*, 1997). To determine whether *gshB* overexpression regulates Gα2 localization, KAx3 and *gshB*^{oe} cells expressing Gα2-GFP were generated and the integrated fluorescence intensity was measured. As the result, there was no significant difference in the mean fluorescence intensity between KAx3 and *gshB*^{oe} cells (Fig. 4.1). However, there was the distinction in Gα2-GFP localization between KAx3 and *gshB*^{oe} cells (Fig. 4.2. A and B). In KAx3 cells, Gα2-GFP was uniformly expressed prior to cAMP stimulation and rapidly translocated to the plasma membrane within 30 s after stimulation (Fig. 4.2.A). However, in *gshB*^{oe} cells, Gα2-GFP was strongly localized at the plasma membrane both before and after the addition of cAMP (Fig. 4.2.A). The averaged ratio of the plasma membrane-to-cytosol fluorescence intensity was significantly higher in *gshB*^{oe} cells (FI_{mem}/FI_{cyt} = 2.74 ± 0.36, n = 15, ***P < 0.0001, Student's *t*-test) than in KAx3 cells (FI_{mem}/FI_{cyt} = 1.12 ± 0.21, n = 15, ***P < 0.0001, Student's *t*-test) (Fig. 4.2.B). Taken together, these results suggest that Gα2 is strongly localized at the plasma membrane regardless of cAMP stimulation in *gshB*^{oe} cells.

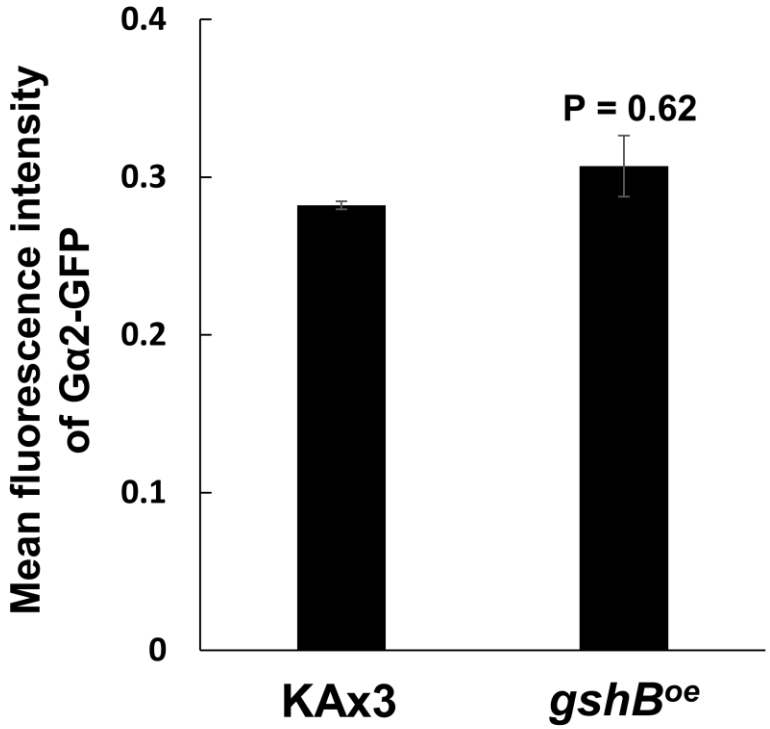

Fig. 4.1. The mean fluorescence intensity of Gα2-GFP in KAx3 and *gshB*^{oe} cells. The mean fluorescence intensity of an unstimulated cell was determined using a Zeiss Zen software package. Data represent the mean and SEM of at least ten independent experiments, using Student's *t*-test.

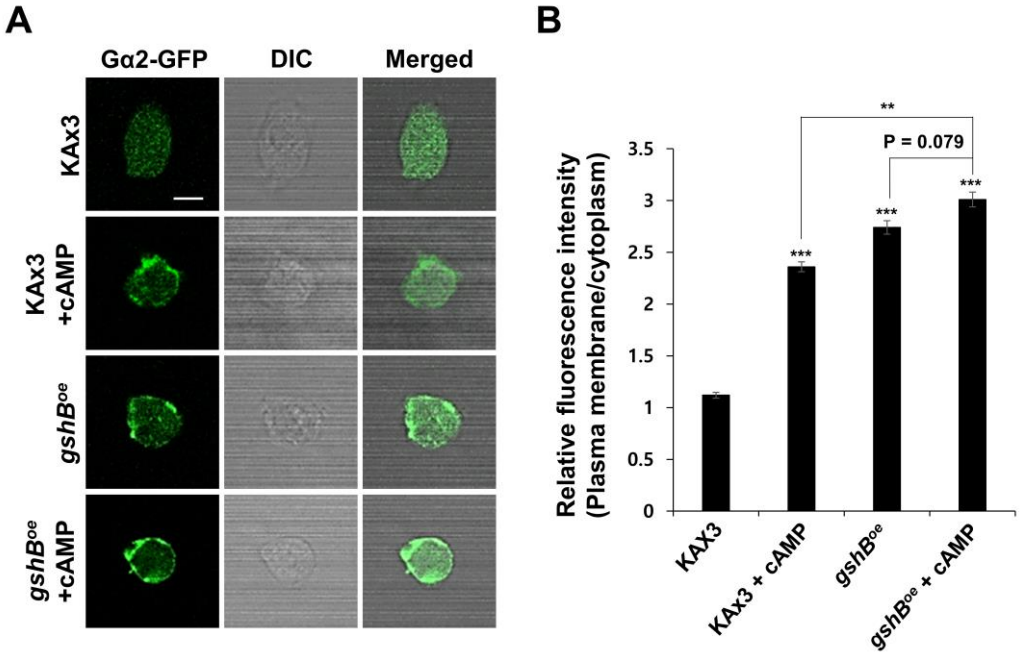

Fig. 4.2. Effect of *gshB* overexpression on Gα2 localization during early development. (A) Changes in localization of Gα2-GFP in response to cAMP in KAx3 and *gpaB*^{oe} cells. (B) The averaged ratio of plasma membrane-to-cytosol fluorescence intensity of Gα2-GFP in KAx3 and *gpaB*^{oe} cells. *gpaB*^{oe} cells showed strong Gα2-GFP fluorescence signals at the plasma membrane, both before and after 1 μM cAMP stimulation. Data represent the mean and SEM of at least ten independent experiments. ***$P < 0.0001$, **$P < 0.0005$, Student's *t*-test. (Scale bars: 5 μm.)

IV. DISCUSSION

The importance of gshB in the regulation of GSH biosynthesis

Intracellular GSH levels are tightly regulated by the synthesis of a variety of enzymes during *Dictyostelium* development (Choi, *et al*., 2006; Kim, *et al*., 2005; Kim, *et al*., 2014). Previous studies demonstrated the roles of GSH during growth and development using GCS null cells (Kim, *et al.*, 2005; Kim, *et al.*, 2014), because GCS, which is encoded by *gcsA*, is a rate-limiting enzyme associated with GSH biosynthesis.

Herein, the gene expression patterns of *gcsA* and *gshB* were examined in KAx3 cells as a preliminary experiment to understand the regulation of intracellular GSH synthesis (Fig. 5.1. A). The expression of *gcsA* was induced when starvation began and decreased thereafter. Then, its expression level peaked a second time during culmination (at 20 h; Fig. 5.1.A), as previously described in (Kim, *et al.*, 2005). In contrast, the expression of *gshB* peaked soon after the onset of starvation (at 0 h) and then decreased (Fig. 5.1.A). These expression patterns indicate that regulation of intracellular GSH levels is necessary for *Dictyostleium* development. Additionally, in KAx3 cells, the intracellular GSH levels were increased during early aggregation (at 4 h) and then decreased, which was similar to the expression pattern of *gshB* (Fig. 5.1.B). These findings suggest that *gshB* expression is closely related to increases in GSH levels. Moreover, GSH levels were significantly increased in *gshB*^{oe} cells throughout the development, while there were no differences in GSH levels between KAx3 and *gcsA*^{oe} cells in spite of *gcsA* overexpression (Fig. 5.1.B). These results indicate that *gshB* plays an important role in modulating GSH biosynthesis.

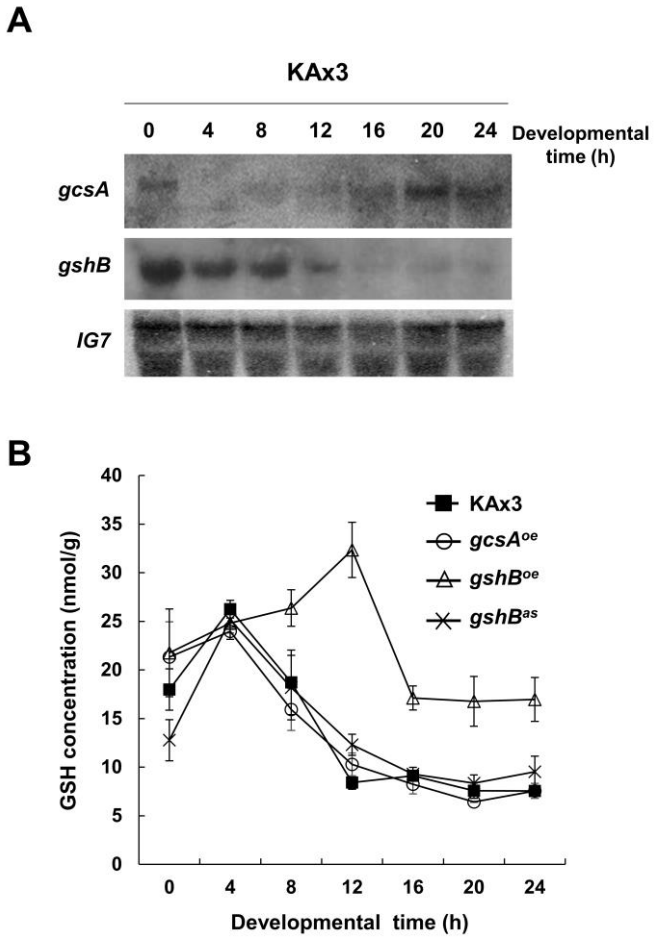

Fig. 5.1. Effect of *gshB* expression on the regulation of GSH biosynthesis during *Dictyostelium* development. (A) Expression patterns of *gcsA* and *gshB* during development in Kax3 cells. (B) Changes in intracellular GSH levels in KAx3, $gcsA^{oe}$, $gshB^{oe}$ and $gshB^{as}$ cells duirng development. *gshB* expression is closely related to increases in GSH levels. Data represent the mean and SEM of at least three independent experiments.

Cell fate is determined by GSH level at the initial development

It has previously been reported that developmental cell fate is dependent on growth conditions in *D. discoideum* (Gomer and Firtel, 1987). Our groups demonstrated previously that entry into development depends on GSH concentration at the onset of development (Kim, *et al.*, 2005; Kim, *et al.*, 2014). In this study, it was supposed that cell fate determination may also be regulated by the intracellular GSH levels at the transition from growth to starvation. *gcsA*^{oe} and *gshB*^{oe} cells exhibited higher GSH levels than KAx3 cells at the initiation of starvation (at 0 h), whereas GSH level of *gshB*^{as} cells was reduced by 30% than that of KAx3 cells at that time, although there were no differences in GSH levels between *gshB*^{as} and KAx3 cells during development (Fig. 5.1.B). When cells were allowed to develop at a low density in submerged culture, both *gcsA*^{oe} and *gshB*^{oe} cells did not form cell streaming (Fig. 2.1.A), while *gshB*^{as} cells produced cell streaming (Fig. 2.1.A) and showed normal cell polarity (Fig. 2.1.B and Fig. 2.2). Additionally, the mounds of *gshB*^{oe} cells and the slugs of *gcsA*^{oe} cells displayed enlarged pre-stalk regions and smaller pre-spore regions, while the slugs of *gshB*^{as} cells were comprised smaller pre-stalk regions and larger pre-spore regions (Fig. 2.4.). Moreover, in chimeric slugs, *gcsA*^{oe} and *gshB*^{oe} cells labelled with GFP markers were primarily localized in the pre-stalk region (Fig. 5.2.). However, GFP-marked *gshB*^{as} cells were primarily distributed in the pre-spore region (Fig. 5.2.). These results indicate that cell fate decision and spatial pattern in multicellular structures are affected by cellular GSH levels at the onset of development in a cell-autonomous manner.

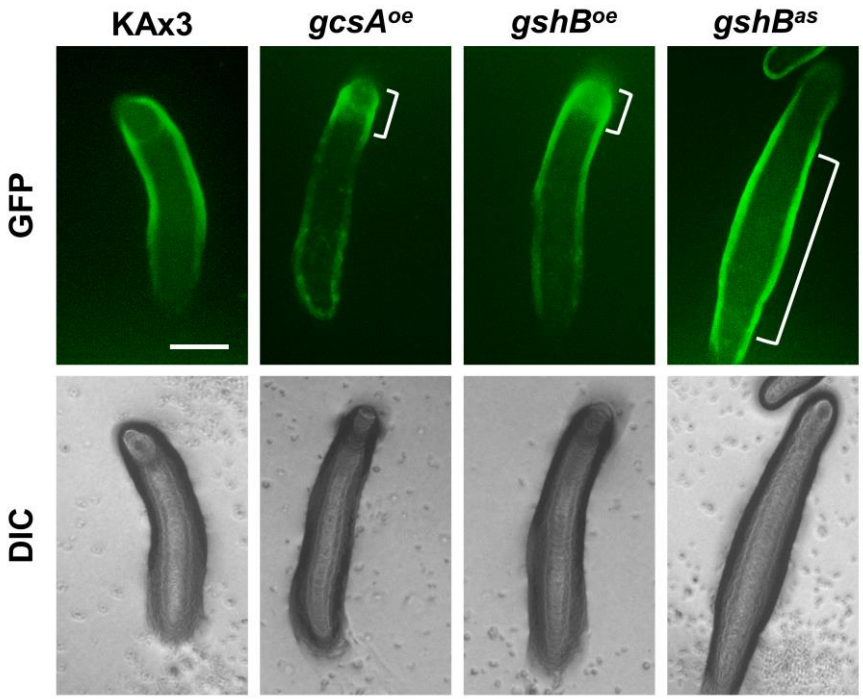

Fig. 5.2. Comparison of the spatial patterning of mutant cells in multicellular structures. GFP-labelled cells were allowed to develop with unlabeled Kax3 cells at a ratio of 1:3. The Kax3 cells in the chimeric slug were provided for the comparison. In the chimeric slugs, *gcsA*^{oe} and *gshB*^{oe} cells labeled with GFP markers were primarily localized in the pre-stalk zone. However, GFP-marked *gshB*^{as} cells were distributed in the pre-spore region. White bars indicate that region of GFP enrichment. (Scale bars: 50 µm.)

The specific relationship between the expression of gshB and gpaB

In this study, *gshB*^{oe} cells were arrested in the mound stage and were not able to produce spores during development (Fig. 1.3.), which was similar to the characteristic defects of cells overexpressing *gpaB,* which encodes G protein alpha 2 (Gα2) (Fig. 3.1.). *gshB*^{oe} cells exhibited increased intracellular cAMP levels in a secondary response to induced expression of *gpaB* (Fig. 2.6. and Fig. 2.7.). *gpaB* expression was also increased in KAx3 cells according to GSH concentrations supplemented in developmental buffer (Fig. 5.3.). Furthermore, KAx3 cells that added GSH exogenously showed delayed developmental processes and reduced sporulation (Fig. 1.4.). Both *gshB*^{oe} and *gpaB*^{oe} cells exhibited defect in multicellular aggregation and abnormal pattern in F-actin polymerization (Fig. 2.1.A, 2.3.A, 3.3.A, and 3.5.A.), which could be due to abnormally elevated cAMP levels because the phenotypes of mutant lacking a cAMP-specific phosphodiesterase (*regA*-null cells) also exhibit similar defects, such as aberrant aggregation and reduced suppression of lateral pseudopod formation (Wessels, *et al*., 2000). We also observed that the expression levels of *pedA* (encoding cAMP/cGMP phosphodiesterase A) were downregulated in *gshB*^{oe} cells during early development (Fig. 5.4.). Furthermore, Gα2 was significantly increased at the plasma membrane of *gshB*^{oe} cells (Fig. 4.2.). Interestingly, defects of *gshB*^{oe} cells were partially rescued by *gpaB* knockdown (Fig. 3. 10-13.). Taken together, our findings suggest that intracellular GSH overproduced by *gshB* overexpression results in deficiencies of cAMP signaling-related development such as aggregation and F-actin polymerization, which may be caused by the defects in enhanced *gpaB* expression and increased cAMP production.

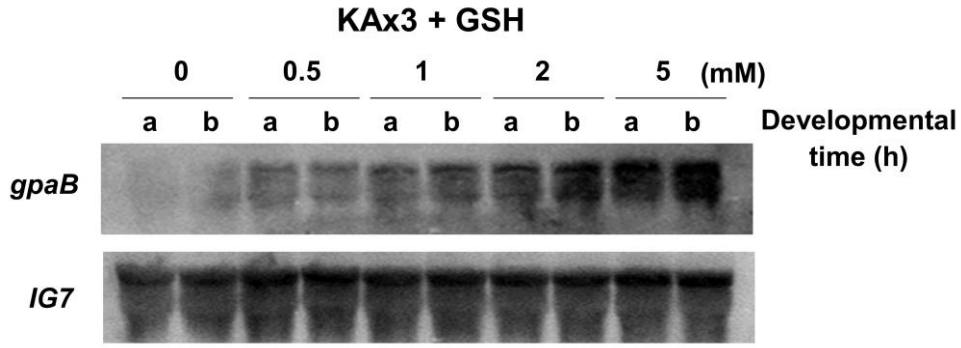

Fig. 5.3. Expression pattern of *gpaB* in Kax3 cells supplemented with or without exogenous GSH (0.5 – 5 mM). In Kax3 cells, *gpaB* expression was increased in a dose-dependent manner. (a and b indicate developmental times of 12 h and 16 h after the onset of development, respectively.)

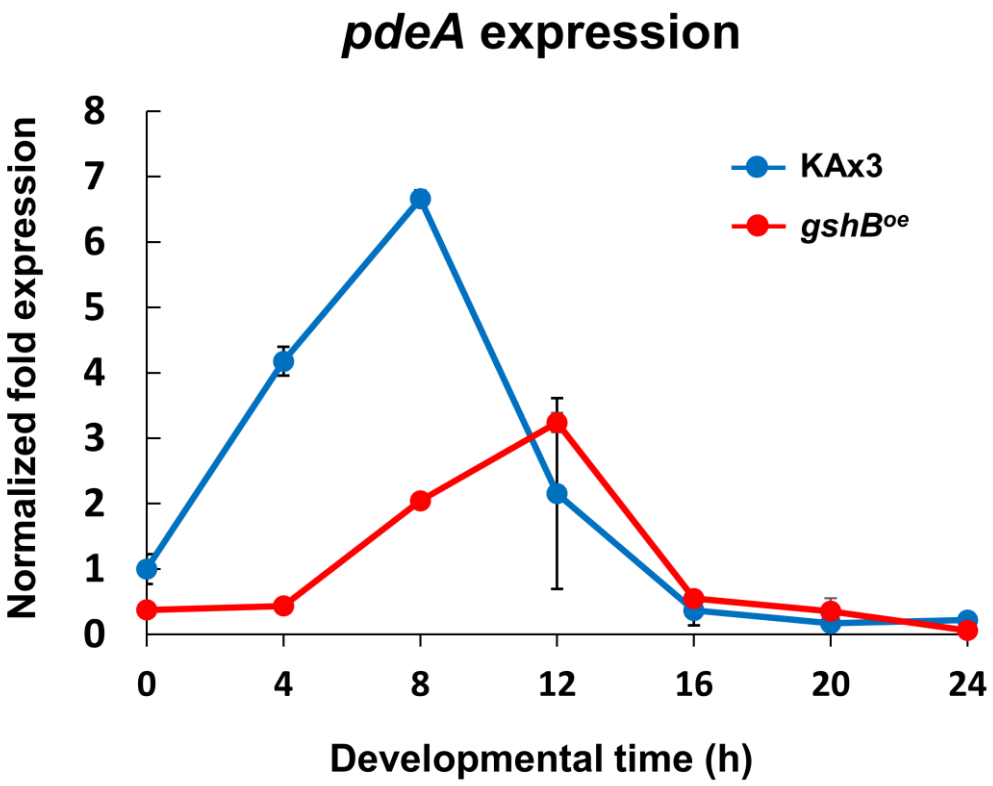

Fig. 5.4. Transcriptional regulation of *pdeA* expression in *gshB*^{oe} cells. *pdeA*, cAMP/cGMP phosphodiesterase A (DdPDE1). *rnlA* was used as a control.

The roles of intracellular GSH on Gα2 localization

Several intracellular signaling pathways activate the motile apparatus associated with *Dictyostelium* chemotaxis (Chen, *et al.*, 2003; Elzie, *et al.*, 2009; Iijima, *et al.*, 2002; Kortholt, *et al.*, 2011; Parent, *et al.*, 1998; Xu, *et al.*, 2005). A few groups have suggested that heterotrimeric G proteins (Gα2βγ) transduce cAMP-binding signals to downstream molecules via cyclic movements between the cytosol (inactive state) and plasma membrane (active state) (Elzie, *et al.*, 2009; Iijima, *et al.*, 2002). In present study, it was demonstrated that an increase in the intracellular GSH levels by *gshB* overexpression leads to changes in expression and localization of Gα2 (Fig. 2.6. and Fig. 4.2.). Although the mechanisms underlying this process remain unclear, several possibilities have been considered. First, the reducing properties of GSH may induce Gα2 gene expression via regulation of redox-sensitive transcription factors. In plants, heterotrimeric G proteins are involved in signaling mediated by ROS production (Joo, *et al.*, 2005). Second, it is possible that GSH level increased by *gshB* overexpression causes conformational changes in Gα2 through alterations of its residues, which may affect its localization and activity. It is reported that in the frontal cortical membrane of the normal human brain, GSH and its analogue (UPF1) stimulate G proteins activity (Karelson, *et al.*, 2002). Third, GSH may directly regulate G proteins via protein S-glutathionylation, an important post-transcriptional modification that regulates protein localization (Dalle-Donne, *et al.*, 2009). Lastly, the enhanced expression of Gα2 gene in $gshB^{oe}$ cells may cause unregulated Gα2 localization in cell and, consequently, the enrichment of Gα2 at the plasma membrane.

In conclusion, tight regulation of the intracellular GSH levels is vitally important in *Dictyostelium* development. During development, GSH regulates

developmental stage and cell-type proportioning by upregulating cAMP signaling via modulation of Gα2 expression and localization. Further studies designed to determine the molecular mechanisms that regulate G protein-related cAMP signaling by GSH may provide insights into general mechanisms underlying cell development.

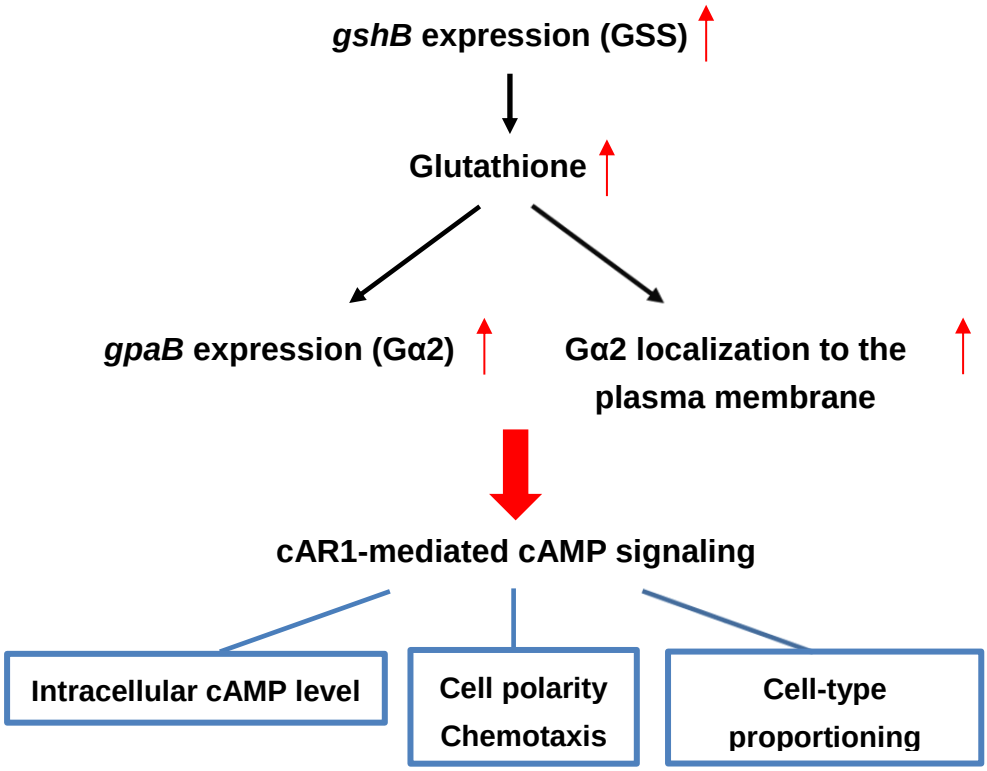

Fig. 5.5. The model of regulatory mechanism of GSH in cAR1-mediated cAMP signaling via Gα2 induced by *gshB* expression during *Dictyostelium discoideum* development

V. REFERENCES

Abe K. and Yanagisawa K. (1983) A new class of rapidly developing mutants in Dictyostelium discoideum: implications for cyclic AMP metabolism and cell differentiation. *Dev Biol* **95,** 200-210

Akerboom T. P., Bilzer M. and Sies H. (1982) The relationship of biliary glutathione disulfide efflux and intracellular glutathione disulfide content in perfused rat liver. *J Biol Chem* **257,** 4248-4252

Allen R. G., Newton R. K., Sohal R. S., Shipley G. L. and Nations C. (1985) Alterations in superoxide dismutase, glutathione, and peroxides in the plasmodial slime mold Physarum polycephalum during differentiation. *J Cell Physiol* **125,** 413-419

Anjard C., Chang W. T., Gross J. and Nellen W. (1998) Production and activity of spore differentiation factors (SDFs) in Dictyostelium. *Development* **125,** 4067-4075

Anjard C., van Bemmelen M., Veron M. and Reymond C. D. (1997) A new spore differentiation factor (SDF) secreted by Dictyostelium cells is phosphorylated by the cAMP dependent protein kinase. *Differentiation* **62,** 43-49

Anjard C., Zeng C., Loomis W. F. and Nellen W. (1998) Signal transduction pathways leading to spore differentiation in Dictyostelium discoideum. *Dev Biol* **193,** 146-155

Araki T., Abe T., Williams J. G. and Maeda Y. (1997) Symmetry breaking in Dictyostelium morphogenesis: evidence that a combination of cell cycle stage and positional information dictates cell fate. *Dev Biol* **192,** 645-648

Aw T. Y. (2003) Cellular redox: a modulator of intestinal epithelial cell proliferation. *News*

Physiol Sci **18,** 201-204

Azhar M., Kennady P. K., Pande G., Espiritu M., Holloman W., Brazill D., Gomer R. H. and Nanjundiah V. (2001) Cell cycle phase, cellular Ca2+ and development in Dictyostelium discoideum. *Int J Dev Biol* **45,** 405-414

Bader S., Kortholt A. and Van Haastert P. J. (2007) Seven Dictyostelium discoideum phosphodiesterases degrade three pools of cAMP and cGMP. *Biochem J* **402,** 153-161

Berks M. and Kay R. R. (1990) Combinatorial control of cell differentiation by cAMP and DIF-1 during development of Dictyostelium discoideum. *Development* **110,** 977-984

Bosgraaf L., Russcher H., Smith J. L., Wessels D., Soll D. R. and Van Haastert P. J. (2002) A novel cGMP signalling pathway mediating myosin phosphorylation and chemotaxis in Dictyostelium. *EMBO J* **21,** 4560-4570

Bretschneider T., Vasiev B. and Weijer C. J. (1997) A Model for Cell Movement During Dictyostelium Mound Formation. *J Theor Biol* **189,** 41-51

Cairns N. G., Pasternak M., Wachter A., Cobbett C. S. and Meyer A. J. (2006) Maturation of arabidopsis seeds is dependent on glutathione biosynthesis within the embryo. *Plant Physiol* **141,** 446-455

Ceaser E. K., Moellering D. R., Shiva S., Ramachandran A., Landar A., Venkartraman A., Crawford J., Patel R., Dickinson D. A., Ulasova E., Ji S. and Darley-Usmar V. M. (2004) Mechanisms of signal transduction mediated by oxidized lipids: the role of the electrophile-responsive proteome. *Biochem Soc Trans* **32,** 151-155

Chaudhuri B., Ingavale S. and Bachhawat A. K. (1997) apd1+, a gene required for red pigment formation in ade6 mutants of Schizosaccharomyces pombe, encodes an enzyme required for glutathione biosynthesis: a role for glutathione and a glutathione-conjugate pump. *Genetics* **145,** 75-83

Chen L., Janetopoulos C., Huang Y. E., Iijima M., Borleis J. and Devreotes P. N. (2003) Two phases of actin polymerization display different dependencies on PI(3,4,5)P3 accumulation and have unique roles during chemotaxis. *Mol Biol Cell* **14,** 5028-5037

Chisholm R. L. and Firtel R. A. (2004) Insights into morphogenesis from a simple developmental system. *Nat Rev Mol Cell Biol* **5,** 531-541

Cho M. Y., Bae C. D., Park J. B. and Lee T. H. (1998) Purification and cloning of glyoxalase II from rat liver. *Exp Mol Med* **30,** 53-57

Choi C. H., Kim B. J., Jeong S. Y., Lee C. H., Kim J. S., Park S. J., Yim H. S. and Kang S. O. (2006) Reduced glutathione levels affect the culmination and cell fate decision in Dictyostelium discoideum. *Dev Biol* **295,** 523-533

Davies L., Satre M., Martin J. B. and Gross J. D. (1993) The target of ammonia action in dictyostelium. *Cell* **75,** 321-327

Devine K. M., Morrissey J. H. and Loomis W. F. (1982) Differential synthesis of spore coat proteins in prespore and prestalk cells of Dictyostelium. *Proc Natl Acad Sci U S A* **79,** 7361-7365

Devreotes P. N. and Zigmond S. H. (1988) Chemotaxis in eukaryotic cells: a focus on leukocytes

and Dictyostelium. *Annu Rev Cell Biol* **4,** 649-686

Dinauer M. C., MacKay S. A. and Devreotes P. N. (1980) Cyclic 3',5'-AMP relay in Dictyostelium discoideum III. The relationship of cAMP synthesis and secretion during the cAMP signaling response. *J Cell Biol* **86,** 537-544

Dingermann T., Reindl N., Werner H., Hildebrandt M., Nellen W., Harwood A., Williams J. and Nerke K. (1989) Optimization and in situ detection of Escherichia coli beta-galactosidase gene expression in Dictyostelium discoideum. *Gene* **85,** 353-362

Dormann D., Vasiev B. and Weijer C. J. (1998) Propagating waves control Dictyostelium discoideum morphogenesis. *Biophys Chem* **72,** 21-35

Dormann D. and Weijer C. J. (2001) Propagating chemoattractant waves coordinate periodic cell movement in Dictyostelium slugs. *Development* **128,** 4535-4543

Elzie C. A., Colby J., Sammons M. A. and Janetopoulos C. (2009) Dynamic localization of G proteins in Dictyostelium discoideum. *J Cell Sci* **122,** 2597-2603

Feinberg A. P. and Vogelstein B. (1983) A technique for radiolabeling DNA restriction endonuclease fragments to high specific activity. *Anal Biochem* **132,** 6-13

Felder M., Szafranski K., Lehmann R., Eichinger L., Noegel A. A., Platzer M. and Glockner G. (2005) DictyMOLD-a Dictyostelium discoideum genome browser database. *Bioinformatics* **21,** 696-697

Forman D. and Garrod D. R. (1977) Pattern formation in Dictyostelium discoideum. II. Differentiation and pattern formation in non-polar aggregates. *J Embryol Exp Morphol* **40,** 229-

243

Franca-Koh J., Kamimura Y. and Devreotes P. (2006) Navigating signaling networks: chemotaxis in Dictyostelium discoideum. *Curr Opin Genet Dev* **16,** 333-338

Franke J., Faure M., Wu L., Hall A. L., Podgorski G. J. and Kessin R. H. (1991) Cyclic nucleotide phosphodiesterase of Dictyostelium discoideum and its glycoprotein inhibitor: structure and expression of their genes. *Dev Genet* **12,** 104-112

Funamoto S., Meili R., Lee S., Parry L. and Firtel R. A. (2002) Spatial and temporal regulation of 3-phosphoinositides by PI 3-kinase and PTEN mediates chemotaxis. *Cell* **109,** 611-623

Galter D., Mihm S. and Droge W. (1994) Distinct effects of glutathione disulphide on the nuclear transcription factor kappa B and the activator protein-1. *Eur J Biochem* **221,** 639-648

Gardiner C. S. and Reed D. J. (1994) Status of glutathione during oxidant-induced oxidative stress in the preimplantation mouse embryo. *Biol Reprod* **51,** 1307-1314

Gerisch G., Malchow D., Roos W. and Wick U. (1979) Oscillations of cyclic nucleotide concentrations in relation to the excitability of Dictyostelium cells. *J Exp Biol* **81,** 33-47

Ghezzi P. (2011) Role of glutathione in immunity and inflammation in the lung. *Int J Gen Med* **4,** 105-113

Ginsburg G. T. and Kimmel A. R. (1997) Autonomous and nonautonomous regulation of axis formation by antagonistic signaling via 7-span cAMP receptors and GSK3 in Dictyostelium. *Genes Dev* **11,** 2112-2123

Gomer R. H. and Firtel R. A. (1987) Cell-autonomous determination of cell-type choice in

Dictyostelium development by cell-cycle phase. *Science* **237,** 758-762

Grant C. M., MacIver F. H. and Dawes I. W. (1997) Glutathione synthetase is dispensable for growth under both normal and oxidative stress conditions in the yeast Saccharomyces cerevisiae due to an accumulation of the dipeptide gamma-glutamylcysteine. *Mol Biol Cell* **8,** 1699-1707

Griffith O. W. (1999) Biologic and pharmacologic regulation of mammalian glutathione synthesis. *Free Radic Biol Med* **27,** 922-935

Griffith O. W. and Mulcahy R. T. (1999) The enzymes of glutathione synthesis: gamma-glutamylcysteine synthetase. *Adv Enzymol Relat Areas Mol Biol* **73,** 209-267, xii

Harloff C., Gerisch G. and Noegel A. A. (1989) Selective elimination of the contact site A protein of Dictyostelium discoideum by gene disruption. *Genes Dev* **3,** 2011-2019

Harwood A. J., Plyte S. E., Woodgett J., Strutt H. and Kay R. R. (1995) Glycogen synthase kinase 3 regulates cell fate in Dictyostelium. *Cell* **80,** 139-148

Hopper N. A., Harwood A. J., Bouzid S., Veron M. and Williams J. G. (1993) Activation of the prespore and spore cell pathway of Dictyostelium differentiation by cAMP-dependent protein kinase and evidence for its upstream regulation by ammonia. *EMBO J* **12,** 2459-2466

Huang H. and Pears C. (1999) Cell cycle-dependent regulation of early developmental genes. *Biochim Biophys Acta* **1452,** 296-302

Huang Y. E., Iijima M., Parent C. A., Funamoto S., Firtel R. A. and Devreotes P. (2003) Receptor-mediated regulation of PI3Ks confines PI(3,4,5)P3 to the leading edge of chemotaxing cells. *Mol Biol Cell* **14,** 1913-1922

Huang Z. A., Yang H., Chen C., Zeng Z. and Lu S. C. (2000) Inducers of gamma-glutamylcysteine synthetase and their effects on glutathione synthetase expression. *Biochim Biophys Acta* **1493,** 48-55

Hwang C., Sinskey A. J. and Lodish H. F. (1992) Oxidized redox state of glutathione in the endoplasmic reticulum. *Science* **257,** 1496-1502

Ibarra N., Blagg S. L., Vazquez F. and Insall R. H. (2006) Nap1 regulates Dictyostelium cell motility and adhesion through SCAR-dependent and -independent pathways. *Curr Biol* **16,** 717-722

Iijima M. and Devreotes P. (2002) Tumor suppressor PTEN mediates sensing of chemoattractant gradients. *Cell* **109,** 599-610

Iijima M., Huang Y. E. and Devreotes P. (2002) Temporal and spatial regulation of chemotaxis. *Dev Cell* **3,** 469-478

Inagi R., Kumagai T., Fujita T. and Nangaku M. (2010) The role of glyoxalase system in renal hypoxia. *Adv Exp Med Biol* **662,** 49-55

Inouye K. and Takeuchi I. (1982) Correlations between prestalk-prespore tendencies and cAMP-related activities in Dictyostelium discoideum. *Exp Cell Res* **138,** 311-318

Janaky R., Ogita K., Pasqualotto B. A., Bains J. S., Oja S. S., Yoneda Y. and Shaw C. A. (1999) Glutathione and signal transduction in the mammalian CNS. *J Neurochem* **73,** 889-902

Janetopoulos C., Jin T. and Devreotes P. (2001) Receptor-mediated activation of heterotrimeric G-proteins in living cells. *Science* **291,** 2408-2411

Janetopoulos C., Ma L., Devreotes P. N. and Iglesias P. A. (2004) Chemoattractant-induced phosphatidylinositol 3,4,5-trisphosphate accumulation is spatially amplified and adapts, independent of the actin cytoskeleton. *Proc Natl Acad Sci U S A* **101,** 8951-8956

Jurgensen C. W., Jacobsen N. R., Emri T., Eriksen S. H. and Pocsi I. (2001) Glutathione metabolism and dimorphism in Aureobasidium pullulans. *J Basic Microbiol* **41,** 131-137

Kalapos M. P. (2008) Methylglyoxal and glucose metabolism: a historical perspective and future avenues for research. *Drug Metabol Drug Interact* **23,** 69-91

Ketterer B., Coles B. and Meyer D. J. (1983) The role of glutathione in detoxication. *Environ Health Perspect* **49,** 59-69

Kim B. J., Choi C. H., Lee C. H., Jeong S. Y., Kim J. S., Kim B. Y., Yim H. S. and Kang S. O. (2005) Glutathione is required for growth and prespore cell differentiation in Dictyostelium. *Dev Biol* **284,** 387-398

Kim J. S., Seo J. H. and Kang S. O. (2014) Glutathione initiates the development of Dictyostelium discoideum through the regulation of YakA. *Biochim Biophys Acta* **1843,** 664-674

Kortholt A., Kataria R., Keizer-Gunnink I., Van Egmond W. N., Khanna A. and Van Haastert P. J. (2011) Dictyostelium chemotaxis: essential Ras activation and accessory signalling pathways for amplification. *EMBO Rep* **12,** 1273-1279

Kriebel P. W., Barr V. A. and Parent C. A. (2003) Adenylyl cyclase localization regulates streaming during chemotaxis. *Cell* **112,** 549-560

Kumagai A., Pupillo M., Gundersen R., Miake-Lye R., Devreotes P. N. and Firtel R. A. (1989) Regulation and function of G alpha protein subunits in Dictyostelium. *Cell* **57,** 265-275

Lilly P., Wu L., Welker D. L. and Devreotes P. N. (1993) A G-protein beta-subunit is essential for Dictyostelium development. *Genes Dev* **7,** 986-995

Loomis W. F. (1993) Lateral inhibition and pattern formation in Dictyostelium. *Curr Top Dev Biol* **28,** 1-46

Louis J. M., Saxe C. L., 3rd and Kimmel A. R. (1993) Two transmembrane signaling mechanisms control expression of the cAMP receptor gene CAR1 during Dictyostelium development. *Proc Natl Acad Sci U S A* **90,** 5969-5973

Lu S. C. (2000) Regulation of glutathione synthesis. *Curr Top Cell Regul* **36,** 95-116

Lushchak V. I. (2012) Glutathione homeostasis and functions: potential targets for medical interventions. *J Amino Acids* **2012,** 736837

MacWilliams H. K. (1982) Numerical simulations of hydra head regeneration using a proportion-regulating version of the Gierer-Meinhardt model. *J Theor Biol* **99,** 681-703

Malchow D., Lusche D. F. and Schlatterer C. (2004) A link of Ca2+ to cAMP oscillations in Dictyostelium: the calmodulin antagonist W-7 potentiates cAMP relay and transiently inhibits the acidic Ca2+-store. *BMC Dev Biol* **4,** 7

Mann S. K. and Firtel R. A. (1989) Two-phase regulatory pathway controls cAMP receptor-mediated expression of early genes in Dictyostelium. *Proc Natl Acad Sci U S A* **86,** 1924-1928

Mann S. K. and Firtel R. A. (1991) A developmentally regulated, putative serine/threonine

protein kinase is essential for development in Dictyostelium. *Mech Dev* **35,** 89-101

Mann S. K. and Firtel R. A. (1993) cAMP-dependent protein kinase differentially regulates prestalk and prespore differentiation during Dictyostelium development. *Development* **119,** 135-146

Martins A. M., Cordeiro C. A. and Ponces Freire A. M. (2001) In situ analysis of methylglyoxal metabolism in Saccharomyces cerevisiae. *FEBS Lett* **499,** 41-44

Meister A. (1983) Selective modification of glutathione metabolism. *Science* **220,** 472-477

Meister A. (1994) Glutathione-ascorbic acid antioxidant system in animals. *J Biol Chem* **269,** 9397-9400

Meister A. (1994) Glutathione, ascorbate, and cellular protection. *Cancer Res* **54,** 1969s-1975s

Meister A. and Anderson M. E. (1983) Glutathione. *Annu Rev Biochem* **52,** 711-760

Meredith M. J. and Reed D. J. (1982) Status of the mitochondrial pool of glutathione in the isolated hepatocyte. *J Biol Chem* **257,** 3747-3753

Milne J. L. and Devreotes P. N. (1993) The surface cyclic AMP receptors, cAR1, cAR2, and cAR3, promote Ca2+ influx in Dictyostelium discoideum by a G alpha 2-independent mechanism. *Mol Biol Cell* **4,** 283-292

Morris H. R., Taylor G. W., Masento M. S., Jermyn K. A. and Kay R. R. (1987) Chemical structure of the morphogen differentiation inducing factor from Dictyostelium discoideum. *Nature* **328,** 811-814

Murata K., Saikusa T., Fukuda Y., Watanabe K., Inoue Y., Shimosaka M. and Kimura A.

(1986) Metabolism of 2-oxoaldehydes in yeasts. Possible role of glycolytic bypath as a detoxification system in L-threonine catabolism by Saccharomyces cerevisiae. *Eur J Biochem* **157,** 297-301

Myers S. A., Han J. W., Lee Y., Firtel R. A. and Chung C. Y. (2005) A Dictyostelium homologue of WASP is required for polarized F-actin assembly during chemotaxis. *Mol Biol Cell* **16,** 2191-2206

Nations C., Allen R. G., Balin A. K., Reimer R. J. and Sohal R. S. (1987) Superoxide dismutase activity and glutathione concentration during the calcium-induced differentiation of Physarum polycephalum microplasmodia. *J Cell Physiol* **133,** 181-186

Newton G. L. and Fahey R. C. (1995) Determination of biothiols by bromobimane labeling and high-performance liquid chromatography. *Methods Enzymol* **251,** 148-166

Njalsson R., Norgren S., Larsson A., Huang C. S., Anderson M. E. and Luo J. L. (2001) Cooperative binding of gamma-glutamyl substrate to human glutathione synthetase. *Biochem Biophys Res Commun* **289,** 80-84

Noctor G., Mhamdi A., Chaouch S., Han Y., Neukermans J., Marquez-Garcia B., Queval G. and Foyer C. H. (2012) Glutathione in plants: an integrated overview. *Plant Cell Environ* **35,** 454-484

Okaichi K., Cubitt A. B., Pitt G. S. and Firtel R. A. (1992) Amino acid substitutions in the Dictyostelium G alpha subunit G alpha 2 produce dominant negative phenotypes and inhibit the activation of adenylyl cyclase, guanylyl cyclase, and phospholipase C. *Mol Biol Cell* **3,** 735-

747

Pang K. M., Lynes M. A. and Knecht D. A. (1999) Variables controlling the expression level of exogenous genes in Dictyostelium. *Plasmid* **41,** 187-197

Parent C. A., Blacklock B. J., Froehlich W. M., Murphy D. B. and Devreotes P. N. (1998) G protein signaling events are activated at the leading edge of chemotactic cells. *Cell* **95,** 81-91

Parent C. A. and Devreotes P. N. (1996) Molecular genetics of signal transduction in Dictyostelium. *Annu Rev Biochem* **65,** 411-440

Pasternak M., Lim B., Wirtz M., Hell R., Cobbett C. S. and Meyer A. J. (2008) Restricting glutathione biosynthesis to the cytosol is sufficient for normal plant development. *Plant J* **53,** 999-1012

Penninckx M. J., Jaspers C. J. and Legrain M. J. (1983) The glutathione-dependent glyoxalase pathway in the yeast Saccharomyces cerevisiae. *J Biol Chem* **258,** 6030-6036

Plyte S. E., O'Donovan E., Woodgett J. R. and Harwood A. J. (1999) Glycogen synthase kinase-3 (GSK-3) is regulated during Dictyostelium development via the serpentine receptor cAR3. *Development* **126,** 325-333

Rennenberg H. and Filner P. (1982) Stimulation of h(2)s emission from pumpkin leaves by inhibition of glutathione synthesis. *Plant Physiol* **69,** 766-770

Richardson D. L., Loomis W. F. and Kimmel A. R. (1994) Progression of an inductive signal activates sporulation in Dictyostelium discoideum. *Development* **120,** 2891-2900

Rietdorf J., Siegert F. and Weijer C. J. (1996) Analysis of optical density wave propagation

and cell movement during mound formation in Dictyostelium discoideum. *Dev Biol* **177,** 427-438

Sasaki A. T., Chun C., Takeda K. and Firtel R. A. (2004) Localized Ras signaling at the leading edge regulates PI3K, cell polarity, and directional cell movement. *J Cell Biol* **167,** 505-518

Schmittgen T. D. and Livak K. J. (2008) Analyzing real-time PCR data by the comparative C(T) method. *Nat Protoc* **3,** 1101-1108

Schnitzler G. R., Briscoe C., Brown J. M. and Firtel R. A. (1995) Serpentine cAMP receptors may act through a G protein-independent pathway to induce postaggregative development in Dictyostelium. *Cell* **81,** 737-745

Segall J. E., Kuspa A., Shaulsky G., Ecke M., Maeda M., Gaskins C., Firtel R. A. and Loomis W. F. (1995) A MAP kinase necessary for receptor-mediated activation of adenylyl cyclase in Dictyostelium. *J Cell Biol* **128,** 405-413

Sen C. K. (1998) Redox signaling and the emerging therapeutic potential of thiol antioxidants. *Biochem Pharmacol* **55,** 1747-1758

Sen C. K. and Packer L. (1996) Antioxidant and redox regulation of gene transcription. *FASEB J* **10,** 709-720

Shi Z. Z., Osei-Frimpong J., Kala G., Kala S. V., Barrios R. J., Habib G. M., Lukin D. J., Danney C. M., Matzuk M. M. and Lieberman M. W. (2000) Glutathione synthesis is essential for mouse development but not for cell growth in culture. *Proc Natl Acad Sci U S A* **97,** 5101-5106

Siems W., Crifo C., Capuozzo E., Uchida K., Grune T. and Salerno C. (2010) Metabolism of 4-hydroxy-2-nonenal in human polymorphonuclear leukocytes. *Arch Biochem Biophys* **503,** 248-252

Sies H. (1999) Glutathione and its role in cellular functions. *Free Radic Biol Med* **27,** 916-921

Snaar-Jagalska B. E., Kesbeke F. and Van Haastert P. J. (1988) G-proteins in the signal-transduction pathways of Dictyostelium discoideum. *Dev Genet* **9,** 215-226

Souza G. M., Lu S. and Kuspa A. (1998) YakA, a protein kinase required for the transition from growth to development in Dictyostelium. *Development* **125,** 2291-2302

Sugiyama K., Izawa S. and Inoue Y. (2000) The Yap1p-dependent induction of glutathione synthesis in heat shock response of Saccharomyces cerevisiae. *J Biol Chem* **275,** 15535-15540

Sun T. J. and Devreotes P. N. (1991) Gene targeting of the aggregation stage cAMP receptor cAR1 in Dictyostelium. *Genes Dev* **5,** 572-582

Sussman M. (1987) Cultivation and synchronous morphogenesis of Dictyostelium under controlled experimental conditions. *Methods Cell Biol* **28,** 9-29

Sutovsky P. and Schatten G. (1997) Depletion of glutathione during bovine oocyte maturation reversibly blocks the decondensation of the male pronucleus and pronuclear apposition during fertilization. *Biol Reprod* **56,** 1503-1512

Tapiero H., Mathe G., Couvreur P. and Tew K. D. (2002) II. Glutamine and glutamate. *Biomed Pharmacother* **56,** 446-457

Thomas D., Klein K., Manavathu E., Dimmock J. R. and Mutus B. (1991) Glutathione levels

during thermal induction of the yeast-to-mycelial transition in Candida albicans. *FEMS Microbiol Lett* **61,** 331-334

Townsend D. M., Tew K. D. and Tapiero H. (2003) The importance of glutathione in human disease. *Biomed Pharmacother* **57,** 145-155

Traynor D., Kessin R. H. and Williams J. G. (1992) Chemotactic sorting to cAMP in the multicellular stages of Dictyostelium development. *Proc Natl Acad Sci U S A* **89,** 8303-8307

Verkerke-van Wijk I., Fukuzawa M., Devreotes P. N. and Schaap P. (2001) Adenylyl cyclase A expression is tip-specific in Dictyostelium slugs and directs StatA nuclear translocation and CudA gene expression. *Dev Biol* **234,** 151-160

Vernoux T., Wilson R. C., Seeley K. A., Reichheld J. P., Muroy S., Brown S., Maughan S. C., Cobbett C. S., Van Montagu M., Inze D., May M. J. and Sung Z. R. (2000) The ROOT MERISTEMLESS1/CADMIUM SENSITIVE2 gene defines a glutathione-dependent pathway involved in initiation and maintenance of cell division during postembryonic root development. *Plant Cell* **12,** 97-110

Wang J., Hou L., Awrey D., Loomis W. F., Firtel R. A. and Siu C. H. (2000) The membrane glycoprotein gp150 is encoded by the lagC gene and mediates cell-cell adhesion by heterophilic binding during Dictyostelium development. *Dev Biol* **227,** 734-745

Weening K. E., Wijk I. V., Thompson C. R., Kessin R. H., Podgorski G. J. and Schaap P. (2003) Contrasting activities of the aggregative and late PDSA promoters in Dictyostelium development. *Dev Biol* **255,** 373-382

Wessels D. J., Zhang H., Reynolds J., Daniels K., Heid P., Lu S., Kuspa A., Shaulsky G., Loomis W. F. and Soll D. R. (2000) The internal phosphodiesterase RegA is essential for the suppression of lateral pseudopods during *Dictyostelium* chemotaxis. *Mol Biol Cell* **11,** 2803-2820

Williams J., Hopper N., Early A., Traynor D., Harwood A., Abe T., Simon M. N. and Veron M. (1993) Interacting signalling pathways regulating prestalk cell differentiation and movement during the morphogenesis of Dictyostelium. *Dev Suppl* 1-7

Wood S. A., Ammann R. R., Brock D. A., Li L., Spann T. and Gomer R. H. (1996) RtoA links initial cell type choice to the cell cycle in Dictyostelium. *Development* **122,** 3677-3685

Wu G., Fang Y. Z., Yang S., Lupton J. R. and Turner N. D. (2004) Glutathione metabolism and its implications for health. *J Nutr* **134,** 489-492

Wu L., Valkema R., Van Haastert P. J. and Devreotes P. N. (1995) The G protein beta subunit is essential for multiple responses to chemoattractants in Dictyostelium. *J Cell Biol* **129,** 1667-1675

Xu X., Meier-Schellersheim M., Jiao X., Nelson L. E. and Jin T. (2005) Quantitative imaging of single live cells reveals spatiotemporal dynamics of multistep signaling events of chemoattractant gradient sensing in Dictyostelium. *Mol Biol Cell* **16,** 676-688

Yang H., Zeng Y., Lee T. D., Yang Y., Ou X., Chen L., Haque M., Rippe R. and Lu S. C. (2002) Role of AP-1 in the coordinate induction of rat glutamate-cysteine ligase and glutathione synthetase by tert-butylhydroquinone. *J Biol Chem* **277,** 35232-35239

Yokoyama H. (2007) [Gamma glutamyl transpeptidase (gammaGTP) in the era of metabolic syndrome]. *Nihon Arukoru Yakubutsu Igakkai Zasshi* **42,** 110-124

Zhang N., Long Y. and Devreotes P. N. (2001) Ggamma in dictyostelium: its role in localization of gbetagamma to the membrane is required for chemotaxis in shallow gradients. *Mol Biol Cell* **12,** 3204-3213

Zhu X., Gallogly M. M., Mieyal J. J., Anderson V. E. and Sayre L. M. (2009) Covalent cross-linking of glutathione and carnosine to proteins by 4-oxo-2-nonenal. *Chem Res Toxicol* **22,** 1050-1059

Zigmond S. H., Joyce M., Borleis J., Bokoch G. M. and Devreotes P. N. (1997) Regulation of actin polymerization in cell-free systems by GTPgammaS and Cdc42. *J Cell Biol* **138,** 363-374

국문 초록

Glutathione 은 진핵생물의 세포 내에서 높은 농도로 존재하는 tripeptide 로 –SH (thiol) 작용기를 가지고 있으며, 다세포 생물의 분화에 중요한 역할을 한다. 하지만 진핵생물이자 점균류에 속하는 *Dictyostelium discoideum* 의 분화에 있어서 glutathione 의 최종 합성단계 효소인 glutathione synthetase (*gshB*/GSS)의 역할에 대해선 아직 연구되어 있지 않다. 본 연구에서 *gshB* 과량발현은 *Dictyostelium* 분화의 초기 단계와 후기 단계 모두에서 세포 내 glutathione 농도를 증가시킨 것을 확인하였고, 따라서 *gshB* 과량발현균주를 통하여 세포 내 높은 농도로 glutathione 이 존재할 경우 *Dictyostelium* 분화에 어떠한 영향을 미치는지 규명하고자 하였다.

Dictyostelium 분화동안 *gshB* 과량발현균주는 분화 마지막 단계인 fruiting body 형성을 하지 못하였고, 대부분이 mound 단계에서 분화가 멈추었다. 따라서 포자 형성이 크게 감소되는 결함을 보였다. 이러한 결함은 야생형균주에 외부에서 glutathione 을 추가적으로 넣어주었을 때에도 관찰되었다. 그 원인을 자세히 분석하고자 먼저 *Dictyostelium* 분화 초기에 나타나는 현상인 세포군집 시 chemotaxis 에 의한 streaming 형성을 시험하였다. 세포를 비교적 낮은 밀도로 분화시켰을 때, 야생형균주는 chemoattractant 인 cAMP 의 농도 차이를 인지하여 한 방향으로 모여들어 다세포의 군집형태를 이루며 streaming 을 형성하는 데 반해 *gshB* 과량발현균주는 정상적인 군집형태를 이루지 못하였고 streaming 역시 형성하지 못하였다. 이런 결함은 세포군집 동안 *gshB*

과량발현 단일세포 내의 F-actin 의 분포가 적절한 극성을 띠지 않았고, 과도한 lateral pseudopods 형성을 저해하는데 결함을 보였기 때문이다. 또한 *gshB* 과량발현세포는 cAMP 에 대한 반응인 *in vivo* F-actin polymerization 에서도 비정상적인 fluctuating pattern 을 보였다.

다음으로 분화후기 cell differentiation 동안 cell-type proportioning 을 관찰하였다. 그 결과 *gshB* 과량발현균주는 야생형균주와 달리 최종적으로 형성된 mound 내에서 pre-stalk 으로의 세포분화가 증가한 반면, pre-spore 로의 세포분화가 크게 감소된 것을 보였다. 이는 이 균주에서 최종적으로 관찰된 포자형성의 감소와 일치하는 결과이다.

Dictyostelium 분화동안 cAMP 신호전달체계는 세포군집에서부터 세포분화까지 거의 모든 단계에 관여한다고 알려져 있다. 따라서 *gshB* 과량발현에 의한 세포 내 glutathione 농도의 증가가 cAMP 신호전달에 어떠한 영향을 주는지 알아보고자 *gshB* 과량발현균주에서 cAMP 신호전달에 관련된 주요 유전자들의 발현을 확인하였고, 그 결과 cAR1 매개 신호전달에 관련된 유전자들 (*carA, gα2, gβ,* 그리고 *acaA*) 의 발현량이 야생형균주에서보다 증가한 것을 확인하였으며 그와 동시에 세포 내 cAMP 농도도 증가한 것을 확인하였다.

Glutathione 에 의한 cAR1 매개 신호전달체계의 조절 메커니즘을 분석하고자, 외부의 cAMP 를 인식하는데 필요한 cAMP receptor (cAR1)의 유전자 *carA* 과 cAMP 합성의 상위 단계에 있는 G protein alpha 2 (Gα2)의 유전자 *gpaB* 를 세포 내에 각각 과량발현시켜 그 균주들의 분화양상을 관찰하였다. *carA* 과량발현균주는 정상적으로 fruiting body 까지 분화하는 반면, *gpaB* 과량발현균주는 분화초기

streaming 형성 저해와 비정상적인 F-actin polymerization 의 결함을 보였고, 세포 내 cAMP 농도 역시 크게 증가한 것으로 관찰되었다. 또한 분화후기 cell-type proportioning 에서도 pre-stalk 세포의 증가와 pre-spore 세포의 감소를 보였다. 즉, *gshB* 과량발현균주와 *gpaB* 과량발현균주의 분화양상이 유사한 것을 확인하였다. 반대로 *gshB* 과량발현균주의 분화결함은 Gα2 의 유전자 발현을 저해시켜줌으로써 일부분 회복된 것을 확인하였다. 이러한 결과들은 chemotaxis 에 중요한 역할을 하는 것으로 알려져 있는 Gα2 의 유전자 발현이 glutathione 에 의해 유도된다는 것을 의미한다.

또한 야생형균주와 *gshB* 과량발현균주에서 세포 내 Gα2-GFP 의 위치를 확인한 결과, cAMP 자극을 주기 전 야생형균주에서는 Gα2-GFP 가 세포 내 고르게 분포되어 있었지만, *gshB* 과량발현균주에서는 세포의 원형질막에 높은 농도로 존재하고 있음을 확인하였다. 이 결과는 glutathione 이 Gα2 의 유전자발현뿐만 아니라 세포 내 위치에도 영향을 미치는 것을 의미한다.

위의 결과들을 종합하여 볼 때, GSS 는 glutathione 의 합성 증가에 중요한 역할을 하며, glutathione 은 *Dictyostelium* 분화과정 동안 초기 세포군집을 위한 chemotaxis 와 후기 cell-type differentiation 에 중요한 역할을 하는 Gα2 을 통하여 cAR1 매개 cAMP 신호전달을 유도하는 것으로 생각된다.

주요어: Glutathione, Glutathione synthetase (GSS), cAR1 매개 cAMP 신호전달, G protein alpha 2 (Gα2), *Dictyostelium discoideum*